

**Regulation of Adipocyte Differentiation and Metabolism by Artificial
Sweeteners and Sweet Taste Receptors**

by

Becky R. Simon

**A dissertation submitted in partial fulfillment
of the requirements for the degree of
Doctor of Philosophy
(Cellular and Molecular Biology)
in the University of Michigan
2013**

Doctoral Committee:

**Professor Ormond A. MacDougald, Chair
Professor Robert T. Kennedy
Associate Professor Jiandie Lin
Assistant Professor Carey N. Lumeng
Associate Professor Scott Pletcher**

© Becky R. Simon 2013

Dedication

To Char, for always believing I was mad enough to be scientist.

Acknowledgments

This work would not have been possible without the assistance and support of many people. First and foremost, members of the MacDougald lab have been a font of sage advice, mom jokes, and lab debauchery. Without their logistical and intellectual support, many of these studies would not have been possible. Ormond's constant enthusiasm and 'big-picture' perspective have allowed me to grow as an independent scientist. I have also been fortunate to have several excellent collaborators, including Fariba Assadi-Porter, Linda Ma, and especially Björn Tyrberg who generously provided valuable skills, reagents, animals, and input. Last but not least, I would like to thank friends and family for their unwavering support and constant supply of hugs.

More pragmatically, this work was supported by grants R01-DK062876 and R01-DK095705 to Ormond MacDougald. I was supported by a Rackham Merit Fellowship, Cellular and Molecular Biology Program Training Grant (T32-GM007315), and the Training Program in Organogenesis (T32HD007505). This work utilized Animal Phenotyping and Morphology and Imaging Core Services supported by NIH grants P30-DK089503 and P60-DK020572, and Metabolomics Core Services supported by grant U24 DK097153 of NIH Common Funds Project to the University of Michigan.

Table of Contents

Dedication	ii
Acknowledgments	iii
Table of Figures	vii
List of Abbreviations	ix
Chapter One	1
Introduction	1
Adipose tissue functions and obesity	1
Adipocyte differentiation	1
Lipolysis.....	3
Adipocyte model systems.....	5
Receptor-mediated nutrient sensing in adipose tissue.....	6
Chemosensory receptors are nutrient sensors in non-neural tissues	8
Nutrient-Sensing Olfactory receptors	8
Nutrient-Sensing Taste Receptors	9
Sweet taste receptor biology	12
Sweet taste receptor signaling	13
Artificial sweetener consumption	14
Effects of artificial sweetener consumption on metabolism.....	15
Model: Sweet taste receptors act as nutrient sensors in adipose tissue.....	16
References	21
Chapter Two	37
Artificial Sweeteners Enhance Adipogenesis and Suppress Lipolysis	
Independent of Sweet Taste Receptors	37
Abstract	37
Introduction.....	38
Results.....	40

<u>Chemosensory receptors are regulated with adiposity.</u>	40
<u>Sweet taste receptors T1R2 and T1R3 are expressed constitutively throughout adipogenesis and in 3T3-L1 cells and eMSCs.</u>	40
<u>Saccharin stimulates adipogenesis of mouse and human precursor cells.</u> ..	41
<u>AceK stimulates adipogenesis of mouse and human precursor cells.</u>	42
<u>Saccharin enhancement of adipogenesis is temporally dependent.</u>	43
<u>Artificial sweetener treatment has minimal effects on the early transcriptional program.</u>	44
<u>Saccharin acutely activates Akt and ERK1/2 signaling pathways in preadipocytes.</u>	44
<u>T1R2 and T1R3 are not required for saccharin-stimulated adipogenesis or Akt phosphorylation.</u>	46
<u>Artificial sweeteners suppress lipolysis.</u>	47
<u>T1R2/T1R3 are not required for suppression of lipolysis by saccharin.</u>	48
Discussion	49
Materials and Methods	52
References	69
Chapter Three	75
Metabolic Phenotyping of Sweet Taste Receptor Knockout Mice	75
Abstract	75
Introduction.....	75
Results.....	77
<u>T1R3 KO mice have reduced adiposity on Western Diet.</u>	77
<u>T1R3 KO mice have fewer large adipocytes but equal adipocyte number on Western Diet.</u>	78
<u>T1R3 KO mice have no changes in glucose sensitivity.</u>	79
<u>T1R3 KO mice have sexually dimorphic reductions in adiposity on chow diet.</u>	79
<u>T1R2 KO mice have reduced adiposity on Western Diet.</u>	80
<u>T1R2 KO mice have smaller adipocytes but equal adipocyte numbers.</u>	81

<u>The reduced-adiposity phenotype of T1R2 KO animals has low penetrance.</u>	82
<u>T1R2 KO mice have fewer bone marrow adipocytes.</u>	82
<u>T1R3 KO animals trend towards fewer bone marrow adipocytes.</u>	83
<u>T1R2 KO animals have increased trabecular bone.</u>	83
<u>T1R3 KO animals have increased cortical and trabecular bone.</u>	84
Discussion	84
Materials and Methods	86
References	103
Chapter Four	106
Future Directions for Sweetener and Taste Receptor Biology	106
Summary	106
What is the function of sweet taste receptors in adipose tissue <i>in vivo</i> ? Is there an endogenous ligand for receptor activation?	109
Do sweet taste receptors play a role in bone biology?	110
Are other chemosensory receptors functional in adipose tissue?	111
References	113

Table of Figures

Figure 1.1. Ectopic olfactory receptor expression.	17
Figure 1.2. Human sweet taste receptors.....	18
Figure 1.3. FDA-approved artificial sweeteners and recommended intake.....	19
Figure 1.4. Proposed role for sweet taste receptors and artificial sweeteners in adipogenesis and adipocyte metabolism.	20
Figure 2.1. Chemosensory receptors are regulated with adiposity.	59
Figure 2.2. Sweet taste receptors T1R2 and T1R3 are expressed constitutively throughout adipogenesis in 3T3-L1 cells and eMSCs.....	60
Figure 2.3. Saccharin stimulates adipogenesis in mouse and human precursor cells.	61
Figure 2.4. AceK stimulates adipogenesis in mouse and human precursor cells.	62
Figure 2.5. Saccharin enhancement of adipogenesis is temporally dependent. .	63
Figure 2.6. Artificial sweetener treatment has minimal effects on the early transcriptional program.....	64
Figure 2.7. Saccharin activates Akt and ERK1/2 signaling pathways in preadipocytes.	65
Figure 2.8. T1R3 and T1R2 are not required for saccharin-stimulated adipogenesis or Akt phosphorylation.	66
Figure 2.9. Artificial sweeteners suppress lipolysis.	67
Figure 2.10. T1R2/T1R3 are not required for suppression of lipolysis by saccharin.	68
Figure 3.1. Male T1R3 KO mice have reduced adiposity on Western Diet.	92
Figure 3.2 T1R3 KO mice have fewer large adipocytes but equal adipocyte number on Western Diet	93
Figure 3.3 T1R3 KO mice have no changes in glucose sensitivity.....	94

Figure 3.4 T1R3 KO mice have sexually dimorphic reductions in adiposity on chow diet.	95
Figure 3.5 T1R2 KO mice have reduced adiposity on Western Diet	96
Figure 3.6 T1R2 KO mice have smaller adipocytes but equal adipocyte numbers.	97
Figure 3.7. T1R2 KO mice have no changes in glucose sensitivity.....	98
Figure 3.8. T1R2 KO mice have fewer bone marrow adipocytes.	99
Figure 3.9. T1R3 KO animals trend towards fewer bone marrow adipocytes. ..	100
Figure 3.10. T1R2 KO animals have increased trabecular bone.....	101
Figure 3.11. T1R3 KO animals have increased cortical and trabecular bone. ..	102

List of Abbreviations

AceK	Acesulfame potassium
ATGL	Adipose Triglyceride Lipase
AUC	Area under the curve
BAT	Brown adipose tissue
BMC	Bone mineral content
BMD	Bone mineral density
BW	Body weight
CCK	Cholecystokinin
D	Dexamethasone
DAG	Diacylglycerol
eMSC	Ear mesenchymal stem cell
eWAT	epididymal white adipose tissue
FBS	Fetal bovine serum
Fsk	Forskolin
GPCR	G protein-coupled receptor
GTT	Glucose tolerance test
gWAT	gonadal white adipose tissue
HSL	Hormone sensitive lipase
I	Insulin
IP3	Inositol triphosphate
ITT	Insulin tolerance test
M	IBMX, 3-isobutyl-1-methylxanthine
MAT	Marrow adipose tissue
NEFA	Non-esterified fatty acid
NTD	N-terminal domain
PDE	Phosphodiesterase

PDK1	3-phosphoinositide dependent protein kinase-1
PI3K	Phosphatidylinositide 3-kinases
PIP2	Phosphatidylinositol 4,5-bisphosphate
PIP3	Phosphatidylinositol (3,4,5)-triphosphate
PKA	Protein kinase A
PLIN	Perilipin
Sacc	Saccharin
Sucr	Sucralose
SVCs	Stromal vascular cells
TMD	Tissue mineral density
WAT	White adipose tissue
WM	Wortmannin
μ CT	Microcomputerized tomography

Chapter One

Introduction

Adipose tissue functions and obesity

Adipose tissue is a dynamic endocrine organ necessary for the storage and release of lipid in concert with energetic requirements. When energy intake surpasses usage, adipose tissue responds by increasing size and/or number of adipocytes to facilitate lipid storage (Hirsch, 1969; Hellman, 1961 ;Bertrand, 1978;Knittle, 1979). Conversely, in intervals of energy deprivation, adipocytes release stored lipid. However, when energetic homeostasis is not maintained due to prolonged energy surplus, adipose tissue expands to pathological levels resulting in obesity and increased risk for obesity-associated disorders, notably type 2 diabetes, hypertension, atherosclerosis, and many types of cancer (Kong, et al)

Adipocyte differentiation

Adipocytes differentiate from committed precursor cells known as preadipocytes through a complex but well-defined transcriptional cascade. Transcription factors PPAR γ and C/EBP α , master regulators of adipogenesis, are necessary and sufficient to drive the expression of target genes such as FABP4, IRS, and GLUT4 (Rosen et al., 2006). These and many other target genes drive the physiological processes characteristic of functional adipocytes, including glucose uptake, lipogenesis, lipolysis, and hormone secretion (Winegrad et al.,1958; Milstein et al.,1956; Halaas et al.,1995; Frerichs et al.,1962). PPAR γ activity is required for both acquisition and maintenance of an adipogenic cell fate. PPAR γ alone is sufficient to drive adipogenesis in fibroblasts (Tontonoz et

al, 1994). Ablation of PPAR γ activity in mature adipocytes results in triacylglycerol loss *in vitro* (Tamori et al, 2002), and cell death *in vivo* (Imai, 2004). While C/EBP α cannot stimulate adipogenesis in the absence of PPAR γ , its expression appears to be necessary to confer insulin sensitivity to mature adipocytes (Wu et al., 1999), in addition to serving as a stimulator of PPAR γ expression and being a strong driver of adipogenesis (Linhart et al, 2001; Rosen et al, 2002; Freytag et al, 1994). Many additional transcription factors function to modulate the activity of PPAR γ and/or C/EBP α through interaction with specific promoters or the transcription factors themselves. These genes include KLFs (Mori, 2005; Banerjee, 2003), GATAs (Tong, 2000), and additional C/EBPs (Tang 2000 et al.; Tang et al., 2003; Tanaka et al.1997), with some families containing both pro- and anti-adipogenic members.

Upstream of transcriptional regulation, adipogenesis is also directed by extracellular signaling factors relaying conditions of the surrounding milieu. Such extracellular signaling factors include developmental signaling pathways like Wnt, Hedgehog, and Notch (Ross et al., 2004; Cousin et al., 2007). Wnt activity is best defined of this group, being a strong inhibitor of adipogenesis (Ross et al., 2000). Other secreted proteins regulating adipogenesis include insulin and IGF-1. While insulin is a well-characterized inducer of adipogenesis, preadipocytes express the insulin receptor at relatively low levels. Hence, the pro-adipogenic effects of supraphysiological concentrations of insulin *in vitro* are therefore thought to be mediated by the IGF-1 receptor (Smith et al.,1988), which is more highly expressed in preadipocytes and also binds insulin, though with reduced affinity (Mynarcik et al.,1997; Rubin et al.,1978). Insulin binding to either insulin receptors or IGF-1 receptors results in autophosphorylation of tyrosine residues and recruitment of scaffolding and substrate proteins, including insulin receptor substrate IRS-1 and Src homology 2 domains SH2 (Bevan, 2001). IRS-1 recruits and activates PI3 kinase (PI3K), which phosphorylates PIP2 to generate PIP3 within the cell membrane. This phospholipid serves as an anchoring point for additional signaling proteins. PDK1 and Akt are recruited to the cell membrane

by PIP3, where PDK1 phosphorylates Akt (also known as PKB) at threonine 308 (Stokoe et al., 1997). An additional phosphorylation of Akt at serine 473 by mTORC2 results in maximal Akt activation (Sarbasov et al., 2005). Akt is a pro-adipogenic kinase in itself, facilitating adipogenesis through numerous mechanisms. These include phosphorylation and nuclear exclusion of the anti-adipogenic FOXO (Nakae et al., 2003) and GATA2 (Menghini et al., 2005), and phosphorylation and activation of the pro-adipogenic CREB (Cypess et al 2001; Reusch et al., 2002). Constitutive Akt activity results in spontaneous differentiation of 3T3-L1 cells (Magun et al., 1996); Akt therefore serves as a major effector of insulin-stimulated adipogenesis.

An additional regulator of adipogenesis sensitive to extracellular milieu is the MAP Kinase pathway (MAPK). However, contradictory roles for ERK1/2 signaling in adipogenesis have been reported. Some groups have shown rapid and transient ERK1/2 activation upon induction of adipogenesis, and inhibition of adipogenesis when this activation is blocked (Prusty et al., 2002). Additional groups have reported that ERK1/2 phosphorylates C/EBP β to allow its eventual transactivation of C/EBP α and PPAR γ (Tang et al., 2005). This observation is supported by ERK1 KO animals, which have decreased adiposity and fewer adipocytes (Bost et al., 2005). However, other groups have reported that sustained ERK activation inhibits adipogenesis and decreases PPAR γ activity (Hu et al., 1996). The reports can be balanced with a model in which ERK1/2 signaling is essential in early, mitotic stages of differentiation, but becomes inhibitory at later stages.

Lipolysis

In contrast to adipogenesis, which is generally stimulated under nutrient-rich conditions, lipolysis is a catabolic pathway that is activated in nutrient-deprived states to supply tissues with fatty acids. This process utilizes lipases to generate free fatty acids and glycerol from stored triglyceride. While a futile cycle of lipid hydrolysis and re-esterification is often maintained within adipocytes

(Kalderon et al., 2000), this equilibrium is strongly shifted to favor lipolysis by stimulation of β -adrenergic receptors. These G protein-coupled receptors (GPCRs) couple to $G\alpha_s$, which stimulates cAMP production. cAMP in turn activates cAMP-dependent protein kinase (PKA), which phosphorylates hormone-sensitive lipase (HSL) (Duncan et al., 2007). Although HSL was long thought to be the primary lipase in lipolysis, HSL knockout mice have surprisingly mild lipolytic phenotypes, suggesting involvement of additional enzymes (Wang et al., 2001; Haemmerle et al., 2002a; Haemmerle et al., 2002b). This possibility was confirmed with the identification of Adipose Triglyceride Lipase (ATGL), (Zimmermann et al., 2004; Villena et al., 2004; Jenkins et al., 2004), presenting a slightly more complex picture of lipolytic regulation. Current data suggests that HSL is a primary contributor to diacylglycerol (DAG) hydrolysis *in vivo*, (Haemmerle, 2002a), but is not strictly required for the initiation of lipolysis. As ATGL has preferential activity against triacylglycerol (TAG), reports have suggested that HSL and ATGL act together in a synergistic fashion and are both essential for lipolytic homeostasis (Zimmermann, 2003; Duncan, 2007).

In addition to lipases, there are multiple adapter and structural proteins with important roles in lipolysis. Perilipin (PLIN) normally surrounds lipid droplets, protecting the latter from cytoplasmic lipases. However, upon phosphorylation by PKA, PLIN remodels to expose the lipid droplet and allow access to lipases (Marcinkiewicz et al., 2006). Perilipin's role in lipid metabolism is supported by the abrogation of hormone-stimulated lipolysis in PLIN KO mice (Tansey et al., 2001). Perilipin also has important roles in controlling protein localization; upon lipolytic stimulation, HSL translocates exclusively to lipid droplets containing perilipin (Sztalryd et al, 2003). Perilipin phosphorylation also directly regulates the localization of CGI-58, a lipase-like protein (Subramanian et al., 2004). CGI-58 dissociates from perilipin upon PKA stimulation and directly interacts with ATGL to increase TAG hydrolysis (Lass et al., 2006). These data suggest a model in which CGI-58 may act as a coactivator of ATGL, but remains sequestered by perilipin until PKA activation (Granneman and Moore, 2008).

Further inhibitory regulation is mediated by phosphodiesterase (PDE) activity, which breaks down cAMP to reduce PKA activation. Insulin signaling is a primary driver of these phosphodiesterases, including PDE3B (Kitamura et al., 1999; Enoksson et al., 1998). Insulin stimulation can also directly reduce phosphorylation of HSL (Stralfors et al., 1989), and suppress lipolysis in the fed state by down-regulating ATGL expression and promoting re-esterification of fatty acids (Kershaw et al., 2006; Campbell et al., 1992).

Adipocyte model systems

Both the adipogenic transcriptional cascade and the basic metabolic functions of adipocytes have been studied thoroughly using *in vitro* model systems. Among the most frequently used of these models are 3T3-L1 cells. This cell line was originally isolated from Swiss mouse embryonic tissue by Howard Green in 1974, and selected for its innate adipogenic potential (Green and Kehinde, 1975; Green and Meuth, 1974). Despite being stimulated from polyploid, immortalized cells, 3T3-L1 adipogenesis is considered a reasonably accurate representation of adipogenesis *in vivo*.

Differentiation is induced in 3T3-L1 cells following two days of maintaining cells at confluence. On the day of induction, termed D0, cells are fed with fresh media containing fetal bovine serum (FBS) and a differentiation cocktail including IBMX (I), dexamethasone (D), and insulin (I). These three compounds, together termed MDI, provide many independent adipogenic stimuli. The numerous mechanisms for adipogenic stimulation by MDI include IBMX-stimulated intracellular cAMP accumulation and CREB activation, (Reusch et al., 2000; Gonzalez et al., 1989); dexamethasone-stimulated CEBP δ expression (Cao et al., 1991), and insulin-stimulated Akt phosphorylation (Magun et al., 1996). MDI can also block inhibitory pathways, including cAMP-dependent suppression of Wnt10b (Bennett et al., 2002). In a standard differentiation protocol, preadipocytes are induced at D0 with MDI, and media is replaced at D2 with FBS media containing insulin alone. Insulin is removed from the media at D4, after

which cells are maintained in FBS media only until they are mature adipocytes at approximately D8. Such a differentiation protocol can routinely convert 90% of 3T3-L1 preadipocytes to adipocytes.

While 3T3-L1 cells are among the most commonly used models of adipogenesis, they are committed preadipocytes with only one possible cell fate in the absence of genetic intervention. Multipotent adipogenic models can therefore also be used to explore preadipocyte commitment and regulation of alternative cell fates. Ear mesenchymal stem cells (eMSCs) are one such model. These primary cells are obtained from collagenase digestion of mouse ears, and have the potential for adipogenic, osteogenic, myogenic, or chondrogenic differentiation (Rim et al., 2005; Gawronska-Kozak et al., 2007). One advantage of eMSCs is that they can be isolated from genetically modified animals to compare adipogenic potential between genotypes, but offer improved adipogenic efficiency over other primary cells, such as stromal vascular cells (SVCs) obtained from digested adipose tissue. eMSCs can also be isolated from small portions of ears without sacrificing an animal. Differentiation protocols for eMSCs are similar to those for 3T3-L1s, with the exception of the use of higher insulin concentrations in the adipogenic cocktail.

Receptor-mediated nutrient sensing in adipose tissue

As a metabolic endocrine organ responsible for the bulk for an organism's energy storage, adipose tissue has unique needs for the sensing states of energetic plight and plenty. Adipose tissue has multiple mechanisms in place to achieve this task. Many adipose nutrient-sensing pathways are hormonal, such as insulin and β adrenergic signaling, and reflect systemic energy levels (Saltiel et al., 2001). Others are a more direct reflection of local or intracellular nutritional input: for example, AMPK and mTORC pathways. (Laplante et al., 2009; Daval, et al., 2006). However, recent studies have suggested that macronutrient-specific G protein-coupled receptors (GPCRs) may play an important role in nutrient sensing in adipocyte biology. These receptors are known pharmacologically for a

wide spectrum of cognate ligands and have large potential for generating macronutrient-specific inputs.

Several GPCRs have been identified as regulators of various aspects of adipose tissue biology. Some of the first characterized were GPR41 and 43 (Brown et al., 2003). These related GPCRs bind to short-chain fatty acids of varying lengths. GPR41 is expressed primarily in adipose tissue, while 43 is also expressed in immune cells. Further work showed that GPR43 (also known as FFA2) stimulates adipogenesis in response to propionate treatment in a GPR43-dependent manner (Hong et al., 2005). Additional work has shown that GPR41 stimulates leptin expression in cultured and mouse adipocytes (Xiong et al., 2004). However, these receptors also suppress lipolysis in mature adipocytes, as observed with fatty acid stimulation of GPR43 (Ge et al., 2008) or lactate stimulation of the orphan receptor GPR81 (Cai et al., 2008; Ge et al., 2008; Liu et al., 2009). The latter receptor is both enriched in adipocytes and upregulated with PPAR γ activity (Jeninga et al., 2009). Similar results have also been extrapolated to GPR108b and 109a, which are highly related to GPR81 (Ahmed et al., 2009).

Similar regulatory roles have been described for long-chain fatty acid-binding GPCRs in adipose tissue. Knockdown of GPR120, an omega-3 receptor enriched in adipose tissue, inhibits adipogenesis (Gotoh et al., 2007). Moreover, knockout of this receptor *in vivo* results in obesity and inflammation, though whether this is attributable specifically to adipose tissue function is unclear (Ichimura et al., 2012). GPR84, which binds to medium-chain fatty acids, is upregulated in adipocytes with high-fat diet and in response to TNF α -induced inflammation (Nagasaki, et al., 2012). Taken together, these data suggest a functional role of G protein-coupled receptors in nutrient sensing in adipose tissue, and open the door to study novel GPCRs that might also perform this role.

Chemosensory receptors are nutrient sensors in non-neural tissues

Chemosensory receptors, classified as olfactory, vomeronasal, or taste receptors, provide a means for detecting and identifying chemical stimuli in the external environment. These GPCRs represent a large family of Class C receptors: mice possess over 1000 distinct olfactory receptors, the largest GPCR family in existence. This expansive repertoire of available receptors is necessary for binding and generating discrete responses to over 10,000 different chemical ligands (Mombaerts, 2004). In many cases, chemosensory ligands have clear positive or negative associations, such as 'food' in response to fructose, or 'danger' in response to bitter toxins. Associations such as these are equally valid whether the stimuli are present externally or internally; this suggests that chemical detection can also be performed internally, particularly in organs and tissues that are most sensitive to the positive or negative outcomes of the stimulus. Logically, this task can most easily be accomplished by expression of chemosensory receptors in non-neural tissues, rather than independent development of additional receptors. Indeed, chemosensory receptors have been described in multiple 'non-canonical' organ systems as detectors of toxins or nutrients.

Nutrient-Sensing Olfactory receptors

Olfactory receptor expression has been reported in numerous tissues outside the nasal epithelium. These extra-nasal tissues include multiple types of non-olfactory neurons, the spleen, colon, brainstem, and prostate (Blache et al., 1998; Raming et al., 1998; Conzelmann et al., 2000; Yuan et al., 2001). Deep Sequencing of 16 assorted tissues (Fig 1.1) showed heterogeneous olfactory receptor expression in all samples (Flegel et al., 2013). Components of canonical olfactory receptor signaling, such as $G_{\alpha_{olf}}$ and adenylyl cyclase III, have been described in the pancreas (Regnauld et al., 2002) and placenta (Itakura et al., 2006). Ectopic expression is so widespread and heterogeneous that some groups have argued that this is consistent with a neutral model of selection (Feldmesser et al., 2006), suggesting ectopic receptors are not functional.

However, other groups have countered that a subset of ectopic olfactory receptors are conserved between species, suggesting a functional significance (De la Cruz et al., 2009).

In 2003, Spehr *et al* presented the first data supporting a functional role for ectopic olfactory receptor expression. In this report, they described the expression and activity of olfactory receptor hOR17-4 in human sperm (Spehr et al., 2003). The receptor was specifically stimulated by bourgeonal, an odorant used in perfumery for its resemblance to lily of the valley. Bourgeonal stimulation in human sperm resulted in dose-dependent calcium flux, as observed in nasal olfactory receptors, along with chemotaxis and increased swimming speed. It has been hypothesized, but not demonstrated, that the olfactory-aided chemosensing ability of sperm cells facilitates locating the egg, which might produce chemoattractant ligands. An additional report of functional ectopic olfactory receptors showed the expression of six olfactory receptors, $G_{\alpha_{olf}}$, and adenylate cyclase III in ciliated cells of the renal tubule (Pluznick et al., 2009). This group hypothesized that a filtering organ such as the kidney might utilize the vast capacity of olfactory receptors for chemical identification. They demonstrated that mice lacking adenylate cyclase III, an enzyme required for canonical olfaction, have reduced glomerular filtration rates. However, they failed to show olfactory receptor activation or the existence of odorants within renal tubules. Although reports demonstrating ectopic olfactory receptor expression are more numerous than those demonstrating ectopic olfactory receptor function, these receptors nonetheless remain an enticing target for pharmacological and physiological study.

Nutrient-Sensing Taste Receptors

Taste receptors are charged with providing a measure of the nutrient density of food. Sweet taste receptors in particular detect simple sugars, some complex carbohydrates, and more recently, artificial sweeteners. Umami, or 'savory' receptors, bind to amino acids as cognate ligands and serve as protein

sensors. Both of these receptors, particularly sweet taste receptors, evoke hedonistic neural pathways and reward systems and promote a positive association and desire for more nutrient-rich food. Bitter taste receptors, on the other hand, are sensitive to a large catalogue of structurally diverse bitter compounds, such as quinine or strychnine, often associated with toxins in plant material (Chandrashekar et al., 2006). While the sensations of reward or avoidance evoked by these receptors are quite divergent, all are expressed and have been functionally characterized outside of the gustatory system.

Bitter taste receptors represent the largest family of taste receptors, the T2Rs, with at least 25 members in humans (Behrens et al., 2009). In the gustatory system they function largely to prevent ingestion of toxic substances; a similar role exists in several other organ systems, including the upper respiratory tract, trachea, and gut (Lee et al., 2012; Deshpande et al., 2010; Jeon et al., 2008). In the respiratory tract, T2R activation results in bronchodilation in response to inhalation of bitterants (Lee et al., 2012; Deshpande et al., 2010). In the hormone-secreting enteroendocrine cell of the gut, activation of bitter taste receptors stimulates cholecystokinin (CCK) secretion (Masuho et al., 2005) in a SREBP-2 dependent manner (Jeon et al., 2008). CCK functions to slow gastric emptying and increase efficiency of fat absorption, while SREBP-2 activity is regulated by cholesterol intake. Bitter taste receptor mT2R138 was also shown to be an SREBP-2 target gene, and the plant-based diets that more often accompany bitter tastants are also low in cholesterol and fat. Taken together, these data suggest that SREBP-2 might 'prime' the gut during a low cholesterol diet by driving expression of mT2R128 to intercept plant-based toxins, which would also stimulate CCK secretion to slow gastric emptying and increase fat absorption.

Umami receptors elicit a savory response in the tongue by binding to amino acids and thereby providing neural cues for high dietary protein content. This receptor consists of a heterodimer of proteins from the T1R family, T1R1

and T1R3 (Zhao et al., 2003). However, recent work has demonstrated that these receptors also sense extracellular amino acids in muscle tissue (Wauson et al., 2012). In this model, amino acids activate T1R1/T1R3 on multiple types of muscle cells and integrate this signal to mTORC1; when T1R1 or T1R3 expression is depleted, mTORC1's sensitivity to amino acids is reduced and autophagy is stimulated. These results were further expanded to show that mice lacking T1R3 have increased autophagy in heart, skeletal muscle, and liver when fasted. Interestingly, the authors also demonstrated a role for amino acid sensing in β cell insulin secretion: loss of T1R3 from MIN6 cells resulted in decreased insulin content and secretion, possibly due to reduced mTORC1-stimulated translation. Lastly, a role of amino acid sensing by taste receptors has also been proposed in the gut. Here, application of glutamate to perfused rat jejunum resulted in activation of canonical taste signal transduction mechanisms and increased peptide absorption (Mace et al., 2009).

Like bitter and umami taste receptors, metabolic roles for sweet taste receptors have also been described. The sweet taste receptor is similar to umami, with the exception that T1R3 heterodimerizes with T1R family protein T1R2 rather than T1R1 (Nelson et al., 2001). The T1R3 subunit is therefore necessary for both sweet and umami taste. An early description of functional sweet taste receptors outside the gustatory system was by Mace *et al* in 2007. In this report, the investigators described expression of sweet taste receptors and multiple gustatory signal transduction components in the rat jejunum, where artificial sweetener perfusion increased apical translocation of GLUT2 to stimulate glucose absorption (Mace et al., 2007). Subsequent reports have shown that sweet taste receptors are expressed in the hormone-secreting enteroendocrine cells of the gut, where their activation stimulates secretion of the incretin hormone GLP-1. Studies conducted in animals deficient in sweet taste receptors or some sweet taste receptor signaling mechanisms have shown abrogated sweetener-stimulated incretin secretion (Kokrashvili et al., 2009; Jang et al., 2007). However, human studies have shown conflicting results (Brown et

al., 2009; Fujita et al., 2009; Ma et al., 2009), with the majority showing no effect of artificial sweeteners on incretin secretion (Brown et al., 2009). Another recent demonstration of metabolically functioning sweet taste receptors has been in the pancreas; artificial sweeteners stimulated insulin release in MIN6 cells and isolated β cells in a calcium and cAMP-dependent manner (Nakagawa et al., 2009). This result has been expanded *in vivo* to suggest that an active ligand of pancreatic sweet taste receptors is actually fructose, and sweet taste receptor knockout mice have ablated pancreatic fructose responses (Kyriazis et al., 2012).

Sweet taste receptor biology

Perception of sweet tastants is initiated on the tongue by binding of specific carbohydrate molecules, including glucose, sucrose, fructose to the sweet taste receptor. Sweet receptor ligands can also include artificial sweeteners such as saccharin and acesulfame potassium, sweet proteins such as brazzein, or inhibitors such as lactisole. These receptor ligands bind to a heterodimer of T1R2 and T1R3 (Nelson et al., 2001), two receptors that, along with T1R1, make up the T1R family of GPCRs. T1R2 heterodimerizes with T1R3 to form a maximally functional sweet taste receptor, though there is some evidence for T1R2 and T1R3 having independent activity (see below). Ligand binding to T1R2 occurs primarily, but not exclusively, in the large extracellular Venus Fly Trap domain of T1R2. However, binding can also occur in the transmembrane and cysteine rich domains of T1R3 (Fig 1.2, Assadi-Porter et al., 2010). Studies indicate that there are no conserved residues in the binding domain of T1R2 that are necessary for binding all ligands; different sugars, and particularly artificial sweeteners, have different structural binding requirements. (Cui et al., 2006; Masuda et al., 2012). A lack of conservation of binding mechanisms is logical in the case of artificial sweeteners, which were developed very recently with no evolutionary selective pressure. There is also significant inter-species variability in sweet taste perception; mice are insensitive to aspartame and cyclamate, two widely used sweeteners in humans, while cats,

dolphins, and several other exclusive carnivores have pseudogenized sweet taste receptors (Jiang et al., 2012).

Sweet taste receptor signaling

While much work has been done to characterize sweet taste receptor signal transduction, some fundamental questions in the field remain unanswered. Immediately downstream of ligand binding, sweet taste receptors have been proposed to couple to gustducin, a G protein closely related to transducin that promotes the breakdown of cAMP. Gustducin knockout mice have reduced, but not completely ablated, sensitivity to sweeteners (Wong et al., 1996; Danilova et al., 2006). This suggests that additional G proteins may contribute to signal transduction *in vivo*. In heterologous expression systems, functional coupling to $G\alpha_{i/o}$ and the concomitant decreases in cAMP concentrations have also been demonstrated with sweetener treatment (Ozeck et al., 2004; Sainz et al., 2007). Unfortunately, many mechanistic experiments are performed in heterologous overexpression systems rather than *in vivo* or *ex vivo*, adding additional limitations to data interpretation.

Downstream of G proteins, *in vitro* data is more consistent between different laboratories. In lingual cells, $G\beta\gamma$ activates phospholipase $C\beta_2$ to produce IP3 and diacylglycerol. IP3 binding to endoplasmic reticulum receptors produces calcium transients and leads to gating of the transient receptor potential protein TRPM5. Accordingly, mice deficient in PLC β_2 , the IP3 receptor, or TRPM5 have impaired, but not completely ablated, taste sensitivities (Hisatsune et al., 2007; Damak et al., 2006; Dotson et al., 2005; Zhang et al., 2003). This mechanism also appears to be largely conserved for sweet taste receptors in non-neural cells; taste receptors in the pancreas stimulate insulin secretion in a PLC β_2 -dependent manner, and taste receptor activation in virtually all ectopic systems generates calcium transients (Nakagawa et al., 2009; Mace et al., 2007; Rozengurt et al., 2006; Wauson et al., 2012).

Although most evidence suggests that T1R2 and T1R3 function as obligate heterodimers, there are some indications that these receptors might function as homodimers or that additional carbohydrate receptors exist. Firstly, the N-terminal domains of T1R2 and T1R3 have been shown to homodimerize in inclusion bodies, and change conformation in response to ligands (Maitrepierre et al., ;Nie et al, 2006). T1R2 and T1R3 have distinct affinities for different sweeteners (Nie et al., 2005). Additionally, neither T1R2 nor T1R3 knockout mice have a complete loss of sweet taste sensitivity (Delay et al., 2006; Treesukosol et al., 2009). Lastly, while T1R3 KO mice have impaired glucose tolerance during an oral glucose tolerance test, this phenotype is not shared with T1R2 KO animals (Geraedts et al., 2012). This data, combined with the observation that loss of signal transduction mechanisms in mice also does not result in complete loss of taste perception, suggests that there may be an alternative receptors or signaling pathways intrinsic to sweet taste detection.

Artificial sweetener consumption

Five artificial sweeteners are currently approved for use in the United States. These are saccharin (Sweet N' Low®, Sweet Twin), aspartame (Nutrasweet, Equal®), acesulfame potassium (Sweet One, Sunnet), sucralose (Splenda®) and neotame (Fig 1.3). Saccharin was the first compound developed, discovered by accident in 1878 when a Johns Hopkins University chemist licked his hand after an experiment (Myers, 2007). Similar accidental discoveries involving poor lab hygiene led to the development of aspartame in 1965 and acesulfame potassium (AceK) in 1967. While most artificial sweeteners are available in individual packets for consumer use, many are also used in diet beverage formulations. Concentrations and identities of sweeteners used in a given beverage will vary with time, logistics, public opinion and preference. Beverage distributors will commonly follow different formulations for bottled versus fountain drinks. Tab® remains one of the few brands widely utilizing saccharin in its diet formulas, while aspartame holds the largest market share with many distributors. AceK is primarily used in conjunction with other

sweeteners, while neotame, the newest product on the market, has relatively little consumer exposure. All five sweeteners have an FDA-recommended maximum daily intake (Fig 1.3) (Kroger et al., 2006).

Effects of artificial sweetener consumption on metabolism

As recent increases in obesity rates occurred in conjunction with the rise in artificial sweetener usage, many studies have investigated a possible link between obesity and artificial sweetener intake. Paranoia surrounding artificial sweetener usage has resulted in erroneous correlations at various times with breast cancer, post-traumatic stress disorder, lupus, and global warming (conspiracritic7, 2013). Controversy around artificial sweeteners and obesity may have begun with a 1986 study showing increased appetite after drinking aspartame-sweetened water relative to plain water (Blundell et al., 1986). This study was among the first to suggest that an 'uncoupling' between taste perception and food intake might have metabolic consequences. However, multiple studies have failed to repeat this observation or show any increase in food intake following artificial sweetener consumption (Rodin et al., 1990; Mattes et al., 1990; Canty et al., 1991). A 2005 study made a stir when it suggested that diet soda consumption was a predictor of obesity (Dergance et al., 2005). However, the cause and effect of this relationship has not been determined, as people who are already overweight may be more likely to favor diet beverages. Still other studies suggest that aspartame consumption may aid in weight loss (Blackburn et al., 1997) or have no effect (Porikos et al., 1977). In the case of aspartame, meta-analysis suggests that reasonable artificial sweetener consumption is associated with a lower body weight (de la Hunty et al., 2006), and dietary societies have endorsed their use (Fitch et al., 2012).

Although data from human studies indicates that artificial sweetener consumption has no effect on glucose homeostasis, insulin or GLP-1 secretion, animal models suggest strong taste receptor effects through the gut and pancreas. Similarly, while few studies have repeatable data demonstrating

weight gain associated with artificial sweetener use, some laboratories have observed this effect in rats. In one study, rats fed a saccharin-supplemented diet showed a greater increase in body weight over rats on a control diet (Swithers et al., 2008). The same group extrapolated these results to show that mice that had previously been exposed to saccharin had impaired glucose tolerance (Swithers et al., 2012). These discrepancies within and between model systems concerning effects of artificial sweeteners on metabolic systems emphasize the need for further study of these widely consumed compounds.

Model: Sweet taste receptors act as nutrient sensors in adipose tissue

During my doctoral research, I have investigated sweet taste receptor activity in adipose tissue. This was initiated based upon three lines of evidence: 1), Adipose tissue is known to utilize nutrient-sensing GPCRs; 2), Sweet taste receptors have been shown to act as carbohydrate sensors in other metabolic tissues; and 3), Preliminary data indicated expression of chemosensory receptors in adipose tissue (see Chapter 2). We reasoned that as a positive nutrient sensor, sweet taste receptor activation might stimulate adipogenesis and anabolic processes such as lipogenesis, while suppressing catabolic processes, such as lipolysis (Fig 1.4). We aimed to address these questions both *in vitro* (Chapter 2) and *in vivo* (Chapter 3) using gain-of-function and loss-of-function approaches. The completion of this study represents a thorough investigation of a novel aspect of adipocyte biology; characterizes previously unknown phenotypes stimulated by artificial sweetener treatment in adipose tissue; and perhaps most importantly, presents evidence for a previously unrecognized saccharin-binding receptor.

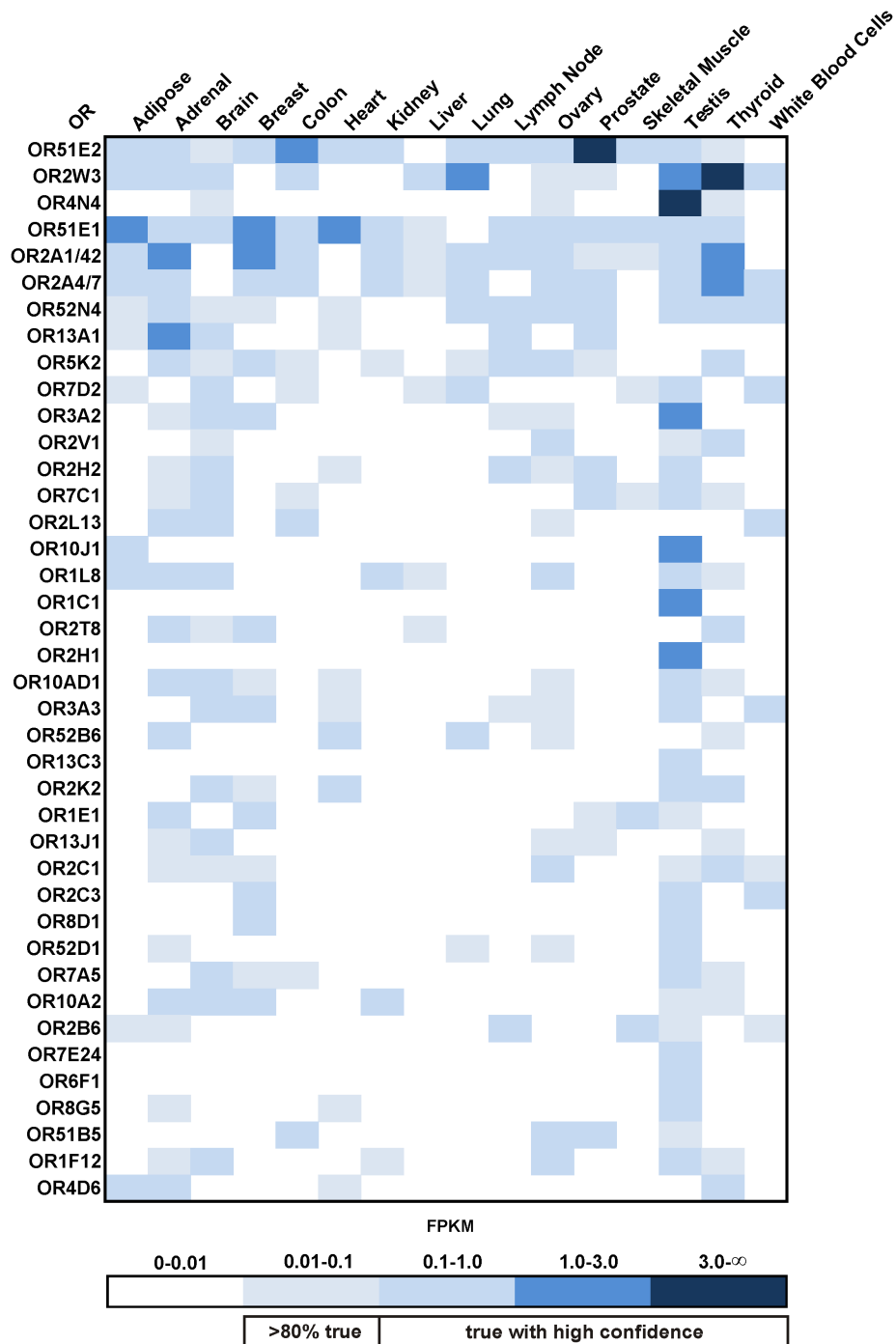


Figure 1.1. Ectopic olfactory receptor expression.

Adapted from (Flegel et al., 2013) Sixteen different human tissues (upper labels) were submitted to Deep Sequencing for assessment of olfactory receptor expression. The heat map (lower panel) indicates which olfactory receptors are expressed with what degree of confidence. Expression of multiple receptors was confirmed in all tested tissues, with the most ubiquitous expression in the testes.

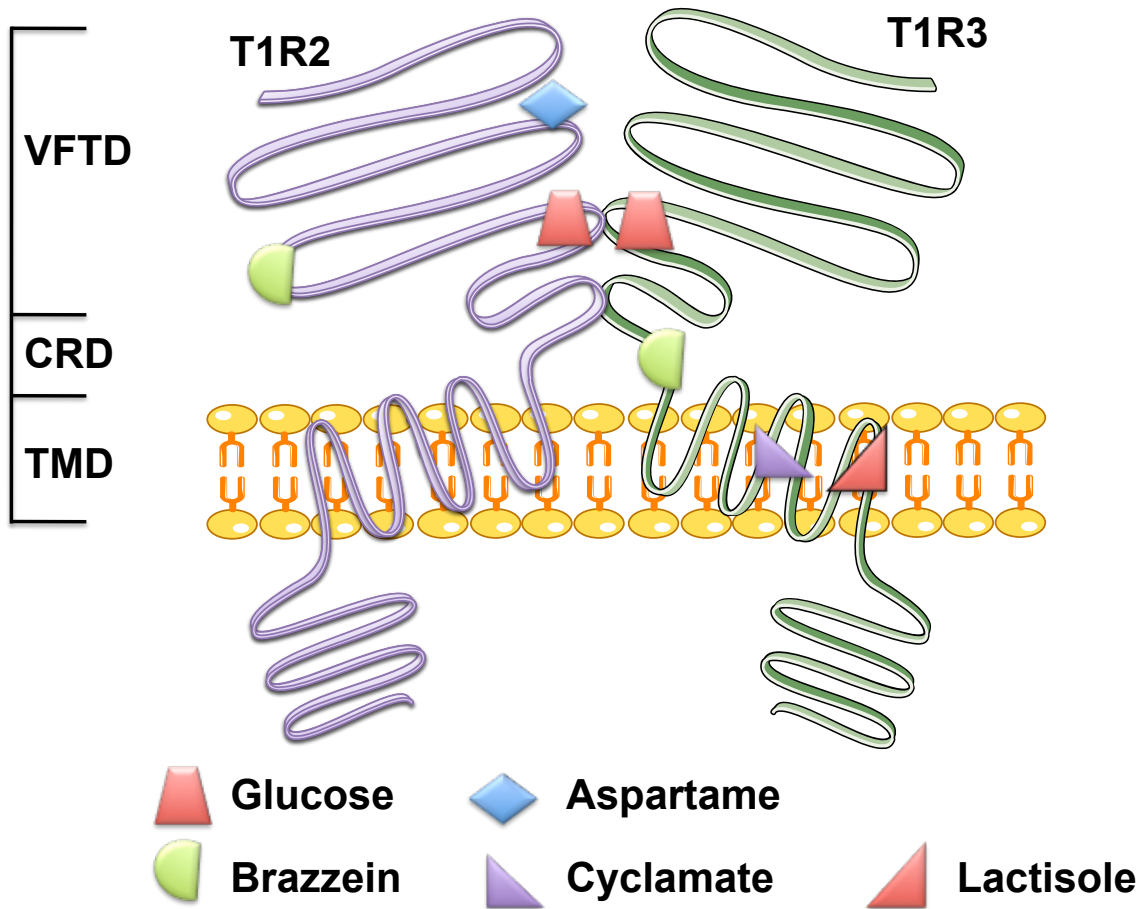


Figure 1.2. Human sweet taste receptors.

Human sweet taste receptors consist of a heterodimer of GPCRs T1R2 and T1R3. Though some ligands bind exclusively to one receptor (aspartame, cyclamate, lactisole), others are capable of binding to either (glucose, brazzein). VFTD, Venus Fly Trap Domain; CRD, cystein-rich domain; TMD, transmembrane domain. The large losses in taste sensitivity in both T1R2 and T1R3 KO mice suggest that the T1R2/T1R3 heterodimer is necessary for maximal receptor function, though several groups have reported homodimer activity.

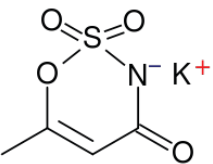
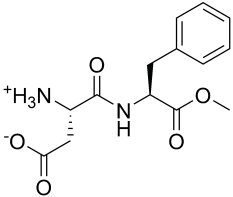
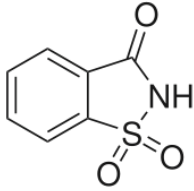
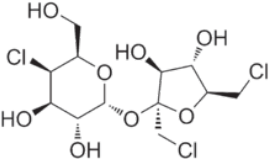
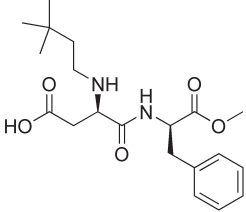
Sweetener	Structure	Sweetness (relative to sucrose)	Accepted Daily Intake (mg/kg body weight/day)	Equivalent Intake
Ace K		200x	15	6 cans diet soda
Aspartame		200x	50	18-19 cans diet soda
Saccharin		300x	5	9-12 sweetener packets
Sucralose		600x	5	6 cans diet soda
Neotame		10,000x	18	NA

Figure 1.3. FDA-approved artificial sweeteners and recommended intake.

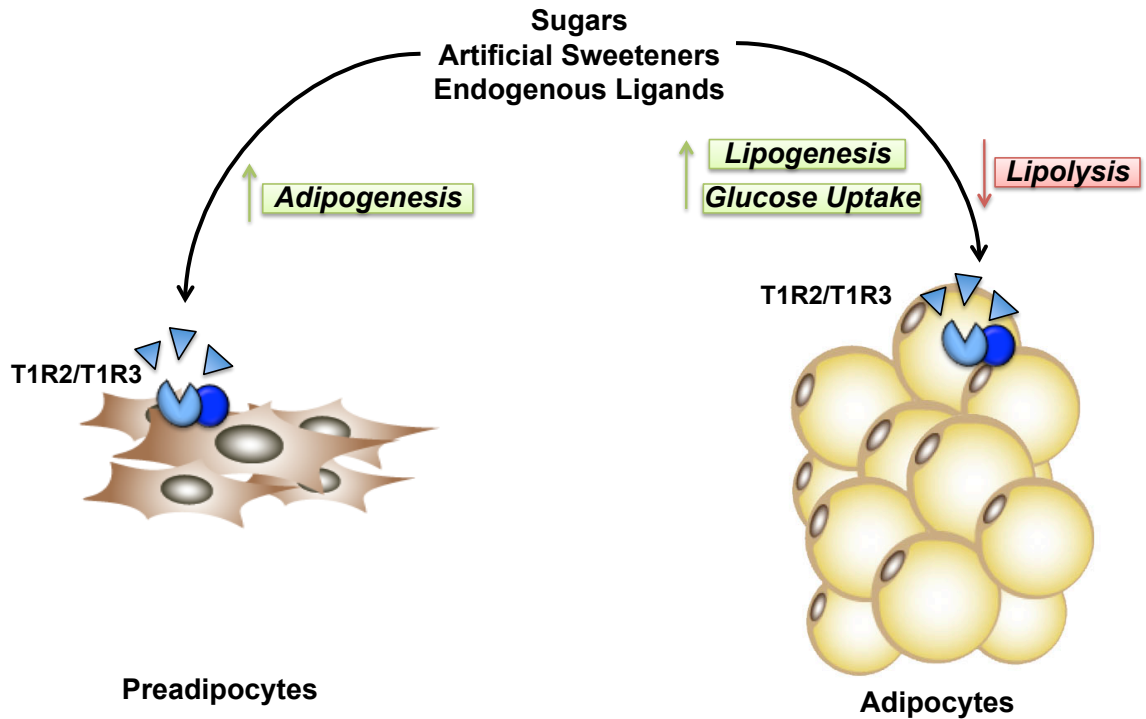


Figure 1.4. Proposed role for sweet taste receptors and artificial sweeteners in adipogenesis and adipocyte metabolism.

We hypothesize that sweet taste receptor activation in preadipocytes stimulates adipogenesis, in accordance with a role as a positive nutrient sensor, and promotes reciprocal regulation of anabolic and catabolic processes in mature adipocytes. These anabolic pathways might include lipogenesis and glucose uptake, which we predict would be stimulated by sweet taste receptor activity. Conversely, lipolysis is a catabolic process that might be inhibited by local carbohydrate sensing. In preadipocytes, we hypothesize that artificial sweetener treatment will enhance adipogenesis in a sweet taste receptor-dependent manner.

References

- Ahmed, K., Tunaru, S., and Offermanns, S. (2009). GPR109A, GPR109B and GPR81, a family of hydroxy-carboxylic acid receptors. *Trends Pharmacol Sci* 30, 557-562.
- Assadi-Porter, FM., Tonelli M., Mailliet E.L., Markley J.L., Max M. (2010). Interactions between the human sweet-sensing T1R2-T1R3 receptor and sweeteners detected by saturation transfer difference NMR spectroscopy. *Biochim Biophys Acta.* 2, 82-86.
- Banerjee, S.S., Feinberg, M.W., Watanabe, M., Gray, S., Haspel, R.L., Denkinger, D.J., Kawahara, R., Hauner, H., and Jain, M.K. (2003). The Kruppel-like factor KLF2 inhibits peroxisome proliferator-activated receptor-gamma expression and adipogenesis. *J Biol Chem* 278, 2581-2584.
- Behrens, M., and Meyerhof, W. (2009). Mammalian bitter taste perception. *Results Probl Cell Differ* 47, 203-220.
- Bertrand, H.A., Masoro, E.J., and Yu, B.P. (1978). Increasing adipocyte number as the basis for perirenal depot growth in adult rats. *Science* 201, 1234-1235.
- Bevan, P. (2001). Insulin signalling. *J Cell Sci* 114, 1429-1430.
- Blache, P., Gros, L., Salazar, G., and Bataille, D. (1998). Cloning and tissue distribution of a new rat olfactory receptor-like (OL2). *Biochem Biophys Res Commun* 242, 669-672.
- Blackburn, G.L., Kandors, B.S., Lavin, P.T., Keller, S.D., and Whatley, J. (1997). The effect of aspartame as part of a multidisciplinary weight-control program on short- and long-term control of body weight. *Am J Clin Nutr* 65, 409-418.
- Blundell, J.E., and Hill, A.J. (1986). Paradoxical effects of an intense sweetener (aspartame) on appetite. *Lancet* 1, 1092-1093.
- Bost, F., Aouadi, M., Caron, L., Even, P., Belmonte, N., Prot, M., Dani, C., Hofman, P., Pages, G., Pouyssegur, J., *et al.* (2005). The extracellular signal-regulated kinase isoform ERK1 is specifically required for in vitro and in vivo adipogenesis. *Diabetes* 54, 402-411.

Brown, A.J., Goldsworthy, S.M., Barnes, A.A., Eilert, M.M., Tcheang, L., Daniels, D., Muir, A.I., Wigglesworth, M.J., Kinghorn, I., Fraser, N.J., *et al.* (2003). The Orphan G protein-coupled receptors GPR41 and GPR43 are activated by propionate and other short chain carboxylic acids. *J Biol Chem* 278, 11312-11319.

Brown, R.J., and Rother, K.I. Non-nutritive sweeteners and their role in the gastrointestinal tract. *J Clin Endocrinol Metab* 97, 2597-2605.

Brown, R.J., Walter, M., and Rother, K.I. (2009). Ingestion of diet soda before a glucose load augments glucagon-like peptide-1 secretion. *Diabetes Care* 32, 2184-2186.

Cai, T.Q., Ren, N., Jin, L., Cheng, K., Kash, S., Chen, R., Wright, S.D., Taggart, A.K., and Waters, M.G. (2008). Role of GPR81 in lactate-mediated reduction of adipose lipolysis. *Biochem Biophys Res Commun* 377, 987-991.

Campbell, P.J., Carlson, M.G., Hill, J.O., and Nurjhan, N. (1992). Regulation of free fatty acid metabolism by insulin in humans: role of lipolysis and reesterification. *Am J Physiol* 263, E1063-1069.

Canty, D.J., and Chan, M.M. (1991). Effects of consumption of caloric vs noncaloric sweet drinks on indices of hunger and food consumption in normal adults. *Am J Clin Nutr* 53, 1159-1164.

Cao, Z., Umek, R.M., and McKnight, S.L. (1991). Regulated expression of three C/EBP isoforms during adipose conversion of 3T3-L1 cells. *Genes Dev* 5, 1538-1552.

Chandrashekar, J., Hoon, M.A., Ryba, N.J., and Zuker, C.S. (2006). The receptors and cells for mammalian taste. *Nature* 444, 288-294.

conspiracritic7 (2013). 'A critical look at the greatest conspiracies of our lifetime'. Crazy People On the Internet.

Conzelmann, S., Levai, O., Bode, B., Eisel, U., Raming, K., Breer, H., and Strotmann, J. (2000). A novel brain receptor is expressed in a distinct population of olfactory sensory neurons. *Eur J Neurosci* 12, 3926-3934.

Cousin, W., Fontaine, C., Dani, C., and Peraldi, P. (2007). Hedgehog and adipogenesis: fat and fiction. *Biochimie* 89, 1447-1453.

Cui, M., Jiang, P., Maillet, E., Max, M., Margolskee, R.F., and Osman, R. (2006). The heterodimeric sweet taste receptor has multiple potential ligand binding sites. *Curr Pharm Des* 12, 4591-4600.

Cypess, A.M., Zhang, H., Schulz, T.J., Huang, T.L., Espinoza, D.O., Kristiansen, K., Unterman, T.G., and Tseng, Y.H. Insulin/IGF-I regulation of necdin and brown adipocyte differentiation via CREB- and FoxO1-associated pathways. *Endocrinology* 152, 3680-3689.

Damak, S., Rong, M., Yasumatsu, K., Kokrashvili, Z., Perez, C.A., Shigemura, N., Yoshida, R., Mosinger, B., Jr., Glendinning, J.I., Ninomiya, Y., *et al.* (2006). Trpm5 null mice respond to bitter, sweet, and umami compounds. *Chem Senses* 31, 253-264.

Danilova, V., Damak, S., Margolskee, R.F., and Hellekant, G. (2006). Taste responses to sweet stimuli in alpha-gustducin knockout and wild-type mice. *Chem Senses* 31, 573-580.

Daval, M., Foufelle, F., and Ferre, P. (2006). Functions of AMP-activated protein kinase in adipose tissue. *J Physiol* 574, 55-62.

De la Cruz, O., Blekhman, R., Zhang, X., Nicolae, D., Firestein, S., and Gilad, Y. (2009). A signature of evolutionary constraint on a subset of ectopically expressed olfactory receptor genes. *Mol Biol Evol* 26, 491-494.

de la Hunty, A., Gibson, S., Ashwell, M. (2006). A review of the effectiveness of aspartame in helping with weight control. *British Nutritional Foundation Nutritional Bulletin* 31, 115-128.

Delay, E.R., Hernandez, N.P., Bromley, K., and Margolskee, R.F. (2006). Sucrose and monosodium glutamate taste thresholds and discrimination ability of T1R3 knockout mice. *Chem Senses* 31, 351-357.

Dergance, J.M., Mouton, C.P., Lichtenstein, M.J., and Hazuda, H.P. (2005). Potential mediators of ethnic differences in physical activity in older Mexican Americans and European Americans: results from the San Antonio Longitudinal Study of Aging. *J Am Geriatr Soc* 53, 1240-1247.

Deshpande, D.A., Wang, W.C., McIlmoyle, E.L., Robinett, K.S., Schillinger, R.M., An, S.S., Sham, J.S., and Liggett, S.B. Bitter taste receptors on airway smooth

muscle bronchodilate by localized calcium signaling and reverse obstruction. *Nat Med* 16, 1299-1304.

Dotson, C.D., Roper, S.D., and Spector, A.C. (2005). PLCbeta2-independent behavioral avoidance of prototypical bitter-tasting ligands. *Chem Senses* 30, 593-600.

Duncan, R.E., Ahmadian, M., Jaworski, K., Sarkadi-Nagy, E., and Sul, H.S. (2007). Regulation of lipolysis in adipocytes. *Annu Rev Nutr* 27, 79-101.

Enoksson, S., Degerman, E., Hagstrom-Toft, E., Large, V., and Arner, P. (1998). Various phosphodiesterase subtypes mediate the in vivo antilipolytic effect of insulin on adipose tissue and skeletal muscle in man. *Diabetologia* 41, 560-568.

Feldmesser, E., Olender, T., Khen, M., Yanai, I., Ophir, R., and Lancet, D. (2006). Widespread ectopic expression of olfactory receptor genes. *BMC Genomics* 7, 121.

Fitch, C., and Keim, K.S. Position of the Academy of Nutrition and Dietetics: use of nutritive and nonnutritive sweeteners. *J Acad Nutr Diet* 112, 739-758.

Flegel, C., Manteniotis, S., Osthold, S., Hatt, H., and Gisselmann, G. Expression profile of ectopic olfactory receptors determined by deep sequencing. *PLoS One* 8, e55368.

Frerichs, H., and Ball, E.G. (1962). Studies on the metabolism of adipose tissue. XI. Activation of phosphorylase by agents which stimulate lipolysis. *Biochemistry* 1, 501-509.

Freytag, S.O., Paielli, D.L., and Gilbert, J.D. (1994). Ectopic expression of the CCAAT/enhancer-binding protein alpha promotes the adipogenic program in a variety of mouse fibroblastic cells. *Genes Dev* 8, 1654-1663.

Fujita, Y., Wideman, R.D., Speck, M., Asadi, A., King, D.S., Webber, T.D., Haneda, M., and Kieffer, T.J. (2009). Incretin release from gut is acutely enhanced by sugar but not by sweeteners in vivo. *Am J Physiol Endocrinol Metab* 296, E473-479.

Gawronska-Kozak, B., Manuel, J.A., and Prpic, V. (2007). Ear mesenchymal stem cells (EMSC) can differentiate into spontaneously contracting muscle cells. *J Cell Biochem* 102, 122-135.

Ge, H., Li, X., Weiszmann, J., Wang, P., Baribault, H., Chen, J.L., Tian, H., and Li, Y. (2008a). Activation of G protein-coupled receptor 43 in adipocytes leads to inhibition of lipolysis and suppression of plasma free fatty acids. *Endocrinology* **149**, 4519-4526.

Ge, H., Weiszmann, J., Reagan, J.D., Gupte, J., Baribault, H., Gyuris, T., Chen, J.L., Tian, H., and Li, Y. (2008b). Elucidation of signaling and functional activities of an orphan GPCR, GPR81. *J Lipid Res* **49**, 797-803.

Geraedts, M.C., Takahashi, T., Vignes, S., Markwardt, M.L., Nkobena, A., Cockerham, R.E., Hajnal, A., Dotson, C.D., Rizzo, M.A., and Munger, S.D. Transformation of postingestive glucose responses after deletion of sweet taste receptor subunits or gastric bypass surgery. *Am J Physiol Endocrinol Metab* **303**, E464-474.

Gonzalez, G.A., and Montminy, M.R. (1989). Cyclic AMP stimulates somatostatin gene transcription by phosphorylation of CREB at serine 133. *Cell* **59**, 675-680.

Gotoh, C., Hong, Y.H., Iga, T., Hishikawa, D., Suzuki, Y., Song, S.H., Choi, K.C., Adachi, T., Hirasawa, A., Tsujimoto, G., *et al.* (2007). The regulation of adipogenesis through GPR120. *Biochem Biophys Res Commun* **354**, 591-597.

Granneman, J.G., and Moore, H.P. (2008). Location, location: protein trafficking and lipolysis in adipocytes. *Trends Endocrinol Metab* **19**, 3-9.

Green, H., and Kehinde, O. (1975). An established preadipose cell line and its differentiation in culture. II. Factors affecting the adipose conversion. *Cell* **5**, 19-27.

Green, H., and Meuth, M. (1974). An established pre-adipose cell line and its differentiation in culture. *Cell* **3**, 127-133.

Haemmerle, G., Zimmermann, R., Hayn, M., Theussl, C., Waeg, G., Wagner, E., Sattler, W., Magin, T.M., Wagner, E.F., and Zechner, R. (2002a). Hormone-sensitive lipase deficiency in mice causes diglyceride accumulation in adipose tissue, muscle, and testis. *J Biol Chem* **277**, 4806-4815.

Haemmerle, G., Zimmermann, R., Strauss, J.G., Kratky, D., Riederer, M., Knipping, G., and Zechner, R. (2002b). Hormone-sensitive lipase deficiency in mice changes the plasma lipid profile by affecting the tissue-specific expression

pattern of lipoprotein lipase in adipose tissue and muscle. *J Biol Chem* 277, 12946-12952.

Halaas, J.L., Gajiwala, K.S., Maffei, M., Cohen, S.L., Chait, B.T., Rabinowitz, D., Lallone, R.L., Burley, S.K., and Friedman, J.M. (1995). Weight-reducing effects of the plasma protein encoded by the obese gene. *Science* 269, 543-546.

Hellman, B., and Hellerstrom, C. (1961). Cell renewal in the white and brown fat tissue of the rat. *Acta Pathol Microbiol Scand* 51, 347-353.

Hirsch, J., and Han, P.W. (1969). Cellularity of rat adipose tissue: effects of growth, starvation, and obesity. *J Lipid Res* 10, 77-82.

Hisatsune, C., Yasumatsu, K., Takahashi-Iwanaga, H., Ogawa, N., Kuroda, Y., Yoshida, R., Ninomiya, Y., and Mikoshiba, K. (2007). Abnormal taste perception in mice lacking the type 3 inositol 1,4,5-trisphosphate receptor. *J Biol Chem* 282, 37225-37231.

Hong, Y.H., Nishimura, Y., Hishikawa, D., Tsuzuki, H., Miyahara, H., Gotoh, C., Choi, K.C., Feng, D.D., Chen, C., Lee, H.G., *et al.* (2005). Acetate and propionate short chain fatty acids stimulate adipogenesis via GPCR43. *Endocrinology* 146, 5092-5099.

Hu, E., Kim, J.B., Sarraf, P., and Spiegelman, B.M. (1996). Inhibition of adipogenesis through MAP kinase-mediated phosphorylation of PPARgamma. *Science* 274, 2100-2103.

Ichimura, A., Hirasawa, A., Poulain-Godefroy, O., Bonnefond, A., Hara, T., Yengo, L., Kimura, I., Leloire, A., Liu, N., Iida, K., *et al.* Dysfunction of lipid sensor GPR120 leads to obesity in both mouse and human. *Nature* 483, 350-354.

Imai, T., Takakuwa, R., Marchand, S., Dentz, E., Bornert, J.M., Messaddeq, N., Wendling, O., Mark, M., Desvergne, B., Wahli, W., *et al.* (2004). Peroxisome proliferator-activated receptor gamma is required in mature white and brown adipocytes for their survival in the mouse. *Proc Natl Acad Sci U S A* 101, 4543-4547.

Itakura, S., Ohno, K., Ueki, T., Sato, K., and Kanayama, N. (2006). Expression of Golf in the rat placenta: Possible implication in olfactory receptor transduction. *Placenta* 27, 103-108.

Jang, H.J., Kokrashvili, Z., Theodorakis, M.J., Carlson, O.D., Kim, B.J., Zhou, J., Kim, H.H., Xu, X., Chan, S.L., Juhaszova, M., *et al.* (2007). Gut-expressed gustducin and taste receptors regulate secretion of glucagon-like peptide-1. *Proc Natl Acad Sci U S A* *104*, 15069-15074.

Jeninga, E.H., Bugge, A., Nielsen, R., Kersten, S., Hamers, N., Dani, C., Wabitsch, M., Berger, R., Stunnenberg, H.G., Mandrup, S., *et al.* (2009). Peroxisome proliferator-activated receptor gamma regulates expression of the anti-lipolytic G-protein-coupled receptor 81 (GPR81/Gpr81). *J Biol Chem* *284*, 26385-26393.

Jenkins, C.M., Mancuso, D.J., Yan, W., Sims, H.F., Gibson, B., and Gross, R.W. (2004). Identification, cloning, expression, and purification of three novel human calcium-independent phospholipase A2 family members possessing triacylglycerol lipase and acylglycerol transacylase activities. *J Biol Chem* *279*, 48968-48975.

Jeon, T.I., Zhu, B., Larson, J.L., and Osborne, T.F. (2008). SREBP-2 regulates gut peptide secretion through intestinal bitter taste receptor signaling in mice. *J Clin Invest* *118*, 3693-3700.

Jiang P, Josue J, Li X, Glaser D, Li W, Brand JG, Margolskee RF, Reed DR, Beauchamp GK. (2012). Major taste loss in carnivorous mammals. *Proc Natl Acad Sci USA*. *109*(13):4956-61.

Kalderon, B., Mayorek, N., Berry, E., Zevit, N., and Bar-Tana, J. (2000). Fatty acid cycling in the fasting rat. *Am J Physiol Endocrinol Metab* *279*, E221-227.

Kershaw, E.E., Hamm, J.K., Verhagen, L.A., Peroni, O., Katic, M., and Flier, J.S. (2006). Adipose triglyceride lipase: function, regulation by insulin, and comparison with adiponutrin. *Diabetes* *55*, 148-157.

Kitamura, T., Kitamura, Y., Kuroda, S., Hino, Y., Ando, M., Kotani, K., Konishi, H., Matsuzaki, H., Kikkawa, U., Ogawa, W., *et al.* (1999). Insulin-induced phosphorylation and activation of cyclic nucleotide phosphodiesterase 3B by the serine-threonine kinase Akt. *Mol Cell Biol* *19*, 6286-6296.

Knittle, J.L., Timmers, K., Ginsberg-Fellner, F., Brown, R.E., and Katz, D.P. (1979). The growth of adipose tissue in children and adolescents. Cross-

sectional and longitudinal studies of adipose cell number and size. *J Clin Invest* 63, 239-246.

Kokrashvili, Z., Mosinger, B., and Margolskee, R.F. (2009). T1r3 and alpha-gustducin in gut regulate secretion of glucagon-like peptide-1. *Ann N Y Acad Sci* 1170, 91-94.

Kong, A.P., Xu, G., Brown, N., So, W.Y., Ma, R.C., and Chan, J.C. Diabetes and its comorbidities-where East meets West. *Nat Rev Endocrinol*.

Kroger, M., Meiser, K., Kava, R. (2006). Low-calorie Sweeteners and Other Sugar Substitutes: A Review of Safety Issues. *Comprehensive Reviews in Food Science and Food Safety* 5, 35-47.

Kyriazis, G.A., Soundarapandian, M.M., and Tyrberg, B. Sweet taste receptor signaling in beta cells mediates fructose-induced potentiation of glucose-stimulated insulin secretion. *Proc Natl Acad Sci U S A* 109, E524-532.

Laplante, M., and Sabatini, D.M. (2009). An emerging role of mTOR in lipid biosynthesis. *Curr Biol* 19, R1046-1052.

Lass, A., Zimmermann, R., Haemmerle, G., Riederer, M., Schoiswohl, G., Schweiger, M., Kienesberger, P., Strauss, J.G., Gorkiewicz, G., and Zechner, R. (2006). Adipose triglyceride lipase-mediated lipolysis of cellular fat stores is activated by CGI-58 and defective in Chanarin-Dorfman Syndrome. *Cell Metab* 3, 309-319.

Lee, R.J., Xiong, G., Kofonow, J.M., Chen, B., Lysenko, A., Jiang, P., Abraham, V., Doghramji, L., Adappa, N.D., Palmer, J.N., *et al.* T2R38 taste receptor polymorphisms underlie susceptibility to upper respiratory infection. *J Clin Invest* 122, 4145-4159.

Linhart, H.G., Ishimura-Oka, K., DeMayo, F., Kibe, T., Repka, D., Poindexter, B., Bick, R.J., and Darlington, G.J. (2001). C/EBPalpha is required for differentiation of white, but not brown, adipose tissue. *Proc Natl Acad Sci U S A* 98, 12532-12537.

Liu, C., Wu, J., Zhu, J., Kuei, C., Yu, J., Shelton, J., Sutton, S.W., Li, X., Yun, S.J., Mirzadegan, T., *et al.* (2009). Lactate inhibits lipolysis in fat cells through

activation of an orphan G-protein-coupled receptor, GPR81. *J Biol Chem* 284, 2811-2822.

Ma, J., Bellon, M., Wishart, J.M., Young, R., Blackshaw, L.A., Jones, K.L., Horowitz, M., and Rayner, C.K. (2009). Effect of the artificial sweetener, sucralose, on gastric emptying and incretin hormone release in healthy subjects. *Am J Physiol Gastrointest Liver Physiol* 296, G735-739.

Mace, O.J., Affleck, J., Patel, N., and Kellett, G.L. (2007). Sweet taste receptors in rat small intestine stimulate glucose absorption through apical GLUT2. *J Physiol* 582, 379-392.

Mace, O.J., Lister, N., Morgan, E., Shepherd, E., Affleck, J., Helliwell, P., Bronk, J.R., Kellett, G.L., Meredith, D., Boyd, R., *et al.* (2009). An energy supply network of nutrient absorption coordinated by calcium and T1R taste receptors in rat small intestine. *J Physiol* 587, 195-210.

Magun, R., Burgering, B.M., Coffey, P.J., Pardasani, D., Lin, Y., Chabot, J., and Sorisky, A. (1996). Expression of a constitutively activated form of protein kinase B (c-Akt) in 3T3-L1 preadipose cells causes spontaneous differentiation. *Endocrinology* 137, 3590-3593.

Maitrepierre, E., Sigoillot, M., Le Pessot, L., and Briand, L. Recombinant expression, in vitro refolding, and biophysical characterization of the N-terminal domain of T1R3 taste receptor. *Protein Expr Purif* 83, 75-83.

Marcinkiewicz, A., Gauthier, D., Garcia, A., and Brasaemle, D.L. (2006). The phosphorylation of serine 492 of perilipin a directs lipid droplet fragmentation and dispersion. *J Biol Chem* 281, 11901-11909.

Masuda, K., Koizumi, A., Nakajima, K., Tanaka, T., Abe, K., Misaka, T., and Ishiguro, M. Characterization of the modes of binding between human sweet taste receptor and low-molecular-weight sweet compounds. *PLoS One* 7, e35380.

Masuh, I., Tateyama, M., and Saitoh, O. (2005). Characterization of bitter taste responses of intestinal STC-1 cells. *Chem Senses* 30, 281-290.

Mattes, R. (1990). Effects of aspartame and sucrose on hunger and energy intake in humans. *Physiol Behav* 47, 1037-1044.

Menghini, R., Marchetti, V., Cardellini, M., Hribal, M.L., Mauriello, A., Lauro, D., Sbraccia, P., Lauro, R., and Federici, M. (2005). Phosphorylation of GATA2 by Akt increases adipose tissue differentiation and reduces adipose tissue-related inflammation: a novel pathway linking obesity to atherosclerosis. *Circulation* 111, 1946-1953.

Milstein, S.W., and Hausberger, F.X. (1956). Lipogenesis and carbohydrate utilization; effects of glucose concentration and insulin in rat liver and adipose tissue. *Diabetes* 5, 89-92.

Mombaerts, P. (2004). Genes and ligands for odorant, vomeronasal and taste receptors. *Nat Rev Neurosci* 5, 263-278.

Mori, T., Sakaue, H., Iguchi, H., Gomi, H., Okada, Y., Takashima, Y., Nakamura, K., Nakamura, T., Yamauchi, T., Kubota, N., *et al.* (2005). Role of Kruppel-like factor 15 (KLF15) in transcriptional regulation of adipogenesis. *J Biol Chem* 280, 12867-12875.

Myers, R.L. (2007). *The 100 most important chemical compounds : a reference guide* (Westport, Conn., Greenwood Press).

Mynarcik, D.C., Williams, P.F., Schaffer, L., Yu, G.Q., and Whittaker, J. (1997). Identification of common ligand binding determinants of the insulin and insulin-like growth factor 1 receptors. Insights into mechanisms of ligand binding. *J Biol Chem* 272, 18650-18655.

Nagasaki, H., Kondo, T., Fuchigami, M., Hashimoto, H., Sugimura, Y., Ozaki, N., Arima, H., Ota, A., Oiso, Y., and Hamada, Y. Inflammatory changes in adipose tissue enhance expression of GPR84, a medium-chain fatty acid receptor: TNFalpha enhances GPR84 expression in adipocytes. *FEBS Lett* 586, 368-372.

Nakae, J., Kitamura, T., Kitamura, Y., Biggs, W.H., 3rd, Arden, K.C., and Accili, D. (2003). The forkhead transcription factor Foxo1 regulates adipocyte differentiation. *Dev Cell* 4, 119-129.

Nakagawa, Y., Nagasawa, M., Yamada, S., Hara, A., Mogami, H., Nikolaev, V.O., Lohse, M.J., Shigemura, N., Ninomiya, Y., and Kojima, I. (2009). Sweet taste receptor expressed in pancreatic beta-cells activates the calcium and cyclic AMP signaling systems and stimulates insulin secretion. *PLoS One* 4, e5106.

Nelson, G., Hoon, M.A., Chandrashekar, J., Zhang, Y., Ryba, N.J., and Zuker, C.S. (2001). Mammalian sweet taste receptors. *Cell* 106, 381-390.

Nie, Y., Hobbs, J.R., Vignes, S., Olson, W.J., Conn, G.L., and Munger, S.D. (2006). Expression and purification of functional ligand-binding domains of T1R3 taste receptors. *Chem Senses* 31, 505-513.

Nie, Y., Vignes, S., Hobbs, J.R., Conn, G.L., and Munger, S.D. (2005). Distinct contributions of T1R2 and T1R3 taste receptor subunits to the detection of sweet stimuli. *Curr Biol* 15, 1948-1952.

Ozeck, M., Brust, P., Xu, H., and Servant, G. (2004). Receptors for bitter, sweet and umami taste couple to inhibitory G protein signaling pathways. *Eur J Pharmacol* 489, 139-149.

Pluznick, J.L., Zou, D.J., Zhang, X., Yan, Q., Rodriguez-Gil, D.J., Eisner, C., Wells, E., Greer, C.A., Wang, T., Firestein, S., *et al.* (2009). Functional expression of the olfactory signaling system in the kidney. *Proc Natl Acad Sci U S A* 106, 2059-2064.

Porikos, K.P., Booth, G., and Van Itallie, T.B. (1977). Effect of covert nutritive dilution on the spontaneous food intake of obese individuals: a pilot study. *Am J Clin Nutr* 30, 1638-1644.

Prusty, D., Park, B.H., Davis, K.E., and Farmer, S.R. (2002). Activation of MEK/ERK signaling promotes adipogenesis by enhancing peroxisome proliferator-activated receptor gamma (PPARgamma) and C/EBPalpha gene expression during the differentiation of 3T3-L1 preadipocytes. *J Biol Chem* 277, 46226-46232.

Raming, K., Konzelmann, S., and Breer, H. (1998). Identification of a novel G-protein coupled receptor expressed in distinct brain regions and a defined olfactory zone. *Receptors Channels* 6, 141-151.

Regnauld, K.L., Leteurtre, E., Gutkind, S.J., Gespach, C.P., and Emami, S. (2002). Activation of adenylyl cyclases, regulation of insulin status, and cell survival by G(alpha)olf in pancreatic beta-cells. *Am J Physiol Regul Integr Comp Physiol* 282, R870-880.

Reusch, J.E., Colton, L.A., and Klemm, D.J. (2000). CREB activation induces adipogenesis in 3T3-L1 cells. *Mol Cell Biol* 20, 1008-1020.

Reusch, J.E., and Klemm, D.J. (2002). Inhibition of cAMP-response element-binding protein activity decreases protein kinase B/Akt expression in 3T3-L1 adipocytes and induces apoptosis. *J Biol Chem* 277, 1426-1432.

Rim, J.S., Mynatt, R.L., and Gawronska-Kozak, B. (2005). Mesenchymal stem cells from the outer ear: a novel adult stem cell model system for the study of adipogenesis. *FASEB J* 19, 1205-1207.

Rodin, J. (1990). Comparative effects of fructose, aspartame, glucose, and water preloads on calorie and macronutrient intake. *Am J Clin Nutr* 51, 428-435.

Rosen, E.D., Hsu, C.H., Wang, X., Sakai, S., Freeman, M.W., Gonzalez, F.J., and Spiegelman, B.M. (2002). C/EBPalpha induces adipogenesis through PPARgamma: a unified pathway. *Genes Dev* 16, 22-26.

Rosen, E.D., and MacDougald, O.A. (2006). Adipocyte differentiation from the inside out. *Nat Rev Mol Cell Biol* 7, 885-896.

Ross, D.A., Rao, P.K., and Kadesch, T. (2004). Dual roles for the Notch target gene Hes-1 in the differentiation of 3T3-L1 preadipocytes. *Mol Cell Biol* 24, 3505-3513.

Ross, S.E., Hemati, N., Longo, K.A., Bennett, C.N., Lucas, P.C., Erickson, R.L., and MacDougald, O.A. (2000). Inhibition of adipogenesis by Wnt signaling. *Science* 289, 950-953.

Rozengurt, N., Wu, S.V., Chen, M.C., Huang, C., Sternini, C., and Rozengurt, E. (2006). Colocalization of the alpha-subunit of gustducin with PYY and GLP-1 in L cells of human colon. *Am J Physiol Gastrointest Liver Physiol* 291, G792-802.

Rubin, C.S., Hirsch, A., Fung, C., and Rosen, O.M. (1978). Development of hormone receptors and hormonal responsiveness in vitro. Insulin receptors and insulin sensitivity in the preadipocyte and adipocyte forms of 3T3-L1 cells. *J Biol Chem* 253, 7570-7578.

Sainz, E., Cavenagh, M.M., LopezJimenez, N.D., Gutierrez, J.C., Battey, J.F., Northup, J.K., and Sullivan, S.L. (2007). The G-protein coupling properties of the human sweet and amino acid taste receptors. *Dev Neurobiol* 67, 948-959.

Saltiel, A.R., and Kahn, C.R. (2001). Insulin signalling and the regulation of glucose and lipid metabolism. *Nature* 414, 799-806.

Sarbassov, D.D., Guertin, D.A., Ali, S.M., and Sabatini, D.M. (2005). Phosphorylation and regulation of Akt/PKB by the rictor-mTOR complex. *Science* 307, 1098-1101.

Smith, P.J., Wise, L.S., Berkowitz, R., Wan, C., and Rubin, C.S. (1988). Insulin-like growth factor-I is an essential regulator of the differentiation of 3T3-L1 adipocytes. *J Biol Chem* 263, 9402-9408.

Spehr, M., Gisselmann, G., Poplawski, A., Riffell, J.A., Wetzel, C.H., Zimmer, R.K., and Hatt, H. (2003). Identification of a testicular odorant receptor mediating human sperm chemotaxis. *Science* 299, 2054-2058.

Stokoe, D., Stephens, L.R., Copeland, T., Gaffney, P.R., Reese, C.B., Painter, G.F., Holmes, A.B., McCormick, F., and Hawkins, P.T. (1997). Dual role of phosphatidylinositol-3,4,5-trisphosphate in the activation of protein kinase B. *Science* 277, 567-570.

Stralfors, P., and Honnor, R.C. (1989). Insulin-induced dephosphorylation of hormone-sensitive lipase. Correlation with lipolysis and cAMP-dependent protein kinase activity. *Eur J Biochem* 182, 379-385.

Subramanian, V., Rothenberg, A., Gomez, C., Cohen, A.W., Garcia, A., Bhattacharyya, S., Shapiro, L., Dolios, G., Wang, R., Lisanti, M.P., *et al.* (2004). Perilipin A mediates the reversible binding of CGI-58 to lipid droplets in 3T3-L1 adipocytes. *J Biol Chem* 279, 42062-42071.

Swithers, S.E., and Davidson, T.L. (2008). A role for sweet taste: calorie predictive relations in energy regulation by rats. *Behav Neurosci* 122, 161-173.

Swithers, S.E., Laboy, A.F., Clark, K., Cooper, S., and Davidson, T.L. Experience with the high-intensity sweetener saccharin impairs glucose homeostasis and GLP-1 release in rats. *Behav Brain Res* 233, 1-14.

Sztalryd, C., Xu, G., Dorward, H., Tansey, J.T., Contreras, J.A., Kimmel, A.R., and Londos, C. (2003). Perilipin A is essential for the translocation of hormone-sensitive lipase during lipolytic activation. *J Cell Biol* 161, 1093-1103.

Tamori, Y., Masugi, J., Nishino, N., and Kasuga, M. (2002). Role of peroxisome proliferator-activated receptor-gamma in maintenance of the characteristics of mature 3T3-L1 adipocytes. *Diabetes* 51, 2045-2055.

Tanaka, T., Yoshida, N., Kishimoto, T., and Akira, S. (1997). Defective adipocyte differentiation in mice lacking the C/EBPbeta and/or C/EBPdelta gene. *EMBO J* 16, 7432-7443.

Tang, Q.Q., Gronborg, M., Huang, H., Kim, J.W., Otto, T.C., Pandey, A., and Lane, M.D. (2005). Sequential phosphorylation of CCAAT enhancer-binding protein beta by MAPK and glycogen synthase kinase 3beta is required for adipogenesis. *Proc Natl Acad Sci U S A* 102, 9766-9771.

Tang, Q.Q., and Lane, M.D. (2000). Role of C/EBP homologous protein (CHOP-10) in the programmed activation of CCAAT/enhancer-binding protein-beta during adipogenesis. *Proc Natl Acad Sci U S A* 97, 12446-12450.

Tang, Q.Q., Otto, T.C., and Lane, M.D. (2003). CCAAT/enhancer-binding protein beta is required for mitotic clonal expansion during adipogenesis. *Proc Natl Acad Sci U S A* 100, 850-855.

Tansey, J.T., Sztalryd, C., Gruia-Gray, J., Roush, D.L., Zee, J.V., Gavrilova, O., Reitman, M.L., Deng, C.X., Li, C., Kimmel, A.R., *et al.* (2001). Perilipin ablation results in a lean mouse with aberrant adipocyte lipolysis, enhanced leptin production, and resistance to diet-induced obesity. *Proc Natl Acad Sci U S A* 98, 6494-6499.

Tong, Q., Dalgin, G., Xu, H., Ting, C.N., Leiden, J.M., and Hotamisligil, G.S. (2000). Function of GATA transcription factors in preadipocyte-adipocyte transition. *Science* 290, 134-138.

Tontonoz, P., Hu, E., and Spiegelman, B.M. (1994). Stimulation of adipogenesis in fibroblasts by PPAR gamma 2, a lipid-activated transcription factor. *Cell* 79, 1147-1156.

Treesukosol, Y., Blonde, G.D., and Spector, A.C. (2009). T1R2 and T1R3 subunits are individually unnecessary for normal affective licking responses to Polydose: implications for saccharide taste receptors in mice. *Am J Physiol Regul Integr Comp Physiol* 296, R855-865.

Villena, J.A., Roy, S., Sarkadi-Nagy, E., Kim, K.H., and Sul, H.S. (2004). Desnutrin, an adipocyte gene encoding a novel patatin domain-containing protein, is induced by fasting and glucocorticoids: ectopic expression of desnutrin increases triglyceride hydrolysis. *J Biol Chem* 279, 47066-47075.

Wang, S.P., Laurin, N., Himms-Hagen, J., Rudnicki, M.A., Levy, E., Robert, M.F., Pan, L., Oligny, L., and Mitchell, G.A. (2001). The adipose tissue phenotype of hormone-sensitive lipase deficiency in mice. *Obes Res* 9, 119-128.

Wauson, E.M., Zaganjor, E., Lee, A.Y., Guerra, M.L., Ghosh, A.B., Bookout, A.L., Chambers, C.P., Jivan, A., McGlynn, K., Hutchison, M.R., *et al.* The G protein-coupled taste receptor T1R1/T1R3 regulates mTORC1 and autophagy. *Mol Cell* 47, 851-862.

Winegrad, A.I., and Renold, A.E. (1958). Studies on rat adipose tissue in vitro. II. Effects of insulin on the metabolism of specifically labeled glucose. *J Biol Chem* 233, 273-276.

Wong, G.T., Gannon, K.S., and Margolskee, R.F. (1996). Transduction of bitter and sweet taste by gustducin. *Nature* 381, 796-800.

Wu, Z., Rosen, E.D., Brun, R., Hauser, S., Adelmant, G., Troy, A.E., McKeon, C., Darlington, G.J., and Spiegelman, B.M. (1999). Cross-regulation of C/EBP α and PPAR γ controls the transcriptional pathway of adipogenesis and insulin sensitivity. *Mol Cell* 3, 151-158.

Xiong, Y., Miyamoto, N., Shibata, K., Valasek, M.A., Motoike, T., Kedzierski, R.M., and Yanagisawa, M. (2004). Short-chain fatty acids stimulate leptin production in adipocytes through the G protein-coupled receptor GPR41. *Proc Natl Acad Sci U S A* 101, 1045-1050.

Yuan, T.T., Toy, P., McClary, J.A., Lin, R.J., Miyamoto, N.G., and Kretschmer, P.J. (2001). Cloning and genetic characterization of an evolutionarily conserved human olfactory receptor that is differentially expressed across species. *Gene* 278, 41-51.

Zhang, Y., Hoon, M.A., Chandrashekar, J., Mueller, K.L., Cook, B., Wu, D., Zuker, C.S., and Ryba, N.J. (2003). Coding of sweet, bitter, and umami tastes: different receptor cells sharing similar signaling pathways. *Cell* 112, 293-301.

Zhao, G.Q., Zhang, Y., Hoon, M.A., Chandrashekar, J., Erlenbach, I., Ryba, N.J., and Zuker, C.S. (2003). The receptors for mammalian sweet and umami taste. *Cell* 115, 255-266.

Zimmermann, R., Haemmerle, G., Wagner, E.M., Strauss, J.G., Kratky, D., and Zechner, R. (2003). Decreased fatty acid esterification compensates for the reduced lipolytic activity in hormone-sensitive lipase-deficient white adipose tissue. *J Lipid Res* 44, 2089-2099.

Zimmermann, R., Strauss, J.G., Haemmerle, G., Schoiswohl, G., Birner-Gruenberger, R., Riederer, M., Lass, A., Neuberger, G., Eisenhaber, F., Hermetter, A., *et al.* (2004). Fat mobilization in adipose tissue is promoted by adipose triglyceride lipase. *Science* 306, 1383-1386.

Chapter Two

Artificial Sweeteners Enhance Adipogenesis and Suppress Lipolysis Independent of Sweet Taste Receptors

Abstract

Adipogenesis is stimulated by the transcription factors PPAR γ and C/EBP α , whose activity is sufficient to form new adipocytes from mesenchymal precursor cells. However, the autocrine, paracrine, and hormonal signaling factors upstream of PPAR γ activity are less defined. GPCRs have been shown to act upstream of transcriptional activators of adipogenesis by binding fatty acids to modulate adipogenesis and adipocyte metabolism. The sweet taste receptors T1R2 and T1R3 have also been shown to act as nutrient sensors in metabolic tissues by binding carbohydrate. Here we report that sweet taste receptors are expressed in adipose tissue, and that treatment of mouse and human precursor cells with artificial sweeteners enhances adipogenesis. Saccharin treatment in 3T3-L1 cells and primary mesenchymal stem cells stimulates Akt phosphorylation and activation of its downstream targets, a probable mechanism for enhanced adipogenesis. Saccharin-stimulated Akt phosphorylation is rapid, PI3K-dependent, and occurs in the presence of high concentrations of insulin and dexamethasone. However, neither saccharin-stimulated adipogenesis nor Akt phosphorylation is dependent on the expression of T1R2 or T1R3. In mature adipocytes, artificial sweetener treatment suppresses lipolysis, concomitant with a reduction in phosphorylation of HSL. Like sweetener-stimulated adipogenesis, lipolytic regulation by saccharin is also independent of T1R2 and T1R3. These results suggest that 1) some artificial sweeteners have previously

uncharacterized metabolic effects on adipose tissue that are potentially important to human populations, and 2) T1R2 and T1R3 may not be the sole receptors sensitive to the artificial sweeteners as used in our studies.

Introduction

Adipogenesis and lipolysis are major mechanisms for the storage and release, respectively, of triacylglycerol. Proper regulation of these processes in adipose tissue is essential for maintenance of energetic homeostasis and prevention of diabetes. In conditions of nutrient excess, adipocytes differentiate from mesenchymal precursor cells to provide additional reservoirs for lipid storage. These same nutritional conditions result in reciprocal regulation of anabolic and catabolic processes in mature adipocytes to promote triglyceride accumulation. In preadipocytes, adipogenic stimulation results in the activation of transcription factors PPAR γ and C/EBP α , primary drivers of the adipogenic program that stimulate expression of terminal adipocyte genes such as FABP4 and GLUT4 (Rosen and MacDougald, 2006). However, the upstream endogenous vascular- or adipocyte-derived factor(s) that are sensed as the key signals to stimulate nutritional excess remain largely unknown. Nutritive signals may serve as such a stimulus, as has been demonstrated by fatty acids acting through GPR43 and GPR120 to promote preadipocyte differentiation *in vitro* (Gotoh et al., 2007; Hong et al., 2005). Available energy is also sensed through a similar mechanism in mature adipocytes, where GPCRs mediate effects on lipolysis of short chain fatty acids, lactate, β -hydroxybutyrate, β -hydroxyoctanoate, and succinate (Ahmed et al., 2009; Duncan et al., 2008; Liu et al., 2009; Ren et al., 2009a; Taggart et al., 2005). A hypothesis explored in this manuscript is whether nutritive signals regulating adipocyte differentiation and metabolism are also mediated in part by sweet taste receptors.

The sweet taste receptor consists of an obligate heterodimer of the GPCRs T1R2 and T1R3 (Nelson et al., 2001; Zhao et al., 2003). Sugars and

artificial sweeteners such as saccharin or AceK bind primarily to T1R2 (Xu et al., 2004), though direct binding to T1R3 has also been described (Nie et al., 2005). Originally characterized in the tongue as a mediator of saccharin preference, these receptors have subsequently been described in the brain, bladder, pancreas, and gut (Dyer et al., 2005; Elliott et al.; Nakagawa et al., 2009; Ren et al., 2009b), with metabolic roles defined in the latter two tissues. Thus, in the enteroendocrine cells of the small intestine, activation of sweet taste receptors promotes glucose uptake and release of incretin hormones such as glucagon-like peptide 1 (Jang et al., 2007; Mace et al., 2007). T1R2/T1R3 also functions in the pancreas, where its activation in β cells mediates stimulatory effect of fructose on glucose-induced insulin secretion (Kyriazis et al., 2012; Nakagawa et al., 2009).

While there have been numerous reports of sweet taste receptor activation in response to artificial sweeteners in ectopic systems, experiments in taste receptor KO animals suggest that an additional receptor(s) may be capable of binding to sweet tastants (Treesukosol et al., 2009; Zhao et al., 2003; Zukerman et al., 2009). In addition, binding of artificial sweeteners to the N-terminal domain of T1R2 or T1R3 in the absence of its dimerization partner suggests that these receptors may be capable of functioning independently (Maitrepierre et al.; Nie et al., 2006; Nie et al., 2005). While the input of T1R2/T1R3 may be important in the tongue and metabolic tissues, these studies indicate that there may be additional receptors sensitive to carbohydrates and sweeteners.

In this manuscript we report that T1R2 and T1R3 are constitutively expressed throughout adipogenesis of cultured cells and within adipose tissue. Treatment with artificial sweeteners such as saccharin or AceK stimulates adipogenesis of mouse and human precursors. Saccharin treatment also stimulates phosphorylation of Akt and its downstream effectors. However, T1R2 and T1R3 are dispensable for both saccharin-stimulated adipogenesis and Akt phosphorylation. In mature adipocytes, exposure to artificial sweeteners

suppresses basal and stimulated lipolysis, which is also not dependent on sweet taste receptor expression. Taken together these data demonstrate unexpected roles for artificial sweeteners in adipocyte differentiation and metabolism, and support the presence of additional 'sweet receptors.'

Results

Chemosensory receptors are regulated with adiposity.

Our investigation of sweet taste receptors in adipose tissue biology was initiated by a screen for novel regulators of obesity. We analyzed RNA isolated from epididymal white adipose tissue (eWAT) in wild-type C57Bl/6 mice on a high-fat diet by Affymetrix microarray. These mice showed a typical response to high fat diet feeding that resulted in a variable distribution of adiposity (0.5-2.1 g eWAT). We then examined adipocyte genes whose expression correlated, either positively or negatively, with the weight of fat pads across the sample set. From this analysis, we identified over 40 chemosensory receptors expressed in adipose tissue. These included olfactory, taste, vomeronasal, and trace amino acid receptors. Surprisingly, correlation analysis also showed a cluster of 12 chemosensory receptors whose expression changed significantly with altered fat pad weight (Fig 2.1). These data represent an early indication that chemosensory receptors are present in adipose tissue, and their surprising pattern of expression suggests that chemosensory receptors could have regulatory functions in adipose tissue.

Sweet taste receptors T1R2 and T1R3 are expressed constitutively throughout adipogenesis and in 3T3-L1 cells and eMSCs.

As microarray data indicated that chemosensory receptors were expressed in adipose tissue, we chose to investigate sweet taste receptors as candidate metabolic regulators. This was because sweet taste receptors have known metabolic roles in other tissues and ligands for sweet taste receptors are well characterized, making a theoretically simple model for receptor activation. To evaluate the expression of taste receptors during adipogenesis, 3T3-L1

preadipocytes were differentiated into mature adipocytes and RNA was isolated at the indicated time points. In 3T3-L1 cells, expression of T1R2 increases two-fold and T1R3 decreases by half within the first four hours of adipogenesis, returning back to baseline by 12 hours (Fig 2.2A). Over the full time course of adipogenesis expression of both T1R2 and T1R3 peaks at day two, returning to near-preadipocyte levels by day eight (Fig 2.2B). We also examined sweet taste receptor expression in eMSCs as an independent adipogenic model. We found that sweet taste receptor expression in this system was reminiscent of 3T3-L1 cells; T1R2 and T1R3 both peak in expression at day two of adipogenesis before returning to preadipocyte levels at day twelve (Fig 2.2C).

Saccharin stimulates adipogenesis of mouse and human precursor cells.

To assess the effects of sweet taste receptor activity on adipogenesis, we utilized the artificial sweeteners saccharin (sacc) and AceK as T1R2/T1R3 ligands. These agonists, as opposed to natural sugars, are useful for metabolic studies because they are not metabolized and are ~500-fold sweeter than sucrose (Renwick, 1986; Sweatman and Renwick, 1979). Firstly, 3T3-L1 cells were treated throughout adipogenesis with an adipogenic cocktail containing dexamethasone and insulin (D, dexamethasone; I, insulin), supplemented with increasing concentrations of saccharin. This supplementation robustly stimulated adipogenesis in a concentration-dependent manner, resulting in increased lipid accumulation and FABP4 expression (Fig 2.3A). FABP4 was then quantified over multiple experiments to empirically determine minimal saccharin concentrations necessary to enhance adipogenesis (Fig 2.3B); this densitometric analysis indicates that 0.45 mM saccharin is the lowest effective dose to significantly increase FABP4 accumulation in 3T3-L1 cells, while higher doses result in a nearly 10-fold increase.

3T3-L1 cells induced with DI and treated with saccharin show enhanced adipogenesis, which could be due to a specific synergistic interaction of the signaling pathways activated by saccharin and DI. To test this, we differentiated

3T3-L1 cells with multiple combinations of the full MDI cocktail (M, methylisobutylxanthine; D, dexamethasone; I, insulin), including each component individually or no induction at all (FBS, fetal bovine serum), in the presence or absence of saccharin (Fig 2.3C). Using this approach, we observed that saccharin treatment is effective regardless of differentiation conditions, with saccharin-stimulated enhancement of adipogenesis observed under all tested conditions and also in the absence of any other adipogenic stimulation. These data suggest that saccharin-stimulated adipogenesis is versatile and does not require a 'priming' effect of growth factors in differentiation media, or prior activation of a specific adipogenic pathway to be effective.

To determine if these effects of saccharin on adipogenesis are relevant in broader contexts, we next evaluated whether saccharin stimulation of adipogenesis could be extrapolated to other cell models. Using multipotent, primary eMSCs, we also observed that saccharin was sufficient to stimulate lipid accumulation and expression of FABP4 (Fig 2.3D). As observed in 3T3-L1s, sweetener effects occurred independently of differentiation conditions, as eMSCs induced with MDI, DI, or FBS alone ubiquitously showed an enhancement of adipogenesis with saccharin treatment.

Finally, we tested the applicability of these findings to human systems by using stromal vascular cells (SVCs) isolated from human WAT. In this model, we found that saccharin markedly enhanced lipid accumulation and FABP4 expression following adipogenic induction with MDI (Fig 2.3E). Taken together, these results indicate that adipogenesis of mouse and human precursors is stimulated by distinct sweet taste receptor ligands, consistent with a model for artificial sweeteners acting as nutritive signals.

AceK stimulates adipogenesis of mouse and human precursor cells.

To test if effects on adipogenesis were conserved among other artificial sweeteners, we repeated the previous experiments in the presence of AceK.

Similar to saccharin, we observed enhancement of adipogenesis in 3T3-L1 cells supplemented with AceK (Fig 2.4A) at similar concentrations observed with saccharin. Similar results were also observed in eMSCs, where AceK supplementation enhanced adipogenesis independent of the differentiation induction conditions (Fig 2.4B). Lastly, we repeated this experiment in human SVCs. In these primary cells, AceK stimulated lipid and FABP4 accumulation (Fig 2.4C). These results suggest that pro-adipogenic effects may be broadly conserved among different types of artificial sweeteners.

Saccharin enhancement of adipogenesis is temporally dependent.

To further characterize sweetener-stimulated adipogenesis, we evaluated the temporal requirements of saccharin treatment to enhance adipogenesis. We treated differentiating 3T3-L1 cells with saccharin at varying time intervals (Fig 2.5A). Cells treated with saccharin for the first two or four days of adipogenesis demonstrate enhanced adipogenesis, with four days of treatment being more pronounced. The effects of four days of saccharin treatment are similar to, but slightly less than, those observed with eight. However, saccharin treatment must begin within this time window, because there is no effect on adipogenesis in cells treated with saccharin from day four through day eight. This observation suggests that the duration of saccharin treatment is not nearly as important as the time of initiation. We then examined the transcriptional profile of cells that had been treated with saccharin for the first four days of adipogenesis (Fig 2.5B,C). We observed that sweetener-stimulated PPAR γ and C/EBP α expression does not differ from control cells until day five, after the removal of saccharin from the differentiation media. PPAR γ expression was doubled and C/EBP α expression tripled by D8 in sweetener-treated cells (Fig 2.5B,C, right panels). No sweetener-stimulated changes between treatments were observed at earlier time points, although saccharin did slightly and transiently increase PPAR γ and C/EBP α expression at 2 hrs post-induction (Fig 2.5B,C, left panels). These data suggest that sweeteners stimulate early events in adipogenesis (D0-D4) that are propagated following termination of the sweetener treatment.

Artificial sweetener treatment has minimal effects on the early transcriptional program.

Because essential elements of sweetener signaling occur in the first 2 or 4 days of adipogenesis, we profiled transcriptional regulators of adipogenesis active in this time period. However, after profiling numerous transcription factors and regulatory genes, including C/EBP δ (Fig 2.6A), C/EBP β (Fig 2.6B), PREF1 (Fig 2.6C), FOXO1, and Wnt10b, (data not shown), we observed few significant alterations in early markers of the adipogenic transcription cascade. These data suggest that although sweeteners clearly have important roles regulating adipogenesis in the first 4 days of adipogenesis, this regulation may not occur transcriptionally, or involves transcription factors we have not evaluated.

Saccharin acutely activates Akt and ERK1/2 signaling pathways in preadipocytes.

In the absence of clear sweetener-stimulated transcriptional regulation of adipogenesis, we examined additional signal transduction cascades that might mediate sweetener effects. In other contexts (taste cells, β cells, and enteroendocrine cells) sweet taste receptor activation produces intracellular Ca²⁺ transients (Kyriazis et al., 2012; Liu and Liman, 2003; Mace et al., 2007). However, while we successfully generated calcium transients with endothelin-1 treatment in 3T3-L1 cells, we did not find evidence for sweetener-stimulated calcium flux in preadipocytes at or above concentrations that stimulate adipogenesis (data not shown). This suggests either an independent pathway or independent receptors are responsible for signal transduction in adipose tissue. Thus, we focused on known adipogenic signaling pathways as a means for sweetener-stimulated lipid accumulation (Rosen and MacDougald, 2006). To evaluate stimulation of such pathways, we treated serum-starved 3T3-L1 preadipocytes with saccharin and screened lysates for activated signaling proteins. Using this approach, we observed that saccharin treatment stimulates phosphorylation of Akt at T308 and S473 (Fig 2.7A), a modification that is well

characterized for its pro-adipogenic effects. Importantly, saccharin also stimulates phosphorylation of CREB and FOXO1, which are known downstream targets of Akt involved in promoting preadipocyte differentiation (Cypess et al.; Klemm et al., 2001; Nakae et al., 2003). Similar to the lack of calcium transients, this is the first known report of artificial sweeteners stimulating Akt signaling, which implicates novel pathways, novel receptors, or both, in transducing metabolic signals from artificial sweeteners.

To further investigate this novel signal transduction mechanism in preadipocytes, we evaluated saccharin-stimulated signaling upstream of Akt phosphorylation by using PI3K, MEK, or PLC β inhibitors. We observed that the ability of saccharin to stimulate Akt phosphorylation is blocked by PI3K inhibitors LY294002 (Fig 2.7B) and wortmannin (Figure 2.7C). Inhibition of MEK signaling with U0216 has no effect on saccharin-stimulated Akt phosphorylation, while inhibition of PKC with U73122 shows a partial block (Fig 2.7C). These data suggest that this novel sweetener-stimulated Akt phosphorylation occurs, like insulin signaling, in a PI3K-dependent manner.

We further examined saccharin-stimulated Akt phosphorylation using timecourses of saccharin treatment in 3T3-L1 cells. Here we observed that Akt phosphorylation is rapid, occurring within 5 min, and persists for at least 1 hr in serum-starved cells (Fig 2.7D). While maximal activation for T308 occurs within 5 min, S473 phosphorylation increases throughout the time course and is maximally activated at 60 min.

Finally, we evaluated the ability of saccharin to stimulate Akt phosphorylation in the context of adipogenesis, when Akt is already strongly activated by high concentrations of insulin. Even in the presence of high basal Akt phosphorylation, 3T3-L1 preadipocytes induced with DI demonstrated augmented phosphorylation in the presence of saccharin (Fig 2.7E). This augmented phosphorylation is observed within 30 minutes and persists to 6 hrs

following induction. Interestingly, phosphorylation of ERK1/2 is also enhanced in differentiating 3T3-L1 cells. However, this saccharin-stimulated ERK1/2 activity is not present in serum-starved cells (data not shown). Although maximal ERK1/2 phosphorylation at 30 min is not influenced by saccharin treatment, the activation of ERK persists to 16 h, with some increase in basal phosphorylation observed out to 72 h post-induction. While further experiments will be required to explain this difference in ERK activity between serum-starved and DI-stimulated conditions, a 'priming' effect of growth factor signaling may be necessary for saccharin-stimulated ERK1/2 phosphorylation.

T1R2 and T1R3 are not required for saccharin-stimulated adipogenesis or Akt phosphorylation.

Our data thus far have suggested that sweet taste receptors are perhaps the most probable candidates for binding sweeteners in adipose tissue; however, some of our observations are not consistent with the current literature on receptor signaling. To determine if sweet taste receptors are the mediators of artificial sweetener effects on adipose tissue, we investigated the dependence of saccharin-stimulated adipogenesis and Akt signaling on the presence of sweet taste receptors. We reasoned that if saccharin acts through T1R2/T1R3, knockout of either receptor would block the effects of artificial sweeteners on both adipogenesis and Akt phosphorylation. We therefore investigated these phenotypes in eMSCs derived from T1R2 or T1R3 knockout mice, beginning with T1R3-null eMSCs. We observed that these progenitor cells had no deficiency in adipogenesis relative to wild-type controls, suggesting that either sweet taste receptor activity is not essential for *in vitro* adipogenesis, or that a suitable taste receptor ligand is not present under *in vitro* conditions (Fig 2.8A, '0 mM saccharin'). We then evaluated the ability of saccharin to stimulate adipogenesis in the absence of T1R3; surprisingly, we observed that T1R3 KO had no effect on saccharin-stimulated lipid accumulation (Fig 2.8A). Accordingly, when we also measured the ability of saccharin to stimulate Akt phosphorylation in the absence

of T1R3, we observed no difference in the timing (Fig 2.8B) or dose-dependence (Fig 2.8C) of Akt phosphorylation between genotypes.

We next investigated saccharin activity in T1R2 KO eMSCs. Firstly, we examined the adipogenic efficiency of T1R2 KO eMSCs relative to wild-type cells; we observed that, like T1R3 KO, T1R2 had no effect on adipogenesis in cells differentiated with dexamethasone and insulin (Fig 2.8D, '0 mM saccharin'). We also evaluated the ability of saccharin to enhance adipogenesis in the absence of T1R2. Like T1R3, we observed that T1R2 is not required for saccharin-stimulated lipid accumulation (Fig 2.8D). This dispensability of T1R2 in sweetener-stimulated adipogenesis coincides with equal sweetener-stimulated Akt phosphorylation in WT and T1R2 KO cells, as measured in both the context of saccharin-stimulated adipogenesis (Fig 2.8E) and dose-dependence in undifferentiated eMSC precursors (Fig 2.8F). These data suggest that neither T1R2 nor T1R3 are individually necessary for saccharin-mediated enhancement of adipogenesis or Akt phosphorylation in preadipocytes. In this case, saccharin could be binding to an uncharacterized receptor, or both T1R2 and T1R3 might be acting as homodimers to transduce metabolic signals.

Artificial sweeteners suppress lipolysis.

Although the receptor identity remains unknown, these data demonstrate robust effects of artificial sweeteners on preadipocytes and adipogenesis. Hence, we speculated that artificial sweeteners might also regulate metabolic processes in mature adipocytes. To address this possibility, we performed an unbiased metabolomic analysis of compounds regulated by saccharin treatment in 3T3-L1 adipocytes (Fig 2.9A). This analysis, which screened a library of metabolites by mass spectrometry, showed a subpopulation of fatty acids, including palmitate (Fig 2.9B) were reduced with saccharin treatment. Based on this data, we hypothesized that saccharin might regulate lipolysis in mature adipocytes. Indeed, while sweetener treatment had no effect on glucose uptake (Fig 2.9C) or lipogenesis (data not shown), we observed that treatment of 3T3-L1 adipocytes

with saccharin reduced glycerol (Fig 2.9D) and non-esterified fatty acid (NEFA, Fig 2.9E) release from adipocytes within 30 min. Importantly this effect is not due to osmotic stress, as equimolar treatment with mannitol has no effect. A similar effect was also observed with the artificial sweeteners AceK and sucralose (sucr, Fig 2.9F). These results could also be extrapolated to an *ex vivo* system, where isolated epididymal fat pads incubated with saccharin for 4 hrs resulted in a reduction in media glycerol. Interestingly, an intraperitoneal injection of saccharin, rather than an *ex vivo* incubation, was also sufficient to reduce glycerol release when the fat pad was excised 20 min post-injection (Fig 2.9G).

T1R2/T1R3 are not required for suppression of lipolysis by saccharin.

While T1R2 and T1R3 were the most likely binding candidates for artificial sweeteners, data in preadipocytes suggests that these receptors might not be involved. We tested for T1R/T1R3 involvement by performing lipolysis assays in T1R2 and T1R3 KO eMSCs. As we observed in preadipocytes, loss of T1R3 (Fig 2.10A) or T1R2 (Fig 2.10B) failed to block saccharin effects on lipolysis, and no significant differences were observed between genotypes. Furthermore, we tested saccharin's effects in the presence of lactisole, a pharmacological inhibitor of human T1R3. In human preadipocytes, saccharin treatment is sufficient to suppress lipolysis, and lactisole treatment fails to block this suppression (Fig 2.10C). These data support our previous observations that saccharin acts in adipocytes in a T1R2/T1R3 independent manner.

We next investigated mechanisms for lipolytic regulation by artificial sweeteners. We observed that the addition of saccharin to 3T3-L1 adipocytes suppresses phosphorylation of HSL (Fig 2.10D). Interestingly, saccharin significantly blunted the stimulation of both glycerol release and HSL phosphorylation by forskolin (Fsk), an adenylyl cyclase activator. We hypothesized that saccharin might act through Akt signaling, as in preadipocytes, to suppress lipolysis in a PI3K dependent manner. However, treatment with LY294002 also failed to block saccharin-mediated suppression of lipolysis (Fig

2.10E). Additionally, although sachharin stimulated Akt phosphorylation adipocytes, this does not occur until 45 min of treatment, inconsistent with the timing of lipolysis suppression (data not shown). As cAMP is an important regulator of lipolytic activity upstream of HSL, we speculated that saccharin treatment might reduce cAMP concentrations in adipocytes. However, saccharin had no effect on cAMP concentrations (Fig 2.10F), suggesting that it may act downstream of PKA. Taken together, these results suggest that saccharin regulates lipolysis independently of T1R2/T1R3 and many known mediators of lipolytic activity.

Discussion

One strategy currently utilized to curtail the obesity epidemic is extensive use of non-nutritive sweeteners. Such artificial sweeteners, including saccharin, AceK, aspartame, sucralose, and neotame, have little to no caloric value but are hundreds of times sweeter than sucrose. However, controversy has erupted over studies suggesting that high-level consumers of artificial sweeteners may actually be at greater risk for overweight and obesity (Dergance et al., 2005). While not all studies agree with this assessment (Blackburn et al., 1997; Porikos and Koopmans, 1988; Rodin, 1990), the hypothesis that artificial sweeteners ‘uncouple’ anticipated caloric density perceived by the tongue from the actual calories ingested has gained a distinct foothold. Some argue that this uncoupling leads to increased insulin secretion, food intake, and weight gain (Swithers and Davidson, 2008; Swithers et al.). This controversy has been further complicated by reports identifying functional sweet taste receptors sensitive to these artificial sweeteners in many tissues outside the tongue. The studies presented in this chapter extend these previous reports by identifying adipose tissue as an additional metabolic tissue harboring sweet taste receptors; however, their functional role in this context remains unclear.

Our results demonstrate that artificial sweeteners, particularly saccharin, can regulate metabolism in adipose tissue. While the active concentrations here are likely higher than would be observed under normal dietary conditions (Colburn et al., 1981; Sweatman et al., 1981), this remains an important proof of principle for potential downstream effects of artificial sweetener use, particularly in the absence of a characterized receptor. Equally interesting are two additional observations of our experiments: firstly, that artificial sweeteners are capable of acting in the absence of T1R2/T1R3; and secondly, that sweet taste receptors are expressed in adipose tissue.

The observation of saccharin activity in the absence of T1R2/T1R3 has several potential explanations. Some groups have hypothesized that T1R2/T1R3 is not actually an obligate heterodimer, as it has been routinely described, but rather each component might function separately as a homodimer. Thus far, homodimer ligand binding has been demonstrated in isolated N-terminal domains (NTDs), though not in intact receptors (Maitrepierre et al.; Nie et al., 2006; Nie et al., 2005). However, some reports suggest that T1R3 in the gut may function independently, as T1R3 but not T1R2 KO mice have impaired glucose tolerance on an oral glucose tolerance test (Geraedts, et al). Both T1R2 and T1R3 knockout mice are highly, but not totally, deficient in sweet-taste sensitivity (Zhao et al., 2003), suggesting that while heterodimerization is important for maximal receptor function, it may not be absolutely required for activity. This homodimerization model has been proposed by an independent group describing sweet taste receptor activity in adipose tissue (Masubuchi et al.). In their model, T1R3, but not T1R2, is required for inhibition of adipogenesis by sweet taste receptors. The authors show conflicting results to our own, in that saccharin treatment inhibits adipogenesis and reduces expression of PPAR γ and C/EBP α . This effect is partially blocked with knockdown of T1R3. We hypothesize that the higher concentrations of sweetener routinely used by this group (20 mM saccharin) may have caused apoptosis or impaired cellular function rather than true inhibition of adipogenesis, as we have observed cell death at higher

saccharin concentrations (data not shown). Further work will be required to elucidate differences between these model systems, and whether T1R2 or T1R3 homodimerize in this context.

A second possibility for saccharin receptor binding is through bitter taste receptors, which are known to bind to saccharin and AceK at high concentrations; this is the cause of aversion and 'metallic' aftertaste with high doses of some sweeteners (Kuhn et al., 2004). To date, expression of one bitter taste receptor has been reported in an adipogenic system- Tas2R46 in human MSCs (Lund et al.). However, saccharin does not appear to activate hTas2R46 *in vitro* (Brockhoff et al., 2007; Meyerhof et al.), arguing against a homologous event in mice. Microarray data suggests that bitter taste receptors T2R106, 108, and 137 are expressed in WAT (Fig 2.1, data not shown). However, the ligands for these receptors have not been characterized and their propensity for saccharin binding is unknown. We also predict saccharin binding would occur at higher concentrations than those at which we observed functional effects (Brockhoff et al.). However, we have not directly tested for the involvement of bitter taste receptors, as these experiments are hampered by complex and overlapping pharmacology among many receptors (Meyerhof et al.). Thus, bitter taste receptor activity mediating saccharin effects is still a small but tenable possibility.

The remaining possibilities to explain saccharin activity in the absence of T1R2 or T1R3 are 1) Saccharin binding to an uncharacterized 'sweet' receptor, or 2) Saccharin passing directly into the cell independent of receptor activity. Mass spectrometry analysis of mouse fat pads following prolonged saccharin exposure in drinking water suggests that saccharin does not readily diffuse into adipose tissue, and what is internalized is cleared quickly (data not shown). Additionally, the vast majority of ingested saccharin is excreted in urine, arguing against significant saccharin internalization in adipose tissue (Sweatman et al., 1981). The most likely candidate of these possibilities is therefore binding of an

uncharacterized receptor. Data supporting the existence of additional receptors sensitive to sweeteners are similar to data supporting T1R2/T1R3 homodimers: R2 and R3 KO mice have greatly impaired, but not ablated sweet sensitivity, and retain relatively normal responses to polycose (Zukerman et al., 2009). However, the observation that TRPM5 and PLC β KO mice also have impaired, but not ablated, sensitivity favors the existence of an independent receptor, a different signaling pathway, or both (Damak et al., 2006; Dotson et al., 2005), rather than exclusively supporting homodimers. Behavioral studies in T1R2 and T1R3 KO also mice support the presence of additional 'sweet' sensors (Treesukosol et al. 2012).

Perhaps the most intriguing question remaining from this study is the physiological role, if any, of sweet taste receptors in adipose tissue. Though we are the second group to describe them (Masubuchi et al. 2013), there has been no consensus on the function of these receptors. We have screened numerous pathways for sensitivity to sweetener treatment, but few had detectable alterations with sweeteners, and none of those changes were dependent on the expression of T1R2/T1R3. However many other candidate pathways remain untested. One possible function for sweet taste receptors in adipose tissue is regulation of hormone secretion, as has been observed in the pancreas and gut. It is also possible that these receptors have significant functionality *in vivo* that is not reflected under *in vitro* culture conditions; adipose-specific T1R2 and T1R3 KO mice would be necessary to address this possibility. Taken together, these data unveil a novel role for artificial sweeteners in adipose biology, and suggest that sweet taste receptors may represent a broader and more complex group of receptors than is currently appreciated.

Materials and Methods

Microarray

Four micrograms of cDNA from male wild-type mice was converted to sense orientation, then fragmented and biotinylated using Ovation FL Module (NuGen Inc.) following standard manufactures protocol. The probe was then hybridized to Affymetrix Mouse Gene ST 1.0 GeneChips for 20 hrs at 45 °C, stained, and washed using a Fluidics FS450 instrument, and then scanned with the Affymetric 7G Scanner 3000. Gene profiling data are available form the GEO database with the accession number GSE37514.

Cell Culture

3T3-L1 cells were differentiated as previously described (Hemati et al., 1997). Briefly, cells two days after confluence (D0) were treated with DMEM containing 10% fetal bovine serum, 1 µM dexamethasone, 1 µg/mL insulin, and 0.5 mM methylisobutylxanthine, or combinations thereof. Cells were fed every two days, with insulin and FBS supplementation on D2, and FBS alone from D4 to the conclusion of the experiment. In general, artificial sweeteners were added to differentiation media at induction and replaced with media every two days. Saccharin, AceK, and sucralose were from the Sigma-Aldrich Co. (St. Louis, MO). Adipogenesis was evaluated by Oil Red-O (Sigma-Aldrich Co., St. Louis, MO) staining as previously described (Cawthorn et al.).

eMSC isolation

eMSCs were isolated from wild-type, T1R2, and T1R3 KO mice as previously described (Rim et al., 2005a, as modified by Mori et al 2012). Briefly, mouse ears were sterilized and incubated for 1 hr in collagenase to obtain a cell suspension. Pre-confluent cells were supplemented with 50 µg/mL FGF during the initial growth period (Mori et al., 2012), and maintained at 5% CO₂ in DMEM/F:12 supplemented with 15% FBS. For differentiation, 1 µM dexamethasone, 5 µg/mL insulin, and 0.5 mM methylisobutylxanthine were added to maintenance media. As in 3T3-L1 cells, cells are fed every two days, with insulin remaining in media for the first four.

Glucose Uptake

3T3-L1 adipocytes were serum-starved in HBSS with 0.5% BSA for 4 hrs. Cells were then incubated with 4 nM insulin for 10 min before treating with 50 μ M cytochalasin B to block background translocation. After 20 min of insulin treatment, 0.1 μ Ci/mL of C14 2-deoxyglucose (Perkin Elmer, Waltham MA) was added. Ten minutes later (30 min-post insulin), adipocytes are placed on ice and lysed in 0.1% SDS. 2-deoxyglucose internalized in the cell was then quantified by scintillation counting.

Lipolysis

Lipolysis assays were conducted in differentiated adipocytes at least eight days after induction of adipogenesis for 3T3-L1 cells or twelve days for eMSCs and human SVCs. Accumulation of glycerol and NEFA in assay media was determined in HBSS with assay kits from Sigma-Aldrich Co (St. Louis, MO; FG0100), and Wako Diagnostics (Richmond, VA; NEFA-HR(2)). Cells were treated for 2 hrs, or the time indicated. Lipolysis in mouse explants was performed as described under 'Animals.' Lipolysis in human adipocytes was performed on human preadipocytes acquired from ZenBio (Research Triangle Park, NC), and induced the provided differentiation media as per manufacturer's instructions. Lactisole was purchased from Sigma (St. Louis, MO). Forskolin (Sigma, St. Louis MO) was used at 10 μ M and saccharin at 4.5 mM unless otherwise indicated.

cAMP

cAMP was measured by ELISA (Cayman Chemical, Ann Arbor MI) according to manufacturer's instructions.

Human SVC isolation

SVCs were isolated from a subcutaneous fat depot of a 54-year-old diabetic patient in the same manner as eMSCs (Rim et al., 2005b). Human SVCs were maintained and differentiated in the same manner as eMSCs. Human samples

were obtained with the approval of the Institutional Review Board of the University of Michigan Medical School Institutional Review Boards (HUM00060733).

Immunoblot analysis

Cell extracts were lysed in a 1% SDS buffer (1% SDS, 12.7 mM EDTA, 60 mM Tris-HCL, pH 6.8) and heated to 95 °C. Lysates were then centrifuged to pellet cell debris, transferred to a fresh tube, and protein concentration was quantified with a BCA assay (Thermo Scientific, Waltham MA). 4x SDS loading buffer (4% SDS, 240 mM Tris-HCl, 40% glycerol, 0.05% bromophenol blue, and 2.5% 2-mercaptoethanol) was added to a constant amount of protein before separation on Bis-Tris polyacrylamide gels (Invitrogen). For evaluation of adipogenesis markers, a constant volume of lysate was used. SDS-PAGE and immunoblotting were performed as described previously (Cawthorn et al.) Membranes were immunoblotted with antibodies from Cell Signaling Technology, Inc. (Danvers, MA) for C/EBPa (#2295), pAkt 308 (#9271) and pAkt473 (#9275 or #4060), pFOXO1 (#9461), pCREB (#9191), pHSL (#4126) and pERK (#9101), total Akt (#9272), total ERK1/2 (#4695), total FOXO1(#9462), total HSL(#4107) and total CREB(9197). Laminin antibody was obtained from Novus Biologicals (Littleton, CO). PPAR γ 1/2 antibody was obtained from Millipore (Temucula, CA). FABP4 antibody was obtained from R&D Systems (MAB1143, Minneapolis, MN).

mRNA quantification by RT-PCR

Total RNA was prepared from frozen tissue or cells using RNA Stat60 according to the manufacturer's protocol (Tel-Test, Inc., Friendsville TX). Total RNA was quantified and reverse transcribed with random hexamers (Taqman Reverse Transcription kit, Applied Biosystems, Foster City CA). Quantitative PCR was performed using the MyiQ real-time PCR detection system with SYBR green reagents (Bio-Rad Laboratoreis, Hercules CA). Reverse transcription, primer design, and qPCR were performed as described previously (Cawthorn et al.). Primer sequences are as follows:

T1R2 F GTCCGCTGCACCAAGCA
 R GTTCGTCTGAAGAAGAGCTGGTT
 T1R3 F CCAGGCAACCAGGTGCCAGTC
 R CGCCTTGCAGTCCACGCAGT
 PPAR γ F CCAGAGCATGGTGCCTTCGC
 R TTCCGAAGTTGGTGGGCCAGA
 C/EBP α F TGGACAAGAACAGCAACGAG
 R TCACTGGTCAACTCCAGCAC
 PREF1 F CCTCCTGTTGCAGTATAACAGCG
 R GGTCATGTCAATCTTCTCGGG
 WNT10b F ACGACATGGACTTCGGAGAGAAGT
 R CATTCTCGCCTGGATGTCCC
 C/EBP β F GGGACTTGATGCAATCCGG
 R AACCCCGCAGGAACATCTTT
 C/EBP δ F CGCCGCAACCAGGAGAT
 R GCTGATGCAGCTTCTCGTTCT
 FOXO1 F GCTTTTGTACATGCAGGT
 R CGCACAGAGCACTCCATAAA

Animals

C57BL/6J mice were purchased from The Jackson Laboratory (Bar Harbor ME). Procedures for this work were approved by the Committee on the Use and Care of Animals at the University of Michigan, with daily care of animals overseen by the unit for laboratory animal medicine (PRO0001369). Animals were maintained on a 12-hour light/dark cycle and fed standard chow *ad libitum* (Purina Lab Diet 5LOD, St. Louis MO). For saccharin effects on *ex vivo* lipolysis, 10-week-old male mice were injected with a sodium saccharin solution at 100 mg/kg. After 20 min, animals were euthanized with CO₂ and epididymal fat depots were excised. Depots were then weighed and cut into ~40 mg pieces, which were then cultured at 5% CO₂ in HBSS for 4 hrs before quantifying glycerol in media. T1R2 and

T1R3 KO animals were acquired from Björn Tyrberg and developed by Charles Zuker; both have been previously described (Zhao et al., 2003).

Unbiased Metabolomics

Sample preparation

To prepare samples for untargeted metabolomics, metabolites were extracted from adipocytes according to the protocol of Lorenz et al (Lorenz et al.). Briefly, 500 μ L of cold 8:1:1 methanol: chloroform: water were added to each well of a 6-well cell culture plate which had previously been aspirated of all media and quenched by freezing with liquid nitrogen. The plate was then scraped with a cell scraper to release and lyse cells. The cell extract was transferred by pipette to a microcentrifuge tube, and residual cell debris was pelleted by centrifugation at 15,000 x g for 10 minutes. The supernatant was directly analyzed by LC-MS.

Unbiased LC-MS analysis

Cell extracts were analyzed by LC-MS using an Agilent 1200 HPLC coupled to an Agilent 6210 time-of-flight mass spectrometer. Chromatographic separation was performed via mixed-mode anion exchange – hydrophilic interaction chromatography using a Phenomenex Luna NH₂ 3 μ column, 15 cm x 2 mm ID. Mobile phase A for the separation was acetonitrile and mobile phase B was 5mM ammonium acetate in water, adjusted to pH 9.9 with ammonium hydroxide. The gradient consisted of a 20 minute linear ramp from 20% to 100% B, followed by a 2-minute hold at 100% B and a subsequent 13-minute re-equilibration period at 20% B. The sample injection volume was 20 μ L and the flow rate was 0.25 mL/min. Detection was performed by electrospray ionization mass spectrometry in negative ion mode. MS parameters were as follows: gas temp 350°C, drying gas 10 L/min, nebulizer 20 psig, capillary voltage 3500V, scan range 50-1200, internal reference mass correction enabled.

Data analysis

Untargeted metabolomics data analysis was performed using Agilent Masshunter Qualitative Analysis and Mass Profiler Professional software. Features in the data were first detected using the Find by Feature algorithm in Masshunter

Qualitative Analysis, and were then aligned between samples by accurate mass and retention time using Mass Profiler Professional. To minimize gaps in the data, recursive detection of aligned features was performed using the Find by Formula algorithm. Once a final list of features was generated, compounds were assigned putative identities by searching against the online Metlin database (<http://metlin.scripps.edu>). In many cases, the Metlin search resulted in multiple possible matches for each feature within a 10 ppm mass error window. Metabolite matches were ranked in order of ascending mass error, and among matches with equivalent mass error, in order of ascending Metlin ID number. The top database ID was not considered to be the valid metabolite identity, but rather as providing guidance for further confirmation using authentic standards as needed. Following putative metabolite identification, statistical analysis and data reduction techniques including principle component analysis were used to determine statistically different features between sample groups and to assess global differences in the metabolome between treatment conditions.

Calcium Imaging

3T3-L1 cells were incubated with Fluo4 (Life Technologies, Grand Island NY) in glass bottom dishes (MatTek, Ashland, MA) for 30 min before imaging by confocal microscopy (Olympus FV500 Confocal Microscope, Olympus IX-71). Sweeteners were delivered by pipette as 10x solutions and allowed to diffuse through dishes maintained at 37 °C while monitoring the green fluorescence channel. Experiments were conducted with the assistance of the Michigan Diabetes Research and Training Center Morphology and Image Analysis Core.

A

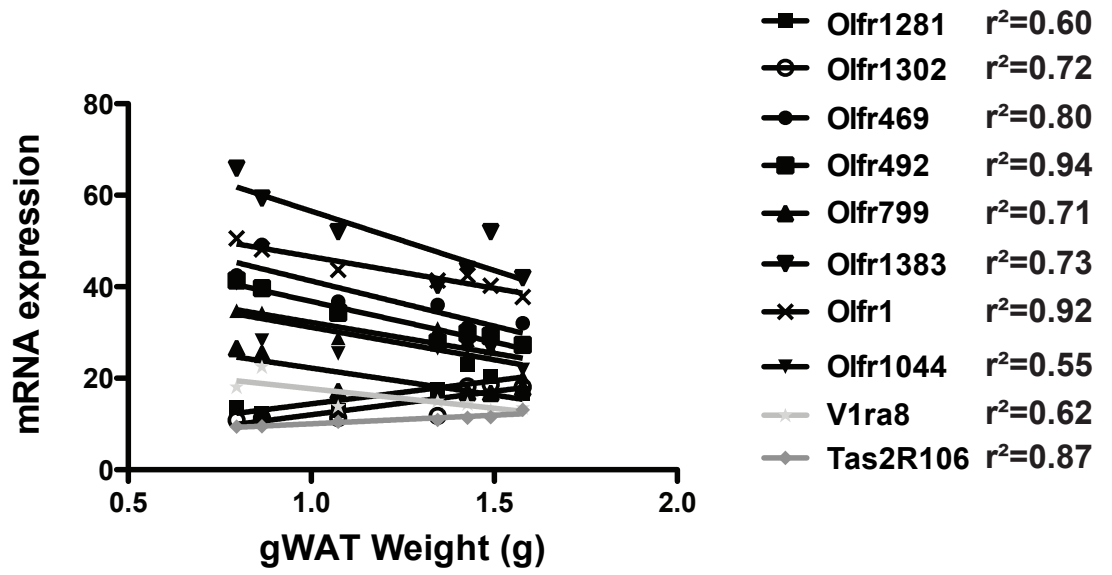


Figure 2.1. Chemosensory receptors are regulated with adiposity.

Ten representative chemosensory receptors show regulated expression with varying adiposity in gonadal white adipose tissue; all olfactory receptors are shown in black, with bitter (Tas2R) or vomeronasal (V1r) receptors in gray. Chemosensory receptor correlations with adiposity may be positive or negative with a wide variety of slopes, suggesting that these receptors may have very divergent functions in adipose tissue.

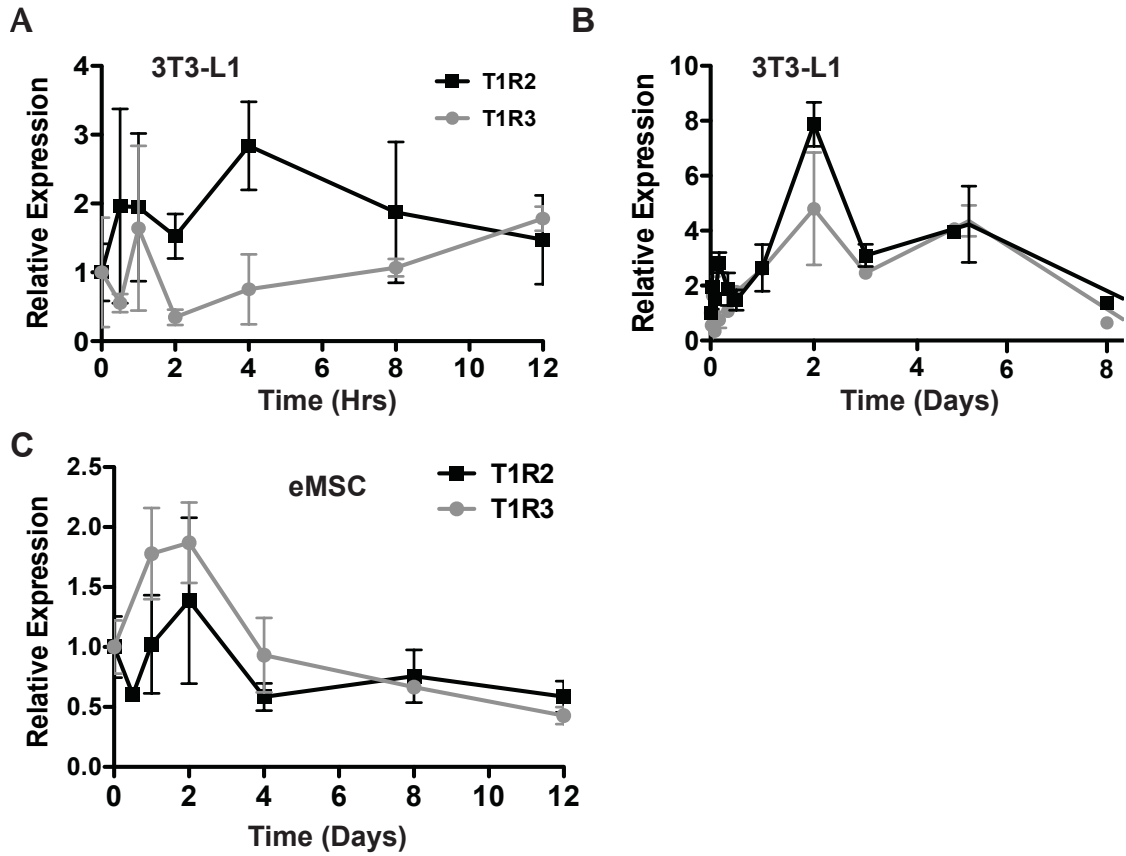


Figure 2.2. Sweet taste receptors T1R2 and T1R3 are expressed constitutively throughout adipogenesis in 3T3-L1 cells and eMSCs.

A) T1R2 and T1R3 expression in the first 12 hours of adipogenesis in 3T3-L1 cells. B) T1R2 and T1R3 expression over eight days of differentiation in 3T3-L1 cells. C) T1R2 and T1R3 expression in differentiating eMSCs. Data are expressed as mean plus S.D.

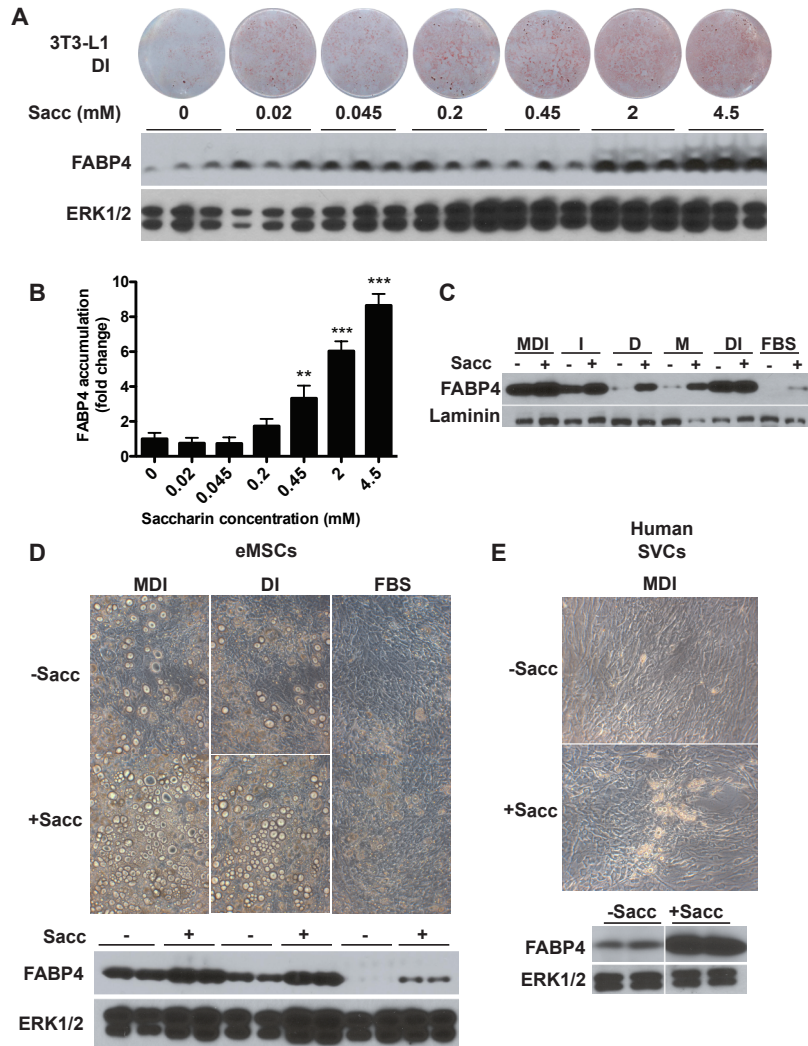


Figure 2.3. Saccharin stimulates adipogenesis in mouse and human precursor cells.

A) 3T3-L1 cells were differentiated with DI in the presence of the indicated concentrations of saccharin. Seven days after induction, cells were stained for neutral lipid with Oil Red-O (upper panel) and lysates were evaluated for expression of FABP4 (lower panel). ERK1/2 was used as a loading control. B) Densitometric quantification of saccharin-stimulated FABP4 accumulation from four independent experiments in DI-treated 3T3-L1 cells. Data are expressed as mean plus S.D. *P-values* <0.01 are indicated with **, and <0.005 with ***. C) 3T3-L1 cells were differentiated with all components of the MDI cocktail together or individually in the presence or absence of 4.5 mM saccharin. Adipogenesis was then evaluated after 8 days in all differentiation conditions by Western blotting for FABP4. D) eMSCs were incubated in the presence of MDI, DI, or FBS media with or without 2 mM saccharin supplementation. At day 16 of differentiation, degree of differentiation was evaluated with photomicrographs (upper panels) and by expression of FABP4 (lower panels). E) Human SVCs were induced with MDI for 14 days in the absence or presence of 4.5 mM saccharin. Adipogenesis was evaluated with photomicrographs and by expression of FABP4.

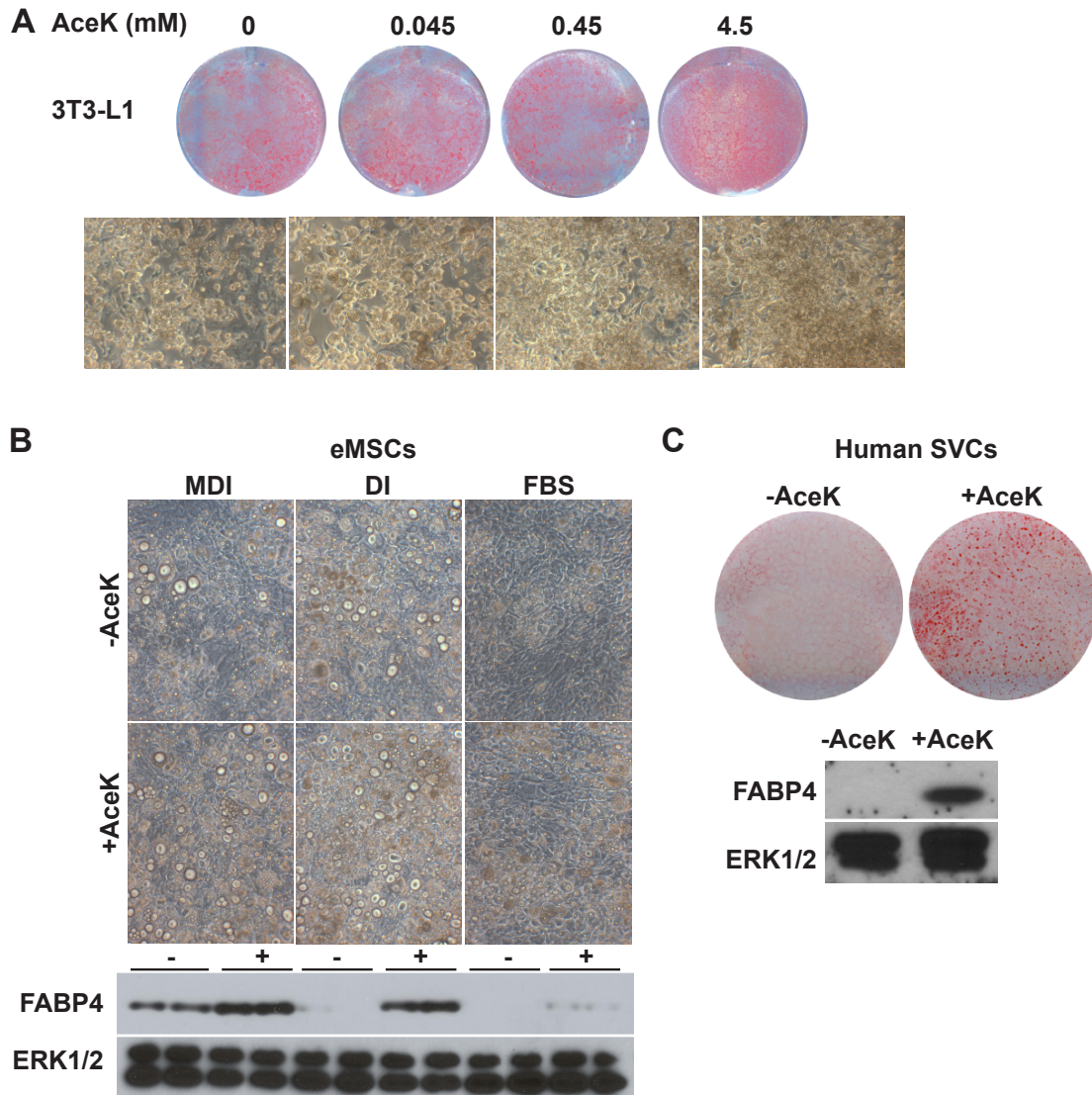


Figure 2.4. AceK stimulates adipogenesis in mouse and human precursor cells.

A) 3T3-L1 cells were induced with DI and treated for 8 days with the indicated concentrations of AceK. After 8 days, cells were stained for neutral lipid with Oil Red-O. B) eMSCs were incubated in the presence of MDI, DI, or FBS media with or without a 2 mM AceK. After 16 days, degree of differentiation was evaluated with photomicrographs (upper panels) and by expression of FABP4 (lower panels). C) Human SVCs were induced with MDI for 14 days in the absence or presence of 4.5 mM AceK. Adipogenesis was determined with photomicrographs (upper panel) and by expression of FABP4 (lower panel).

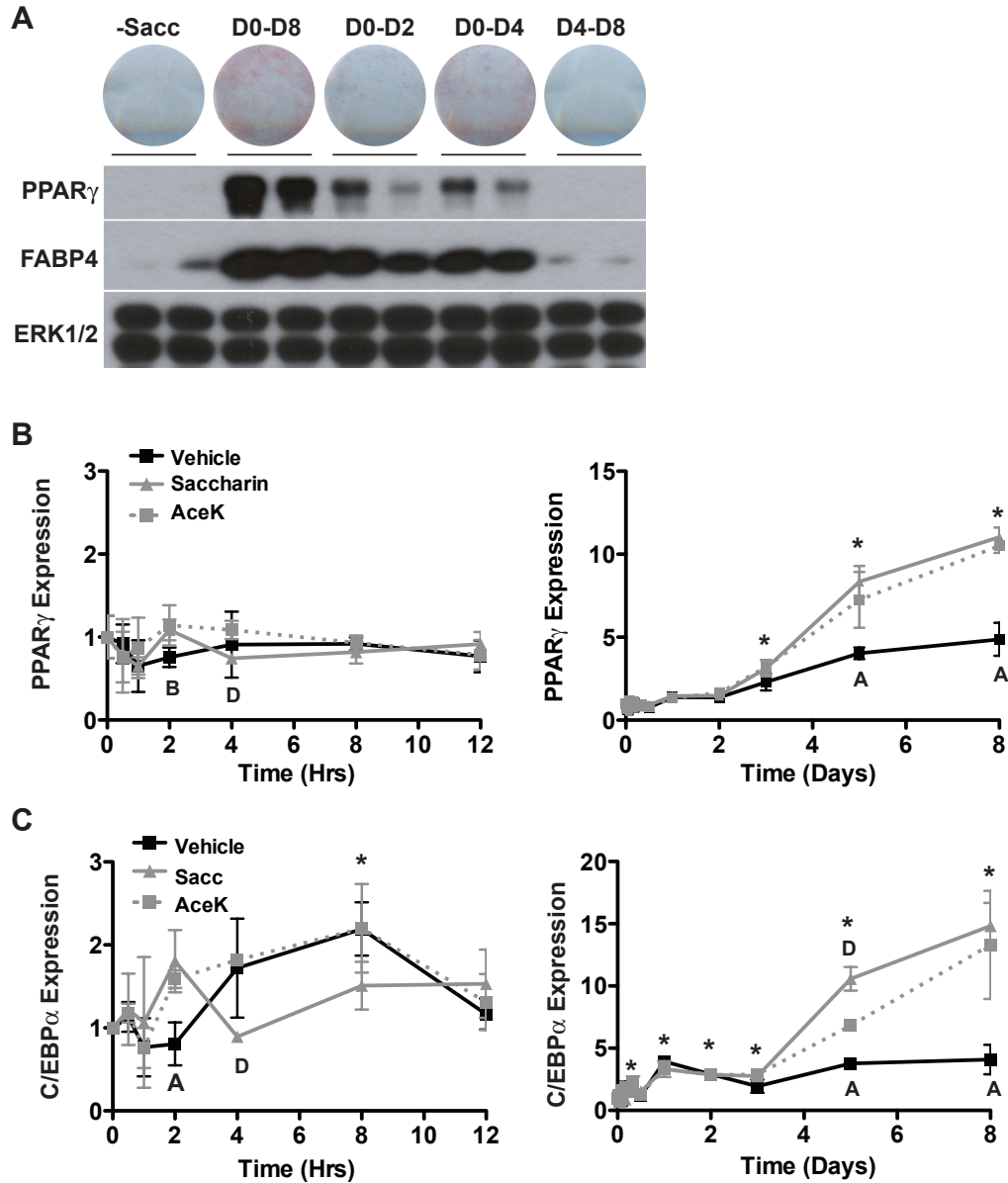


Figure 2.5. Saccharin enhancement of adipogenesis is temporally dependent. A) 3T3-L1 cells were induced for differentiation with DI and supplemented with 4.5 mM sacc at the indicated time points. Cells were stained with Oil Red-O (upper panel) and lysates collected for immunoblotting after 8 days (lower panels). B) PPAR γ and C) C/EBP α expression were measured over a time course of adipogenesis in 3T3-L1 cells induced with DI and treated with vehicle, 4.5 mM sacc, or 4.5 mM AceK for 4 days. Left panels indicate the first 12 hours of differentiation, while right panels indicate the full adipogenesis time course. Significance was determined using Student's t-test. Significant differences (P -value < 0.05) between vehicle and both sacc and AceK are denoted 'A', between vehicle and sacc denoted 'B', between vehicle and AceK denoted 'C', and between sacc and AceK denoted 'D.' Significant differences between vehicle treatment and preadipocytes (Time 0) controls denoted *. Data are expressed as mean plus S.D.

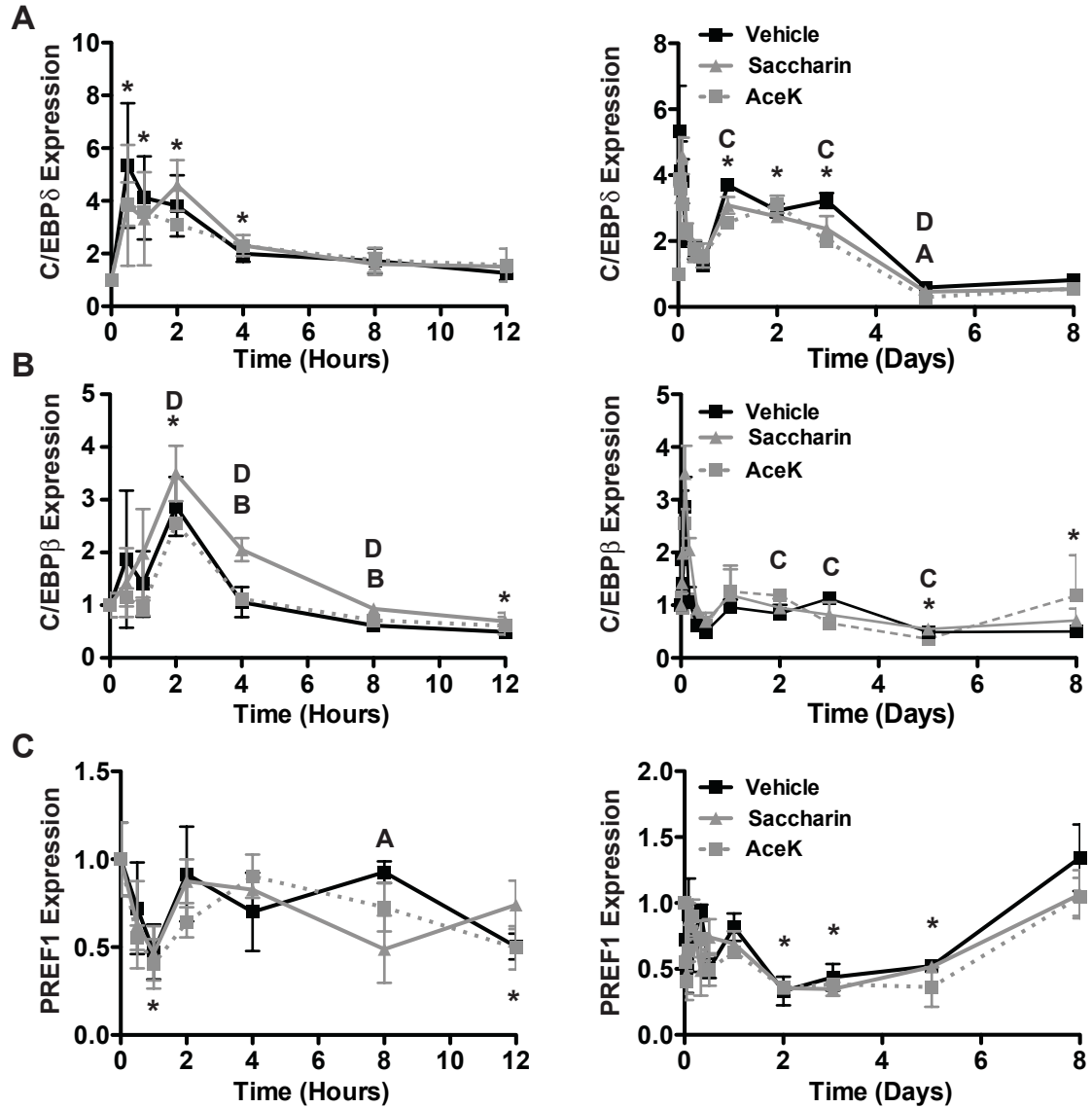


Figure 2.6. Artificial sweetener treatment has minimal effects on the early transcriptional program.

A) Samples obtained as in Fig 2.5B,C, were evaluated for the expression CEBP δ (A), CEBP β (B), and PREF1 (C). Left panels indicate the first 12 hours of differentiation, while right panels indicate full adipogenic time course. Significance was determined using Student's t-test. Significant differences (P -value <0.05) between vehicle and both sacc and AceK are denoted 'A', between vehicle and sacc denoted 'B', between vehicle and AceK denoted 'C', and between sacc and AceK denoted 'D.' Significant differences between vehicle treatment and preadipocytes (Time 0) controls denoted *. Data are expressed as mean plus S.D.

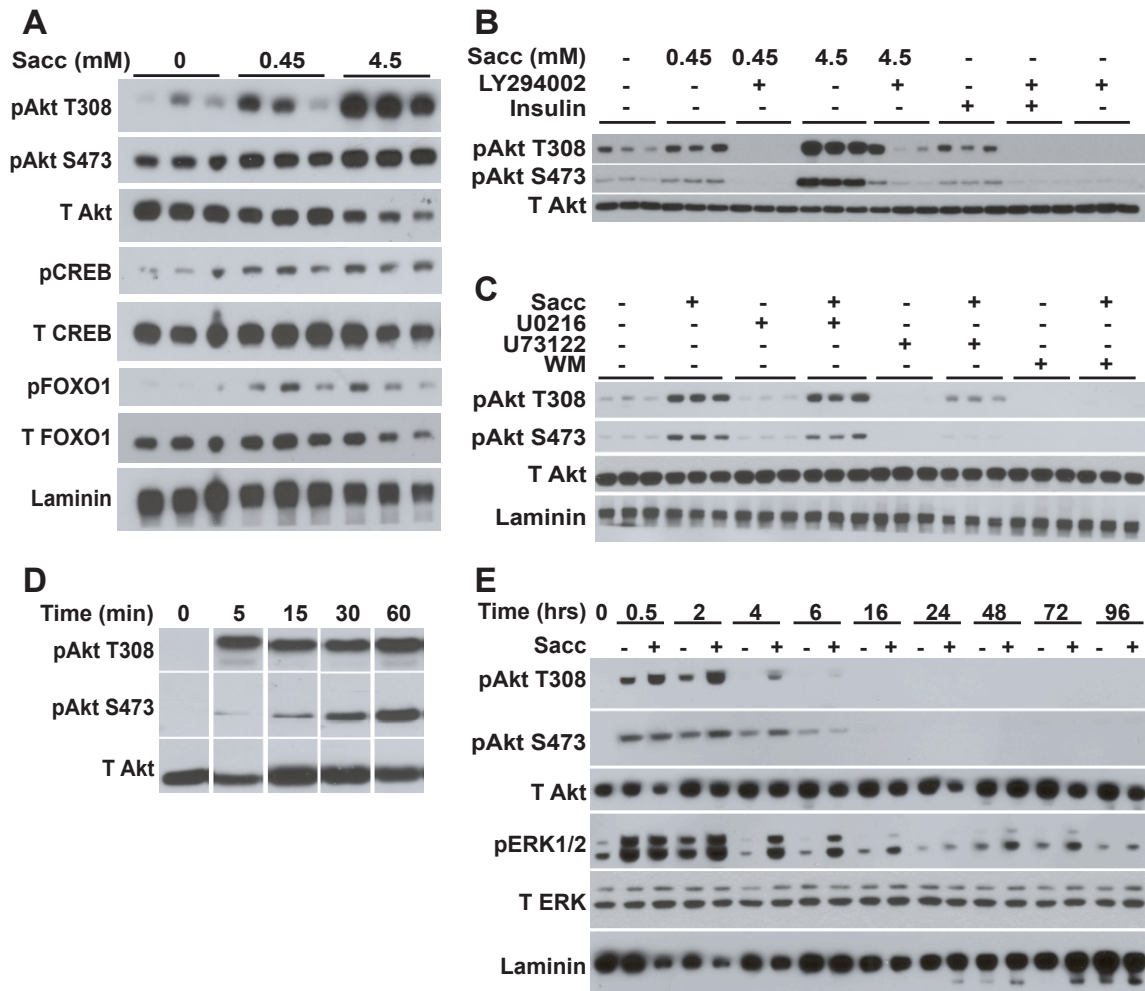


Figure 2.7. Saccharin activates Akt and ERK1/2 signaling pathways in preadipocytes.

A) 3T3-L1 preadipocytes were serum-starved for two hours in HBSS, then treated with 0.45 or 4.5 mM saccharin for 30 min before lysis and immunoblot analyses with the indicated antibodies. B) 3T3-L1 cells were serum-starved in HBSS for two hrs, and pretreated with 50 μ M LY 294002 for 1 hr. Cells were then treated with the indicated concentrations of saccharin in the absence or presence of LY294002 for 30 min. After lysis, samples were probed by immunoblot with the indicated antibodies. 25 nM insulin was used in the presence of LY as a control. C) 3T3-L1 cells were serum starved in HBSS for 2 h, and pretreated with 1 μ M U0216, 5 μ M U73122, or 2 μ M wortmannin for 1 hr. Cells were then treated with 4.5 mM saccharin in the absence or presence of each inhibitor for 30 min before immunoblotting for the indicated proteins. D) 3T3-L1 preadipocytes were serum-starved in HBSS for 2 hrs and treated with 4.5 mM saccharin for the indicated time periods before harvesting for immunoblotting. E) 3T3-L1 cells were stimulated with DI in the presence or absence of 4.5 mM saccharin. Lysates were prepared at the indicated time points and probed by immunoblot for the indicated proteins. T308, threonine 308; S473, serine 473; T Akt, total Akt; T CREB, total CREB; T FOXO1, total FOXO1; T ERK1/2, total ERK1/2; WM, wortmannin.

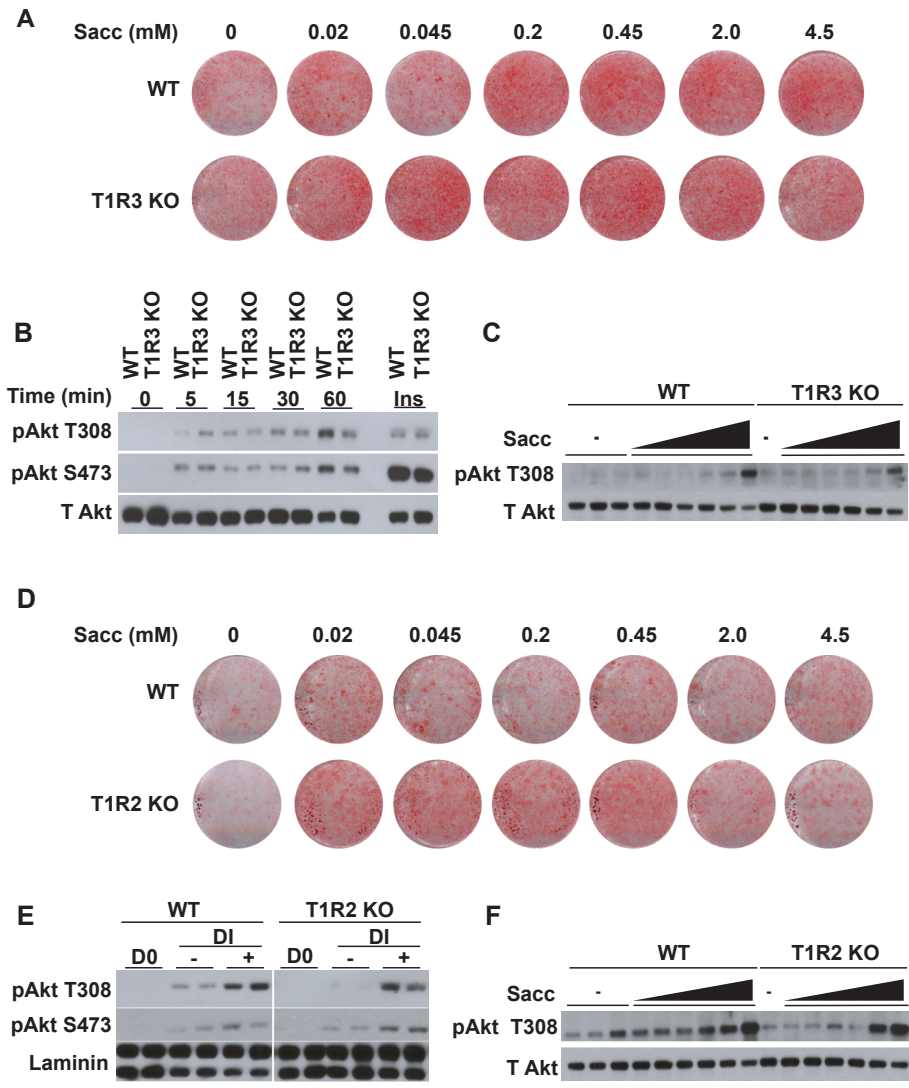


Figure 2.8. T1R3 and T1R2 are not required for saccharin-stimulated adipogenesis or Akt phosphorylation.

A) WT and T1R3 KO eMSCs were allowed to differentiate in FBS supplemented with increasing concentrations of saccharin. After 12 days, lipid accumulation was evaluated with Oil Red-O. B) WT and T1R3 KO eMSCs were serum starved for 2 hrs in HBSS treated with 4.5 mM saccharin for the time periods indicated. Lysates were collected for immunoblotting against the indicated proteins. C) WT and T1R3 KO eMSCs were serum starved for 2 hrs in HBSS and treated for 30 min with increasing concentrations of saccharin (0.02-4.5 mM) before collecting lysates for immunoblotting. D) WT and T1R2 KO eMSCs were allowed to differentiate in FBS supplemented with increasing concentrations of saccharin. After 12 days, lipid accumulation was evaluated with Oil Red-O. E) WT and T1R2 KO eMSCs were either maintained in calf serum media (D0) or treated with induction media containing DI for 30 min in the absence (-) or presence (+) of 4.5 mM saccharin. Lysates were then collected for immunoblotting. F) WT and T1R2 KO eMSCs were starved for 2 hrs in HBSS and treated for 30 min with increasing concentrations of saccharin (0.02-4.5 mM) before collecting lysates for immunoblotting.

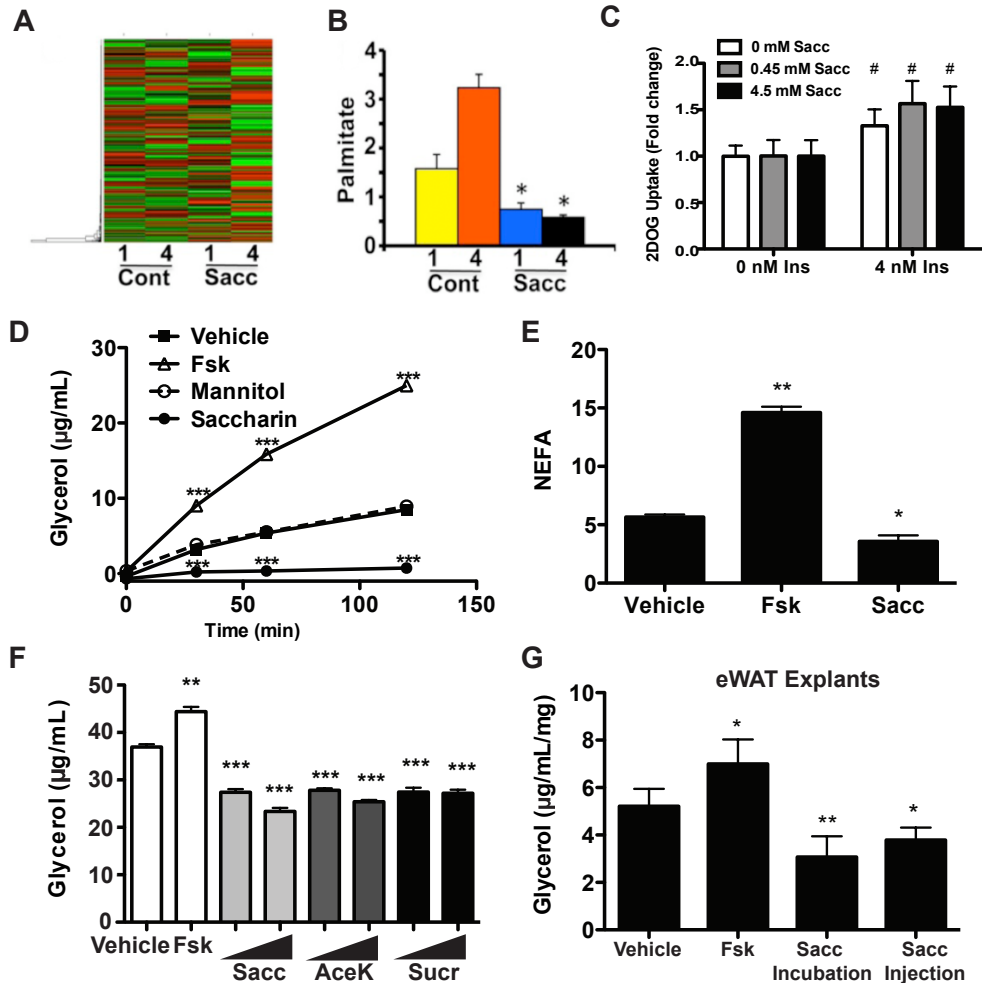


Figure 2.9. Artificial sweeteners suppress lipolysis.

A) Following 1 or 4 hr saccharin treatment, 3T3-L1 adipocytes were flash frozen and intracellular metabolites were evaluated on a LC-MS platform by the University of Michigan Molecular Phenotyping Core. Metscape software was used for pathway visualization and interpretation. Hierarchical clustering shows metabolites that vary with time and/or saccharin treatment, with red being more abundant. B) LC-MS quantification of palmitate following 1 or 4 hr treatment with vehicle or saccharin in 3T3-L1 cells as described in A. C) Glucose uptake was measured in 3T3-L1 adipocytes as described in Methods. Significant differences (P -value <0.05) between 0 and 4 nM insulin denoted #. D) 3T3-L1 adipocytes were serum starved for two hours in HBSS before treatment with 4.5 mM sacc, 4.5 mM mannitol, or 10 μ M of adenylate cyclase activator forskolin (Fsk). Glycerol content of the media was assayed at the indicated time points. E) NEFA (μ M) was measured from assay media under same conditions as D. F) Glycerol content of assay media was measured following 1 hr treatment with sacc, AceK or sucralose at 0.45 and 4.5 mM. G) Epididymal white adipose tissue (eWAT) explants were collected from wild-type mice 20 min following injection of saccharin. Glycerol content of the media was then measured following 4 hr incubation with vehicle, fsk, or saccharin. Significant differences from vehicle treatment (P -values <0.05 , <0.01 , or <0.005) are denoted *, **, or *** respectively. Data are expressed as mean plus S.D. Significance was determined using Student's t-test.

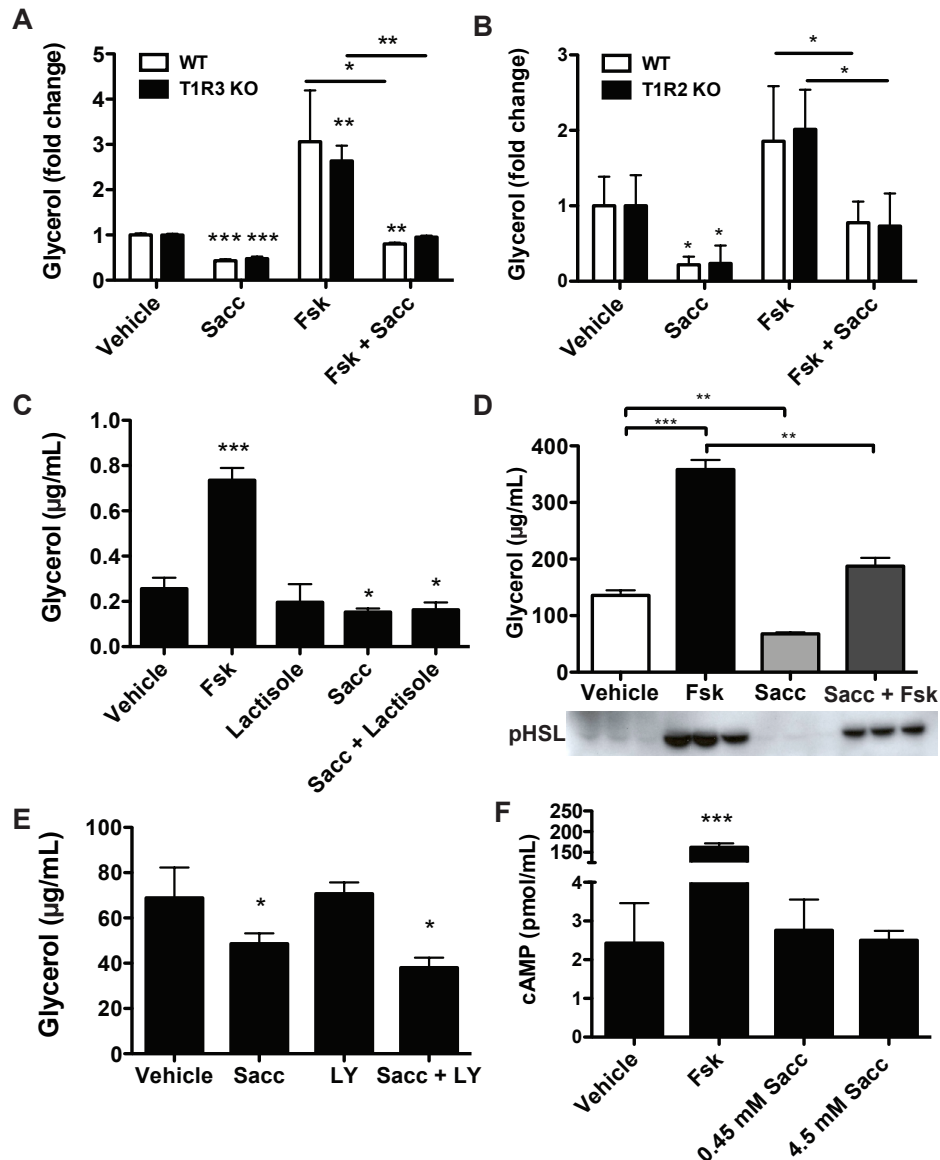


Figure 2.10. T1R2/T1R3 are not required for suppression of lipolysis by saccharin.

A) T1R3 and B) T1R2 KO eMSC adipocytes were treated with sacc, Fsk, or both for 4 hrs before measuring glycerol accumulation in media. C) Human adipocytes were starved in serum-free media for 2 hr and pre-treated with 1.25 mM lactisole for 1 hr before a 2 hr saccharin treatment. Glycerol content was then assayed in media. D) 3T3-L1 adipocytes were treated for one hour with saccharin, forskolin, or both. Glycerol concentration in the media was measured (upper panel) before collecting protein lysates from treated and control cells. Lysates were then probed for phosphorylated hormone sensitive lipase (pHSL) by Western blotting (lower panel). E) 3T3-L1 adipocytes were serum starved for two hours and pre-treated with LY294002 for one hour before a 2 hr saccharin treatment. Glycerol was then measured in assay media. F) 3T3-L1 adipocytes were serum-starved for 2 hrs, then treated for 45 min with Fsk or saccharin. cAMP concentration was then quantified by ELISA. Significant differences (P -values <0.05 , <0.01 , or <0.005) are denoted *, **, or *** respectively. Data are expressed as mean plus S.D. Significance was determined using Student's t-test.

References

- Ahmed, K., Tunaru, S., and Offermanns, S. (2009). GPR109A, GPR109B and GPR81, a family of hydroxy-carboxylic acid receptors. *Trends Pharmacol Sci* 30, 557-562.
- Blackburn, G.L., Kanders, B.S., Lavin, P.T., Keller, S.D., and Whatley, J. (1997). The effect of aspartame as part of a multidisciplinary weight-control program on short- and long-term control of body weight. *Am J Clin Nutr* 65, 409-418.
- Brockhoff, A., Behrens, M., Massarotti, A., Appendino, G., and Meyerhof, W. (2007). Broad tuning of the human bitter taste receptor hTAS2R46 to various sesquiterpene lactones, clerodane and labdane diterpenoids, strychnine, and denatonium. *J Agric Food Chem* 55, 6236-6243.
- Brockhoff, A., Behrens, M., Roudnitzky, N., Appendino, G., Avonto, C., and Meyerhof, W. Receptor agonism and antagonism of dietary bitter compounds. *J Neurosci* 31, 14775-14782.
- Cawthorn, W.P., Bree, A.J., Yao, Y., Du, B., Hemati, N., Martinez-Santibanez, G., and MacDougald, O.A. Wnt6, Wnt10a and Wnt10b inhibit adipogenesis and stimulate osteoblastogenesis through a beta-catenin-dependent mechanism. *Bone* 50, 477-489.
- Colburn, W.A., Bekersky, I., and Blumenthal, H.P. (1981). Dietary saccharin kinetics. *Clin Pharmacol Ther* 30, 558-563.
- Cypess, A.M., Zhang, H., Schulz, T.J., Huang, T.L., Espinoza, D.O., Kristiansen, K., Unterman, T.G., and Tseng, Y.H. Insulin/IGF-I regulation of necdin and brown adipocyte differentiation via CREB- and FoxO1-associated pathways. *Endocrinology* 152, 3680-3689.
- Damak, S., Rong, M., Yasumatsu, K., Kokrashvili, Z., Perez, C.A., Shigemura, N., Yoshida, R., Mosinger, B., Jr., Glendinning, J.I., Ninomiya, Y., *et al.* (2006). Trpm5 null mice respond to bitter, sweet, and umami compounds. *Chem Senses* 31, 253-264.
- Dergance, J.M., Mouton, C.P., Lichtenstein, M.J., and Hazuda, H.P. (2005). Potential mediators of ethnic differences in physical activity in older Mexican

Americans and European Americans: results from the San Antonio Longitudinal Study of Aging. *J Am Geriatr Soc* 53, 1240-1247.

Dotson, C.D., Roper, S.D., and Spector, A.C. (2005). PLCbeta2-independent behavioral avoidance of prototypical bitter-tasting ligands. *Chem Senses* 30, 593-600.

Duncan, R.E., Sarkadi-Nagy, E., Jaworski, K., Ahmadian, M., and Sul, H.S. (2008). Identification and functional characterization of adipose-specific phospholipase A2 (AdPLA). *J Biol Chem* 283, 25428-25436.

Dyer, J., Salmon, K.S., Zibrik, L., and Shirazi-Beechey, S.P. (2005). Expression of sweet taste receptors of the T1R family in the intestinal tract and enteroendocrine cells. *Biochem Soc Trans* 33, 302-305.

Elliott, R.A., Kapoor, S., and Tincello, D.G. Expression and distribution of the sweet taste receptor isoforms T1R2 and T1R3 in human and rat bladders. *J Urol* 186, 2455-2462.

Geraedts, M.C., Takahashi, T., Vignes, S., Markwardt, M.L., Nkobena, A., Cockerham, R.E., Hajnal, A., Dotson, C.D., Rizzo, M.A., and Munger, S.D. Transformation of postingestive glucose responses after deletion of sweet taste receptor subunits or gastric bypass surgery. *Am J Physiol Endocrinol Metab* 303, E464-474.

Gotoh, C., Hong, Y.H., Iga, T., Hishikawa, D., Suzuki, Y., Song, S.H., Choi, K.C., Adachi, T., Hirasawa, A., Tsujimoto, G., *et al.* (2007). The regulation of adipogenesis through GPR120. *Biochem Biophys Res Commun* 354, 591-597.

Hemati, N., Ross, S.E., Erickson, R.L., Groblewski, G.E., and MacDougald, O.A. (1997). Signaling pathways through which insulin regulates CCAAT/enhancer binding protein a (C/EBP α) phosphorylation and gene expression in 3T3-L1 adipocytes: Correlation with GLUT4 gene expression. *J Biol Chem* 272, 25913-25919.

Hong, Y.H., Nishimura, Y., Hishikawa, D., Tsuzuki, H., Miyahara, H., Gotoh, C., Choi, K.C., Feng, D.D., Chen, C., Lee, H.G., *et al.* (2005). Acetate and propionate short chain fatty acids stimulate adipogenesis via GPCR43. *Endocrinology* 146, 5092-5099.

Jang, H.J., Kokrashvili, Z., Theodorakis, M.J., Carlson, O.D., Kim, B.J., Zhou, J., Kim, H.H., Xu, X., Chan, S.L., Juhaszova, M., *et al.* (2007). Gut-expressed gustducin and taste receptors regulate secretion of glucagon-like peptide-1. *Proc Natl Acad Sci U S A* *104*, 15069-15074.

Klemm, D.J., Leitner, J.W., Watson, P., Nesterova, A., Reusch, J.E., Goalstone, M.L., and Draznin, B. (2001). Insulin-induced adipocyte differentiation. Activation of CREB rescues adipogenesis from the arrest caused by inhibition of prenylation. *J Biol Chem* *276*, 28430-28435.

Kuhn, C., Bufe, B., Winnig, M., Hofmann, T., Frank, O., Behrens, M., Lewtschenko, T., Slack, J.P., Ward, C.D., and Meyerhof, W. (2004). Bitter taste receptors for saccharin and acesulfame K. *J Neurosci* *24*, 10260-10265.

Kyriazis, G.A., Soundarapandian, M.M., and Tyrberg, B. (2012). Sweet taste receptor signaling in beta cells mediates fructose-induced potentiation of glucose-stimulated insulin secretion. *Proc Natl Acad Sci U S A* *109*, E524-532.

Liu, C., Wu, J., Zhu, J., Kuei, C., Yu, J., Shelton, J., Sutton, S.W., Li, X., Yun, S.J., Mirzadegan, T., *et al.* (2009). Lactate inhibits lipolysis in fat cells through activation of an orphan G-protein-coupled receptor, GPR81. *J Biol Chem* *284*, 2811-2822.

Liu, D., and Liman, E.R. (2003). Intracellular Ca²⁺ and the phospholipid PIP₂ regulate the taste transduction ion channel TRPM5. *Proc Natl Acad Sci U S A* *100*, 15160-15165.

Lorenz, M.A., Burant, C.F., and Kennedy, R.T. Reducing time and increasing sensitivity in sample preparation for adherent mammalian cell metabolomics. *Anal Chem* *83*, 3406-3414.

Lund, T.C., Kobs, A.J., Kramer, A., Nyquist, M., Kuroki, M.T., Osborn, J., Lidke, D.S., Low-Nam, S.T., Blazar, B.R., and Tolar, J. Bone marrow stromal and vascular smooth muscle cells have chemosensory capacity via bitter taste receptor expression. *PLoS One* *8*, e58945.

Mace, O.J., Affleck, J., Patel, N., and Kellett, G.L. (2007). Sweet taste receptors in rat small intestine stimulate glucose absorption through apical GLUT2. *J Physiol* *582*, 379-392.

Maitrepierre, E., Sigoillot, M., Le Pessot, L., and Briand, L. Recombinant expression, in vitro refolding, and biophysical characterization of the N-terminal domain of T1R3 taste receptor. *Protein Expr Purif* 83, 75-83.

Masubuchi, Y., Nakagawa, Y., Ma, J., Sasaki, T., Kitamura, T., Yamamoto, Y., Kurose, H., Kojima, I., and Shibata, H. A novel regulatory function of sweet taste-sensing receptor in adipogenic differentiation of 3T3-L1 cells. *PLoS One* 8, e54500.

Meyerhof, W., Batram, C., Kuhn, C., Brockhoff, A., Chudoba, E., Bufe, B., Appendino, G., and Behrens, M. The molecular receptive ranges of human TAS2R bitter taste receptors. *Chem Senses* 35, 157-170.

Mori, H., Prestwich, T.C., Reid, M.A., Longo, K.A., Gerin, I., Cawthorn, W.P., Susulic, V.S., Krishnan, V., Greenfield, A., and Macdougald, O.A. (2012). Secreted frizzled-related protein 5 suppresses adipocyte mitochondrial metabolism through WNT inhibition. *J Clin Invest* 122, 2405-2416.

Nakae, J., Kitamura, T., Kitamura, Y., Biggs, W.H., 3rd, Arden, K.C., and Accili, D. (2003). The forkhead transcription factor Foxo1 regulates adipocyte differentiation. *Dev Cell* 4, 119-129.

Nakagawa, Y., Nagasawa, M., Yamada, S., Hara, A., Mogami, H., Nikolaev, V.O., Lohse, M.J., Shigemura, N., Ninomiya, Y., and Kojima, I. (2009). Sweet taste receptor expressed in pancreatic beta-cells activates the calcium and cyclic AMP signaling systems and stimulates insulin secretion. *PLoS One* 4, e5106.

Nelson, G., Hoon, M.A., Chandrashekar, J., Zhang, Y., Ryba, N.J., and Zuker, C.S. (2001). Mammalian sweet taste receptors. *Cell* 106, 381-390.

Nie, Y., Hobbs, J.R., Vignes, S., Olson, W.J., Conn, G.L., and Munger, S.D. (2006). Expression and purification of functional ligand-binding domains of T1R3 taste receptors. *Chem Senses* 31, 505-513.

Nie, Y., Vignes, S., Hobbs, J.R., Conn, G.L., and Munger, S.D. (2005). Distinct contributions of T1R2 and T1R3 taste receptor subunits to the detection of sweet stimuli. *Curr Biol* 15, 1948-1952.

Porikos, K.P., and Koopmans, H.S. (1988). The effect of non-nutritive sweeteners on body weight in rats. *Appetite* 11 Suppl 1, 12-15.

Ren, N., Kaplan, R., Hernandez, M., Cheng, K., Jin, L., Taggart, A.K., Zhu, A.Y., Gan, X., Wright, S.D., and Cai, T.Q. (2009a). Phenolic acids suppress adipocyte lipolysis via activation of the nicotinic acid receptor GPR109A (HM74a/PUMA-G). *J Lipid Res* 50, 908-914.

Ren, X., Zhou, L., Terwilliger, R., Newton, S.S., and de Araujo, I.E. (2009b). Sweet taste signaling functions as a hypothalamic glucose sensor. *Front Integr Neurosci* 3, 12.

Renwick, A.G. (1986). The metabolism of intense sweeteners. *Xenobiotica* 16, 1057-1071.

Rim, J.S., Mynatt, R.L., and Gawronska-Kozak, B. (2005a). Mesenchymal stem cells from the outer ear: a novel adult stem cell model system for the study of adipogenesis. *Faseb J* 19, 1205-1207.

Rim, J.S., Mynatt, R.L., and Gawronska-Kozak, B. (2005b). Mesenchymal stem cells from the outer ear: a novel adult stem cell model system for the study of adipogenesis. *FASEB J* 19, 1205-1207.

Rodin, J. (1990). Comparative effects of fructose, aspartame, glucose, and water preloads on calorie and macronutrient intake. *Am J Clin Nutr* 51, 428-435.

Rosen, E.D., and MacDougald, O.A. (2006). Adipocyte differentiation from the inside out. *Nat Rev Mol Cell Biol* 7, 885-896.

Sweatman, T.W., and Renwick, A.G. (1979). Saccharin metabolism and tumorigenicity. *Science* 205, 1019-1020.

Sweatman, T.W., Renwick, A.G., and Burgess, C.D. (1981). The pharmacokinetics of saccharin in man. *Xenobiotica* 11, 531-540.

Swithers, S.E., and Davidson, T.L. (2008). A role for sweet taste: calorie predictive relations in energy regulation by rats. *Behav Neurosci* 122, 161-173.

Swithers, S.E., Martin, A.A., and Davidson, T.L. High-intensity sweeteners and energy balance. *Physiol Behav* 100, 55-62.

Taggart, A.K., Kero, J., Gan, X., Cai, T.Q., Cheng, K., Ippolito, M., Ren, N., Kaplan, R., Wu, K., Wu, T.J., *et al.* (2005). (D)-beta-Hydroxybutyrate inhibits adipocyte lipolysis via the nicotinic acid receptor PUMA-G. *J Biol Chem* 280, 26649-26652.

Treesukosol, Y., Blonde, G.D., and Spector, A.C. (2009). T1R2 and T1R3 subunits are individually unnecessary for normal affective licking responses to Polycose: implications for saccharide taste receptors in mice. *Am J Physiol Regul Integr Comp Physiol* 296, R855-865.

Treesukosol, Y., Smith, K.R., and Spector, A.C. Behavioral evidence for a glucose polymer taste receptor that is independent of the T1R2+3 heterodimer in a mouse model. *J Neurosci* 31, 13527-13534.

Xu, H., Staszewski, L., Tang, H., Adler, E., Zoller, M., and Li, X. (2004). Different functional roles of T1R subunits in the heteromeric taste receptors. *Proc Natl Acad Sci U S A* 101, 14258-14263.

Zhao, G.Q., Zhang, Y., Hoon, M.A., Chandrashekar, J., Erlenbach, I., Ryba, N.J., and Zuker, C.S. (2003). The receptors for mammalian sweet and umami taste. *Cell* 115, 255-266.

Zukerman, S., Glendinning, J.I., Margolskee, R.F., and Sclafani, A. (2009). T1R3 taste receptor is critical for sucrose but not Polycose taste. *Am J Physiol Regul Integr Comp Physiol* 296, R866-876.

Chapter Three

Metabolic Phenotyping of Sweet Taste Receptor Knockout Mice

Abstract

While functional expression of sweet taste receptors (T1R2 and T1R3) has been reported in many metabolic tissues, including the gut, pancreas, and adipose tissue, adipose tissue phenotypes of T1R2 and T1R3 KO mice have not been reported. Here we provide data to demonstrate that both T1R2 and T1R3 KO mice have reduced adiposity and smaller adipocytes when on an obesogenic diet. However, this is in the absence of any other noted metabolic dysfunction; KO animals show no indication of altered glucose or insulin tolerance. T1R2 KO mice also show no differences in food intake, oxygen consumption, or activity. We observed that while taste receptor KO did not affect adipocyte number in peripheral adipose depots, the number of bone marrow adipocytes is significantly reduced in T1R2 KO animals. Finally, we present data demonstrating that taste receptor KO animals have increased cortical and trabecular bone mass. This report identifies novel metabolic functions for sweet taste receptors in the regulation of adipose and bone biology *in vivo*.

Introduction

Sweet taste perception by the tongue is mediated by the G protein-coupled receptors T1R2 and T1R3 (Nelson et al.; Zhao et al., 2003). These receptors are reported to function as an obligate heterodimer to provide input on the caloric and macronutrient content of ingested food. However, sweet taste receptors have been identified in an increasing number of extra-gustatory tissues

(Elliott et al.; Merigo et al.; Ren et al., 2009), often regulating metabolic processes (Jang et al., 2007; Kokrashvili et al., 2009; Kyriazis et al., 2012; Mace et al., 2007; Margolskee et al., 2007; Nakagawa et al., 2009). Previous reports have shown that mice lacking gustducin, a mediator of taste receptor signaling, have reduced GLP-1 and insulin secretion. This is reportedly on account of the loss of sweet taste receptor activity in GLP-1-secreting enteroendocrine cells in the gut (Jang et al., 2007). In pancreatic β cells, sweet taste receptors act to augment glucose (Nakagawa et al., 2009) or fructose-induced (Kyriazis et al., 2012) insulin secretion.

More recent data suggests that in addition to contributing to insulin and incretin secretion (Kokrashvili et al., 2009; Kyriazis et al., 2012), sweet taste receptors may also have metabolic roles in adipose tissue. T1R2 and T1R3 expression has been reported in 3T3-L1 cells (Fig 2.2; Masubuchi et al., 2013), with the receptors reportedly mediating inhibition of adipogenesis by artificial sweeteners. However, this observation runs counter to our own observations (Fig 2.3) and the paradigm of sweet taste receptors acting as glucose sensors to drive anabolic processes, as had been described in the gut and pancreas. An additional study has shown that T1R3 KO animals are resistant to sucrose-induced obesity and have smaller fat depots on a high-sucrose diet (Glendinning et al. 2012), consistent with a role for sweet taste receptors in facilitating adipose tissue expansion. Despite this contradictory evidence for the role of sweet taste receptors in adipose tissue and the known metabolic functions for these receptors in other tissues, evaluation of adipose tissue phenotypes in T1R2 and T1R3 KO mice has not been performed.

In this report, we investigate whether lack of T1R2 or T1R3 affects metabolic homeostasis by characterizing responses of T1R2 and T1R3 KO mice to a Western diet. We demonstrate that both KO genotypes show a reduction in adiposity and adipocyte size following this dietary intervention. Female, but not male, T1R3 KO animals maintain reduced adiposity on a standard chow diet.

Despite the impaired adipose tissue expansion in taste receptor KO mice, we detected no changes in glucose tolerance, insulin sensitivity, food intake, or oxygen consumption. However, we unexpectedly observed that taste receptor KO reduces adipocyte number in the bone marrow compartment, and increases cortical and trabecular bone mass. These data represent the first demonstration of adipose tissue and bone phenotypes in sweet taste receptor-deficient animals, thereby providing valuable insight into the functions of sweet taste receptors *in vivo*.

Results

T1R3 KO mice have reduced adiposity on Western Diet.

We hypothesized that sweet taste receptors would serve as mediators of 'positive' nutrient signals derived from binding taste receptor ligands in adipose tissue. We therefore anticipated that mice lacking sweet taste receptors might be deficient in adipogenesis or anabolic pathways such as glucose uptake and lipogenesis, and that this might lead to metabolic dysfunction. To assess effects of sweet taste receptor KO on adipose tissue, we subjected WT and T1R3 KO mice to a Western diet challenge for 24 weeks (41% kcal fat, 43% kcal protein, 15% kcal protein, high sucrose and high cholesterol). At the end of this treatment, body weight was identical between genotypes (Fig 3.1A). However, when the body composition of these animals was evaluated, we observed that T1R3 KO animals had reduced fat mass and increased lean mass as percent of body weight (Fig 3.1B). Absolute fat mass was also reduced, though absolute lean mass was unchanged (Fig 3.1C).

To further characterize differences in adiposity in T1R3 KO animals, we measured the weight of individual fat depots (Fig 3.1D). However, we observed no differences in the weights of inguinal, epididymal, or perirenal fat depots. There was also no change in liver or BAT (brown adipose tissue) weight. This disparity between whole body adiposity and fat depot mass could be due to

greater differences in fat depots that were not isolated; accumulation of lipid outside of adipose tissue depots; or it could result from the amalgamation of small changes within individual fat pads that are not grossly apparent. The trend towards reduced mass in all KO tissues suggests that the latter might be the case. Taken together, these data are supportive of a role for taste receptors in regulating adiposity *in vivo*.

T1R3 KO mice have fewer large adipocytes but equal adipocyte number on Western Diet.

Reduced adiposity in T1R3 KO animals could be due to decreased adipocyte number, decreased adipocyte size, or both. To determine if T1R3 was affecting hyperplasia or hypertrophy we measured the areas of adipocytes in epididymal fat of WT and KO mice. We found that the T1R3 KO animals had a shift towards smaller adipocytes (Fig 3.2A), such that the proportion of large adipocytes was significantly reduced (Fig 3.2B). To further explore this observation and estimate relative adipocyte numbers between genotypes, we correlated average adipocyte volume with fat depot weight for each animal. There was no difference between slopes in this correlation analysis (Fig 3.2C), suggesting each genotype had similar numbers of adipocytes per gram fat depot between genotypes. We then estimated the total number of adipocytes in the epididymal fat pad by dividing fat pad weight by average adipocyte weight, as has been previously described (Hirsch and Batchelor, 1976; Nestel et al., 1969; Pasarica et al., 2009). This analysis also suggests that there was no significant change in adipocyte number between genotypes (WT= 7,020,000, S.D. 1,803,301; T1R3 KO= 7,470,000, S.D. 2,270,000). These data indicate that while T1R3 KO animals have no deficiency in adipogenesis in peripheral fat depots, they do maintain smaller adipocytes. This phenotype could be a cause or a consequence of metabolic disturbances elsewhere.

T1R3 KO mice have no changes in glucose sensitivity.

Given the smaller adipocytes present with T1R3 KO, we hypothesized that these animals might have elevated rates of lipolysis. To test this, we measured plasma NEFA concentrations in WT and T1R3 KO animals (Fig 3.3A). However, we observed no alterations in circulating NEFA between genotypes. We next hypothesized that the reduced adiposity in T1R3 KO animals might lead to reduced leptin secretion. However as with NEFA, we observed no differences between genotypes (Fig 3.3B). We next investigated whether sweet taste receptor KO animals were glucose intolerant, as this might be a consequence of impaired adipose tissue expansion. To assess this, we performed intraperitoneal glucose tolerance tests (GTTs) on male and female T1R3 KO mice. Firstly, we observed that in male T1R3 KO mice there was no significant difference in blood glucose at any time point following glucose injection, suggesting that these animals are not acutely deficient in glucose clearance (Fig 3.3C, left panel). However, the area under of the curve (AUC) of GTTs from T1R3 KO animals was significantly greater (Fig 3.3C, right panel), suggesting that male T1R3 KO mice may be mildly glucose intolerant. However, fasting glucose was not different between genotypes (Fig 3.3C, left panel). In female mice, we observed no differences in individual time points or AUC of the GTT time course, and fasting glucose also did not differ between females (Fig 3.3D). To further investigate the possible impairment of glucose tolerance in male KO animals, we performed an intraperitoneal insulin tolerance test (ITT). However, these animals showed no difference in this measure of insulin sensitivity at either individual time points or in total AUC (Fig 3.3E). These data suggest that while T1R3 expression may be a regulator of adipocyte size and adiposity, this phenotype does not result in glucose intolerance or clear metabolic impairments.

T1R3 KO mice have sexually dimorphic reductions in adiposity on chow diet.

The above observations indicate that T1R3 KO mice fed a Western diet have reduced adiposity and smaller adipocytes. However, we were unsure if a

Western diet challenge was necessary to drive this phenotype, or if it would also be observed under non-obesogenic conditions. To answer this question, we maintained WT and T1R3 KO mice on a chow diet into adulthood (~12 weeks), after which body weight and body composition were periodically measured. Using this strategy, we observed no difference in body weight (Fig 3.4A, left panel), fat mass (Fig 3.4A, middle panel), or lean mass (Fig 3.4A, right panel) in male mice throughout 18 weeks of monitoring. Upon removing and weighing adipose depots and other tissues from male mice, we noted that the gonadal fat depot and liver were significantly lighter (Fig 3.4B, left panel), although these differences were no longer apparent when tissue weights were normalized to body weights (right panel). However, when we evaluated female mice from the same cohort, we observed a much stronger phenotype. Female animals had reduced body weight from adulthood and throughout the 18 weeks of monitoring (Fig 3.4A, left panel). In addition, female mice had significantly reduced fat mass (Fig 3.4A, middle panel) and lean mass (Fig 3.4A, right panel). This contrasts with the increased lean mass of males fed a Western diet (Fig 3.1B). Adipose depots were also significantly lighter in females (Fig 3.4B, left panel). Unlike in males, tissue weight reductions were not entirely negated after normalizing to body weight (Fig 3.4B, right panel), as gonadal and inguinal depots remained significantly lighter. These data suggest that while T1R3 KO may contribute to regulation of adiposity on a chow diet, this regulation is only pronounced in female mice.

T1R2 KO mice have reduced adiposity on Western Diet.

We continued our investigation of sweet taste receptor functions in adipose tissue by examining the adiposity of T1R2 KO mice under Western diet challenge. As T1R2 and T1R3 are reported to heterodimerize to form a fully functional taste receptor, we anticipated that T1R2 KO animals should mirror the phenotypes of T1R3. We therefore placed adult T1R2 KO animals on Western diet and evaluated their body composition throughout a time course of diet-induced obesity. At the initiation of the experiment, T1R2 KO animals were

heavier than wild type controls. However, after 14 weeks of Western diet feeding there was no significant difference in body weight (Fig 3.5A). After 5 weeks of feeding, fat mass was reduced in T1R2 KO both as percent of body weight (Fig 3.5B) or in absolute mass (Fig 3.5C), which persisted for the remainder of the experiment. Likewise, lean mass was also increased (Fig 3.5D,E). Examining individual fat depots to further characterize loss of adiposity, we observed that like T1R3, several adipose depots were significantly lighter following Western diet feeding (Fig 3.5F). As we predicted, these data are consistent with observations in T1R3 KO animals and a model of T1R2 and T1R3 regulating adiposity.

T1R2 KO mice have smaller adipocytes but equal adipocyte numbers.

As the reduced adiposity in T1R2 KO mice mirrored that of T1R3 KO animals, we investigated whether adipocyte size was similarly altered between genotypes. We performed frequency analysis of adipocyte size in WT and T1R2 KO epididymal fat depots, and observed a shift towards smaller adipocytes (Fig 3.6A), as observed in T1R3 KO animals. Indeed, T1R2 KO animals had a significantly greater proportion of small adipocytes and a significantly lower proportion of large adipocytes (Fig 3.6B). Finally, we again estimated relative adipocyte number between genotypes by correlating average adipocyte volume with fat depot weight (Fig 3.6C). As observed T1R3 KO animals, there was no difference between slopes in these correlations, suggesting an equal number of adipocytes per gram of adipose tissue. We further estimated adipocyte number in the epididymal fat depot by the same method used in T1R3 adipocytes. We calculated 6,850,000 (S.D 1,170,000) adipocytes in the WT fat depot, and 6,370,000 (S.D. 1,020,000) in T1R2 KO depot. This effect, like that in T1R3 KO animals, was not significant. However, the phenocopying of adipocyte size between genotypes supports a role for a heterodimeric T1R2/T1R3 sweet taste receptor in regulating adipose tissue biology.

T1R2 KO mice have no changes in glucose sensitivity.

As T1R2 KO mice also had reduced adiposity, we evaluated energy balance in these animals to determine if they had altered lipid utilization or increased activity might contribute to this effect. However, after utilizing Comprehensive Animal Monitoring System (CLAMS) cages, we observed no differences in RQ (Fig 3.7A), total activity (Fig 3.7B), or oxygen consumption (data not shown). Food intake was also not different (Fig 3.7C). We next evaluated glucose homeostasis in T1R2 KO animals and observed that, like T1R3 KO mice, there was no difference in random-fed glucose (Fig 3.7D) or glucose tolerance (Fig 3.7E). Lastly, we measured circulating NEFA concentrations, as reduced adipocyte size could reflect increased lipolytic rates. However as with T1R3 KO, T1R2 KOs showed no difference in serum NEFA (Fig 3.7F).

The reduced-adiposity phenotype of T1R2 KO animals has low penetrance.

Our first cohort of T1R2 KO mice showed reduced adiposity relative to WT animals (Fig 3.5). We aimed to further verify this phenotype by repeating Western diet feeding in additional T1R2 KO animals. However, we failed to observe any changes in adiposity in three subsequent cohorts of T1R2 KO animals (data not shown). These data may indicate that T1R2 effects on adiposity are very subtle and easily overwhelmed by animal variation. This is supported by a trend towards smaller fat pads in several KO cohorts. Further experiments will be necessary to determine the reproducibility of this observation.

T1R2 KO mice have fewer bone marrow adipocytes.

Both T1R2 and T1R3 KO results in reduced adiposity and smaller adipocytes in peripheral adipose tissue depots. However, these are not the only metabolically important adipocyte populations; bone marrow adipocytes are emerging as an increasingly important regulator of metabolism (Lecka-Czernik; Shockley et al., 2009). We therefore examined adipocyte populations in the bone marrow cavity of T1R2 KO mice by osmium tetroxide staining (Fretz et al.; Pasarica et al., 2009). Interestingly, μ CT scans of osmium-stained tibiae showed

a reduction in the number of bone marrow adipocytes in KO animals (Fig 3.8A). Quantification of this staining confirmed that adipose tissue volume in bone marrow of medial tibiae was significantly reduced in T1R2 KO animals (Fig 3.8B). This was further verified by histological analysis, in which fewer bone marrow adipocytes were apparent in osmium-stained sections of T1R2 KO tibias (Fig 3.8C). These observations suggest that lack of T1R2 may block adipogenesis in the bone marrow microenvironment.

T1R3 KO animals trend towards fewer bone marrow adipocytes.

To comprehensively assess the contribution of taste receptors to adipocyte number in the bone marrow compartment, we also quantified bone marrow adipocytes in T1R3 KO animals (Fig 3.9A). Here we observed that while there is a trend towards reduced numbers of adipocytes in the media tibia ($P=0.17$), this effect is not significant. These results suggest that while T1R2 may be essential for adipogenesis in the bone marrow compartment, this necessity might not be maintained with T1R3.

T1R2 KO animals have increased trabecular bone.

Our data indicate that loss of T1R2 and T1R3 in the bone marrow cavity may inhibit adipogenesis. As osteogenesis and adipogenesis are known to be reciprocally regulated (Akune et al., 2004; Kawai and Rosen) we evaluated the bone mass of these animals to determine if osteogenesis was also stimulated. We performed μ CT scans of WT and T1R2 KO mouse tibiae to assess the quantity and architecture of cortical and trabecular bone. We observed that T1R2 KO animals on Western diet had increased trabecular area (Fig 3.10A) and increased trabecular bone mineral content (BMC, Fig 3.10B). This combination results in very little change in trabecular bone mineral density (BMD, Fig 3.10C), as greater BMC is diffused over the larger trabecular area. Alterations in cortical bone were more modest; we observed an increase in cortical area (Fig 3.10D), but no change in cortical BMC (Fig 3.10E) or BMD (Fig 3.10F). These results

suggest that T1R2 activation may have a role in blocking osteogenesis, consistent with a pro-adipogenic role in the bone marrow cavity.

T1R3 KO animals have increased cortical and trabecular bone.

To determine if T1R2 KO effects on bone formation were conserved with T1R3, we independently evaluated bone mass in femurs of T1R3 KO mice on Western Diet for 24 weeks. We observed several significant differences within cortical bone (Fig 3.11A). Cortical area (Fig 3.11A, left panel) and cortical BMC (Fig 3.11A, middle panel) were both increased, with cortical BMD (Fig 3.11A, right panel) unchanged. This increase in cortical bone was reflected in the larger inner and outer cortical perimeter in T1R3 KO mice (Fig 3.11B, left and middle panel), and a larger marrow area (Fig 3.11B, right panel). T1R3 KO also produced pronounced changes in trabecular bone. Trabecular BMD and tissue mineral density (TMD) were both increased (Fig 3.11C, right and middle panels), as was the thickness of individual trabeculae (Fig 3.11C, right panel). These data, taken together with increased bone mass in T1R2 KO animals, suggest that sweet taste receptors may have a previously uncharacterized role in the development or maintenance of both adipose tissue and bone.

Discussion

In this chapter, we present results demonstrating reduced adiposity and smaller adipocytes in T1R3 and T1R2 KO animals on Western diet. In accordance with a previously published report (Geraedts et al., 2012), we observed no effect on intraperitoneal glucose tolerance with either T1R2 or T1R3 KO. We also observed no differences in any other measured metabolic parameters, including circulating NEFA or random-fed glucose. Surprisingly, we also observed that T1R2 and T1R3 KO mice have increased bone mass; to our knowledge, this is also the first report of sweet taste receptors having a role in bone or bone marrow biology.

While our *in vitro* studies have thus far failed to identify a specific function for sweet taste receptors in 3T3-L1 cells or eMSCs (Chapter Two), the presence of an adipose tissue phenotype in T1R2 and T1R3 KO animals suggests that these receptors may be involved in adipose biology *in vivo*. While the mechanism for reduced adiposity and smaller adipocytes remains unclear, we can speculate on the driving forces behind this phenotype. Smaller adipocytes are unlikely to be driven by alterations in lipolysis, as lipolytic effects observed *in vitro* are independent of sweet taste receptor activity (Fig 2.10). It is also unlikely that lighter pads are due to failures in adipogenesis, as adipocyte number in epididymal fat depots was similar between genotypes. In the absence of changes in food intake and activity, these results allow speculation that sweet taste receptors could have a role in lipid utilization, adipocyte expansion, or hormone secretion that results in reduced adiposity. However, in the absence of adipose tissue-specific sweet taste receptor knockout animals, it remains possible that sweet taste receptors impact adipose biology by acting in other tissues, such as the gut or pancreas.

Reciprocal regulation of bone mass and bone marrow adipocytes is perhaps the most surprising finding of this study. While we cannot interpret the loss of bone marrow adipocytes in T1R2 KO animals as a failure of adipogenesis *per se*, the concurrent increase in bone mass suggests taste receptor involvement in an osteogenesis-adipogenesis development axis. Further studies will be necessary to delineate taste receptor expression profiles in osteoblasts and osteoclasts, and to evaluate the effects of sweet taste receptor agonism on bone development. An additional surprising finding is sexual dimorphism of T1R3 effects on adiposity on a chow diet. The factors that might make female mice more susceptible to the effects of taste receptor deficiency are unknown, but estrogens or other sex hormones may play an uncharacterized role in taste receptor metabolism.

While there have been some reports of metabolic phenotypes in taste receptor KO animals, these studies have primarily been performed to characterize sweet taste receptor activity in the gut and pancreas. In such studies, T1R3 KO mice have impaired glucose tolerance in response to oral, but not intraperitoneal glucose tolerance tests (Geraedts et al., 2012). This result emphasizes taste receptor-stimulated GLP-1 secretion in the gut, rather than taste receptor-stimulated insulin secretion in the pancreas, as a primary driver of glucose homeostasis. However, an independent report shows that T1R2 expression is necessary for fructose-, but not glucose-stimulated insulin secretion from the pancreas (Kyriazis et al., 2012). Taken together, these results suggest that the sweet taste receptors of the gut and pancreas may have differential impacts on glucose homeostasis when presented with different diets. A similar paradigm may affect adipose tissue, in which the availability of an endogenous ligand may affect receptor activation and our interpretation of the role of sweet taste receptors.

Interestingly, there is also evidence that sweet taste receptors in the gut, like those in tongue, might function as homodimers. Geraedts *et al* noted that T1R3 KO mice have impaired glucose tolerance in an oral GTT, but T1R2 KO had no effect. This study, among others, suggests that T1R3 may be capable of binding sweeteners in the absence of T1R2 (Nie et al., 2005), or be able to compensate for the absence of T1R2. In the context of this study, it appears that both T1R2 and T1R3 may contribute to adiposity *in vivo*. However, it is possible that the less penetrant T1R2 effects on adiposity imply a solely T1R3-dependent mechanism. Further studies will be necessary to clarify possible independent roles for sweet taste receptors *in vivo*.

Materials and Methods

Animal Care and Maintenance

T1R2 and T1R3 KO animals were obtained from Björn Tyrberg (Sanford-Burnham Medical Research Institute, Lake Nona, FL), and originally developed by (Zhao et al., 2003) (Charles Zuker; Columbia University, NY). Mice had been backcrossed to 95-99% congenicity with C57BL/6J and were then further backcrossed up to four generations. *Lep^{db/db}* were obtained from The Jackson Laboratory (Bar Harbor, ME). Mice were maintained on either a normal chow diet (5001, LabDiet, PMI Nutrition International, St. Louis MO) or Western Diet (D12079B, Research Diets, New Brunswick NJ) as indicated. All mice were housed on a 12-hour light/12-hour dark cycle in the Unit for Laboratory Animal Medicine (ULAM) at the University of Michigan, with free access to food and water. Procedures for this work were approved by the Committee on the Use and Care of Animals at the University of Michigan, with daily care of animals overseen by the unit for laboratory animal medicine (PRO0001369).

Animal Measurements

Blood glucose levels were measured on an automated blood glucose reader (Accu-Check, Roche Diagnostics, Indianapolis, IN). Body fat, lean mass, and free fluid were measured in conscious animals using an NMR analyzer (Minispec LF9011, Brucker Optics, Billerica MA) in the phenotyping core of the Nutrition Obesity Research Center at the University of Michigan. Oxygen consumption (VO_2), carbon dioxide production (VCO_2), spontaneous motor activity and food intake were measured using the OxyMax Comprehensive Lab Animal Monitoring System (CLAMS, Columbus Instruments; Columbus OH), an integrated open-circuit calorimeter equipped with an optical beam activity-monitoring device. The measurements were carried out continuously for 72 h. During this time, animals were provided free access to food and water through the equipped feeding and drinking devices located inside the chamber. Respiratory quotient (RQ) was calculated as VCO_2 / VO_2 .

Adipocyte Size Quantification

To begin analyzing the adipose tissue, 100-500 mg of epididymal white adipose tissue (eWAT) acquired during murine necropsy was weighed, placed into a 2.5 mL tube and covered with 4% formalin for a minimum of 3 days. 48 hours prior to paraffin fixation samples were removed from formalin and placed into 70% ethanol. A Leica 2155 rotary paraffin microtome was subsequently used to face-off to the apex of the fixed tissue following which a minimum of five 5 μm sections were made at 100 μm intervals across the entire sample. Slides were then placed in a 60°C oven for 1 hour to initiate deparaffinization, stained using Gills' hematoxylin and eosin and mounted with a xylene based mounting media for a minimum of 24 hours prior to image acquisition. Using a Zeiss inverted confocal microscope 1-5 representative photos of each section were taken at 40X objective in black and white using an AxioCAM MrC. To quantify the area of the individual adipocytes a semi-automated custom image analysis was developed using MetaMorph Microscopy Automation and Image Analysis software. A description of the program is as follows. Based on the magnification, each image was first calibrated to a distance of 0.6812 μm pixel⁻¹. Adipocyte cell membranes were enhanced by 3 pixels through erosion filtration to improve the cell boundaries. Histological images were segmented by an inclusive threshold filtration (200 low and 255 high) creating a binary mask and converting the image to a 1-bit configuration. Any adipocytes with visible lacerations to the membranes were closed manually prior to continuing with the automated area quantification. To quantify the adipocyte areas, images were analyzed and adipocytes highlighted if they met the following four criteria; 1. The adipocyte contained an area between 500-15000 μm^2 , 2. The adipocyte had a shape factor of 0.35-1 (a shape factor of 0 indicating a straight line and 1 a perfect circle), 3. The adipocyte had an equivalent sphere surface area between 5000-1000000 μm^2 , 4. The adipocyte did not border the image frame. 70% of tissue adipocytes met these criteria and were picked up automatically while 10% of remaining adipocytes that met the aforementioned criteria, were not picked up by the automated program but were none-the-less incorporated in the analysis manually. To visualize the adipocytes more clearly and provide traceability for

their respective quantified areas, each adipocyte was subsequently labeled with a unique number. The unique adipocyte number and their respective area could then be exported for statistical analysis. To analyze the data, adipocyte areas from each tissue were grouped and distributed according to their areas into bins representing 500 μm^2 increments.

Glucose Tolerance

Mice were fasted for 16 hours with free access to water. Each mouse was then weighed and glucose measured from tail blood with Accu-Chek Aviva Glucometer (Roche). After obtaining baseline glucose measurements, each mouse was then injected intraperitoneally with a sterile solution of D-glucose at 1mg/kg. Blood glucose measurements were then taken from tail bleeds for each animal at 15, 30, 60, 90 and 120 minutes.

Insulin Tolerance

Mice were fasted for 6 hours with free access to water. Each mouse was then weighed and glucose measured from tail blood with Accu-Chek Aviva Glucometer (Roche). After obtaining baseline glucose measurements, each mouse was then injected intraperitoneally with a sterile solution of insulin at 0.75U/kg. Blood glucose measurements were then taken from tail bleeds for each animal at 15, 30, 60, 90 and 120 minutes.

Food Intake

Food dispensed into animal cages was initially weighed, and subsequently reweighed every 7 days for 5 weeks. Wasted food was also measured by sifting animal bedding and was deducted from consumed food weights.

Osmium Staining

BM adipocytes were labeled with osmium tetroxide as follows: first, bones were decalcified for 14 days in 14% EDTA, pH7.4; second, wash bones for 3 x 10 min in Sorensen's Phosphate buffer, pH 7.4, or in PBS; third, stain bones in 1%

osmium tetroxide for 24 h; fourth, wash bones for 3 x 4-6 h in Sorensen's Phosphate buffer, pH 7.4; fifth, re-scan bones with μ CT, as described above; sixth, identify the tibia/fibula junction; seventh, determine the number of slices between the tibia/fibula junction and the growth plate in the same bone prior to decalcification, and then subtract this number to identify the growth plate on the osmium scan; eighth, use a threshold of 400 to quantify the marrow fat (exclude any fat in attached tissues) between the growth plate and tibia/fibula junction on the osmium-stained bone. Decalcification, osmium staining and wash steps were done at room temperature.

μ CT Scanning

Mouse specimens were embedded in 1% agarose and scanned using a microCT system (μ CT100 Scanco Medical, Bassersdorf, Switzerland). Agarose-embedded femoral heads of rabbits were placed in a 48 mm diameter tube prior to scanning the femoral neck using the following settings: voxel size 36 μ m, 70 kVp, 114 μ A, 0.5 mm AL filter, and integration time 500 ms. Trabeculae were analyzed by contouring the inner trabecular compartment using the manufacturer's software (Analysis #15: trabecular, threshold 220), starting 20 slices away from the growth plate and contouring every 10 slices for a total of 30 slices. Agarose-embedded mouse bones were placed in a 19 mm diameter tube prior to scanning the length of the bones using the following settings: voxel size 12 μ m, medium resolution, 70 kVp, 114 μ A, 0.5 mm AL filter, and integration time 500 ms. Density measurements were calibrated to the manufacturer's hydroxyapatite phantom. Analysis was performed using the manufacturer's evaluation software. Mouse cortical bone was analyzed with a threshold of 280, as follows: 1, the growth plates and tibia/fibula junction were identified and the distance in slices between the two calculated; 2, 70% of this distance was calculated and added to the growth plate landmark; 3, contour at this slice; 4, contour 30 slices up from this initial slice; 4, iterate between these two contours using an outer value of 0 and an inner value of 280, using the stop button to stop. Mouse trabeculae were

analyzed using a threshold of 180, as follows: 1, identify the growth plate and go down five slices; 2, draw an internal outline every 10 slices for 50 slices; 3, back-calculate using an outer value of 272 and an inner value of 0. The total volume of mouse bones was determined by contouring around the entire bone between the growth plate and tibia/fibula junction, and then calculating the bone volume and total volume using a threshold of 220.

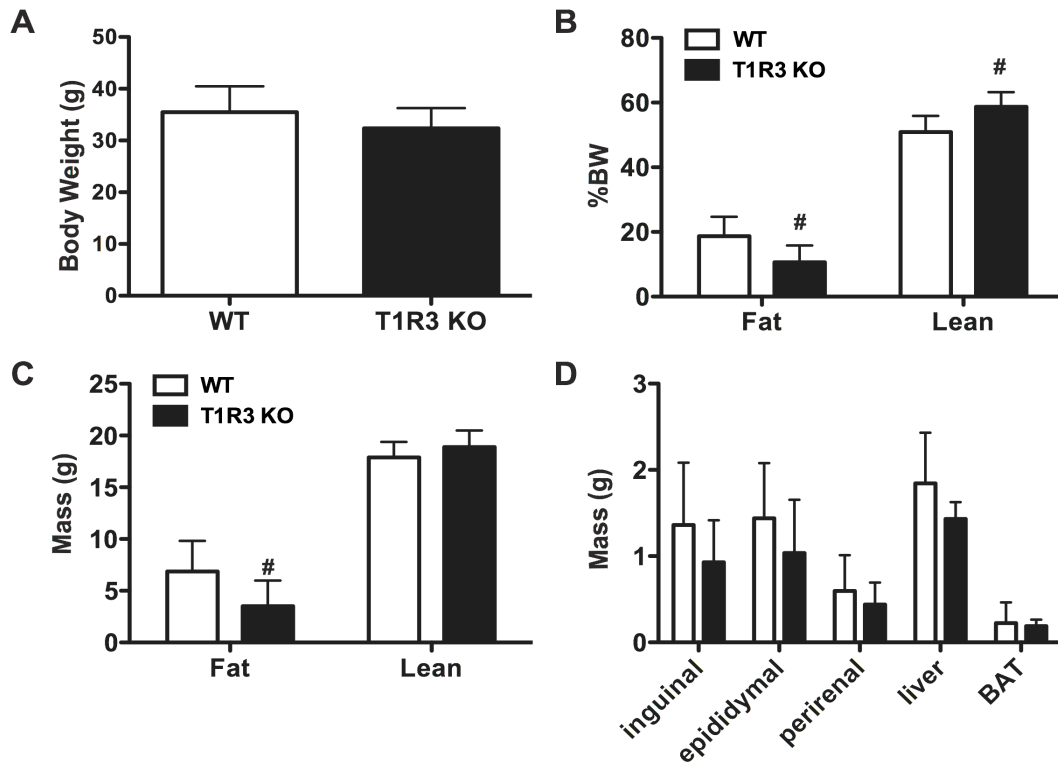


Figure 3.1. Male T1R3 KO mice have reduced adiposity on Western Diet.

A) Body weight in WT (n=7) and T1R3 KO (n=8) animals after 24 weeks of Western Diet feeding. Data are expressed as mean plus S.D. Fat mass and lean mass as percent of body weight B) or in absolute mass C) measured by NMR in WT (n=7) and T1R3 KO (n=8) animals after 24 weeks Western Diet. Data are expressed as mean plus S.D. D) Mass of inguinal, epididymal, or perirenal fat pads, liver, and brown adipose tissue (BAT) following 24 weeks of Western Diet feeding. Data are expressed as mean plus S.D. Significance was determined using Student's t-test. *P*-values <0.05 are indicated with #.

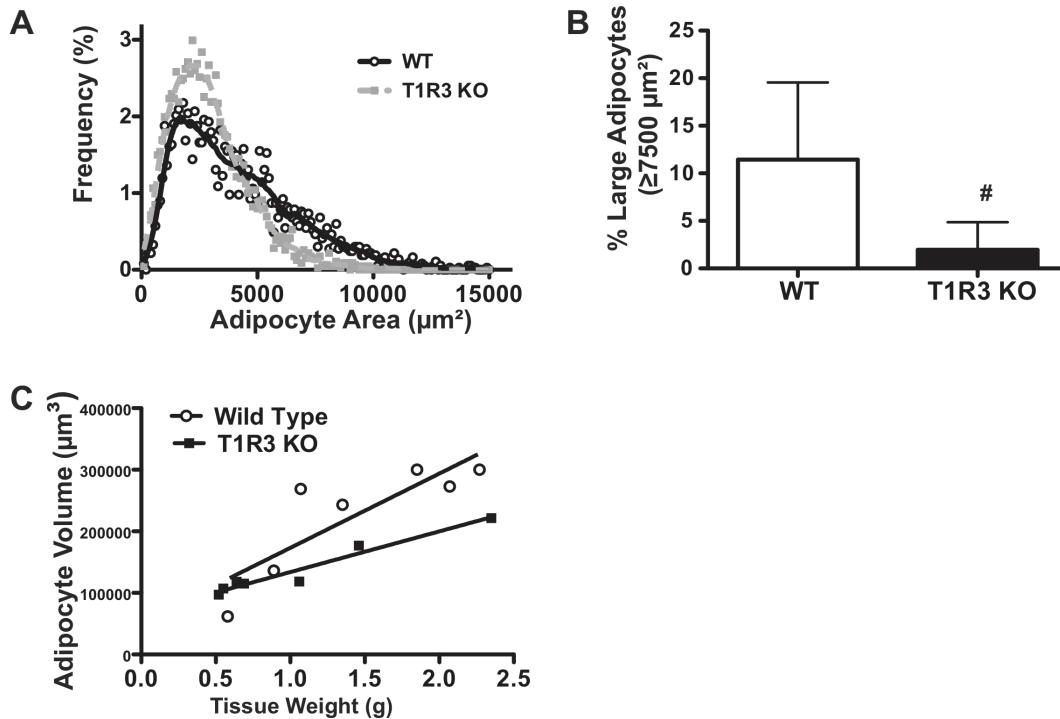


Figure 3.2 T1R3 KO mice have fewer large adipocytes but equal adipocyte number on Western Diet

A) Adipocyte size frequency distribution in WT and T1R3 KO mice on Western Diet shows a shift towards smaller adipocytes in T1R3 KO animals. B) T1R3 KO animals show a decreased frequency of large adipocytes, defined as having a surface area greater than $7500 \mu\text{m}^2$, relative to WT animals following Western Diet feeding. Significance was determined using Student's t-test. *P*-values <0.05 are indicated with # in male mice. Data are expressed as mean plus S.D. C) Epididymal fat pad weight was correlated with average adipocyte volume of WT and T1R3 KO mice to estimate number of adipocytes per gram adipose tissue.

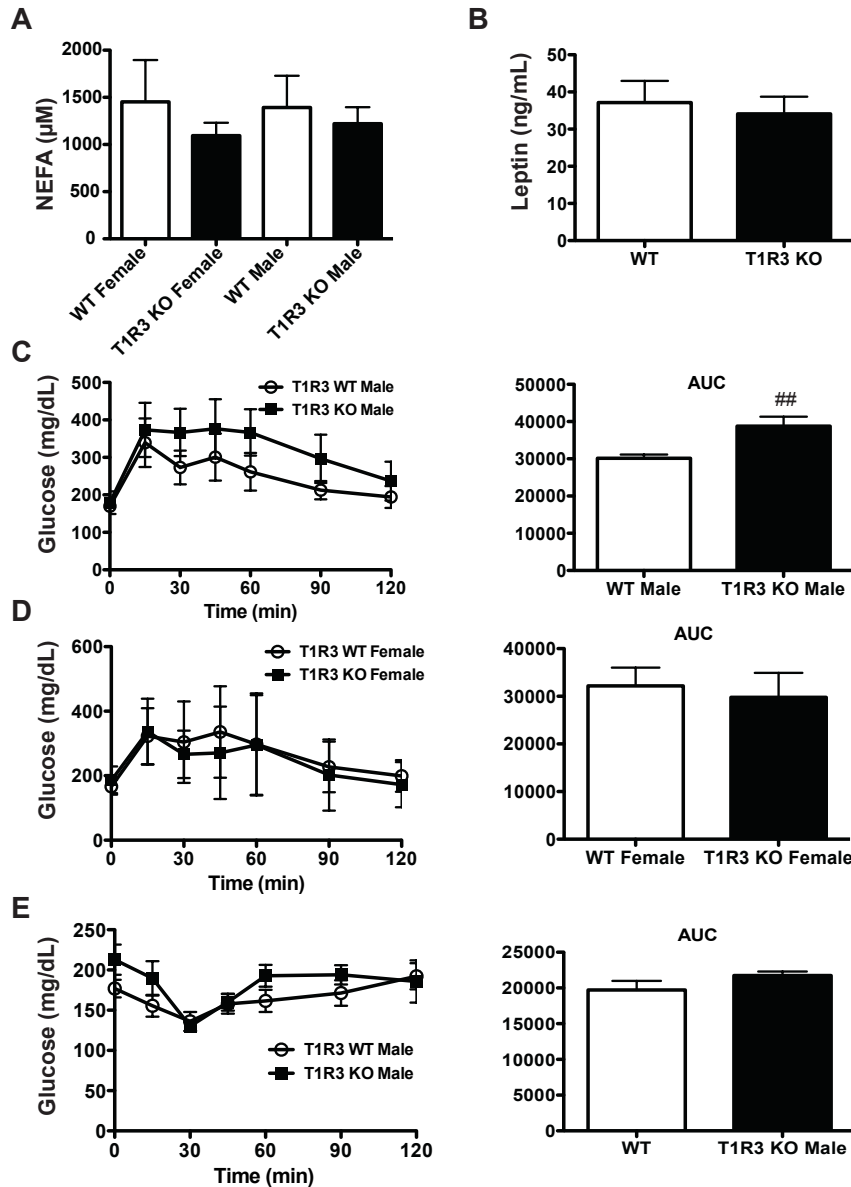


Figure 3.3 T1R3 KO mice have no changes in glucose sensitivity.

A) Non-esterified fatty acids measured from serum of WT (n=6) and T1R3 KO (n=9) mice. NEFA, non-esterified fatty acid. Data are expressed as mean plus S.D. B) Leptin measured from serum of male WT (n=7) and T1R3 KO (n=8) mice on Western Diet for 24 weeks. Data are expressed as mean plus S.D. C) Intraperitoneal glucose tolerance test (left panel) in male WT (n=6) and T1R3 KO (n=9) mice on Western diet for 24 weeks. Quantification of area under the curve (right panel). Data are expressed as mean plus S.D. D) Intraperitoneal glucose tolerance test (left panel) in female WT (n=8) and T1R3 KO (n=6) mice on Western diet for 24 weeks. Quantification of area under the curve (right panel). Data are expressed as mean plus S.D. E) Intraperitoneal insulin tolerance test (left panel) in male WT and T1R3 KO mice from C. Quantification of area under the curve (right panel). Data are expressed as mean plus S.D. Significance was

determined using Student's t-test. P-values <0.01 are indicated with ##.

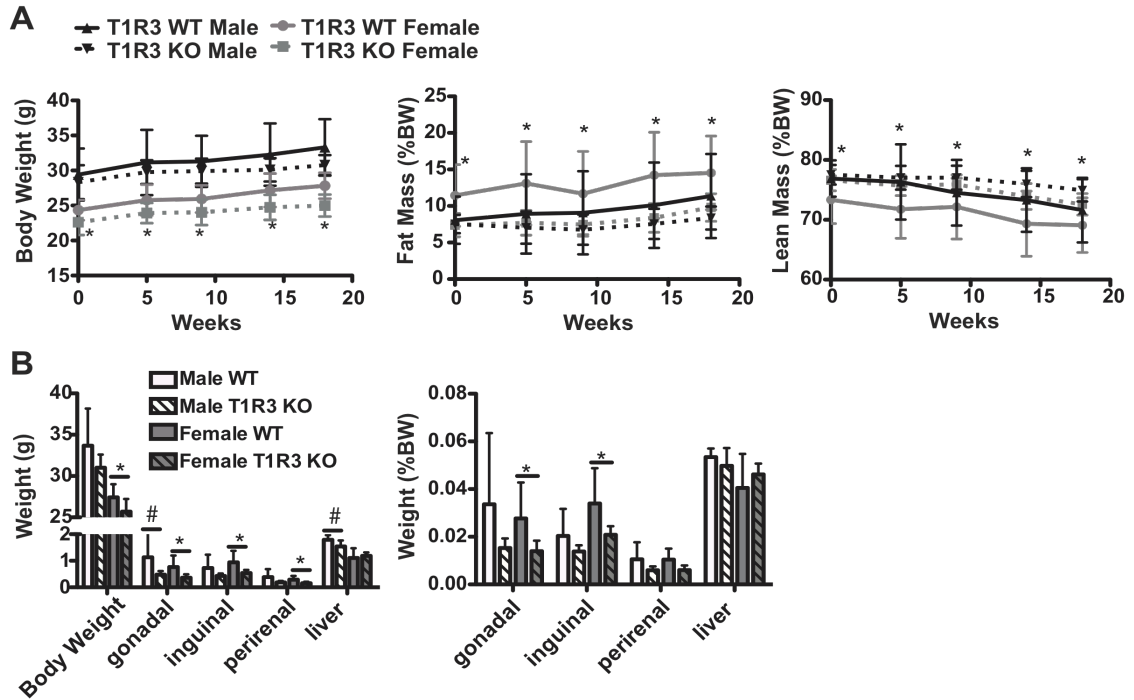


Figure 3.4 T1R3 KO mice have sexually dimorphic reductions in adiposity on chow diet.

A) Body weight (left panel), fat mass (middle panel), and lean mass (right panel) of male and female WT and T1R3 KO mice on chow diet were monitored for 18 weeks, starting at ~12 weeks of age. Male WT n=9, male KO n=9, female WT n=10, female KO n=9. B) Final body and tissue weights in grams (left panel) or as percent of body weight (left panel) of WT and T1R3 KO mice on Chow diet. Significance was determined using Student's t-test. P-values <0.05 are indicated with * in female mice and # in male mice. Data are expressed as mean plus S.D.

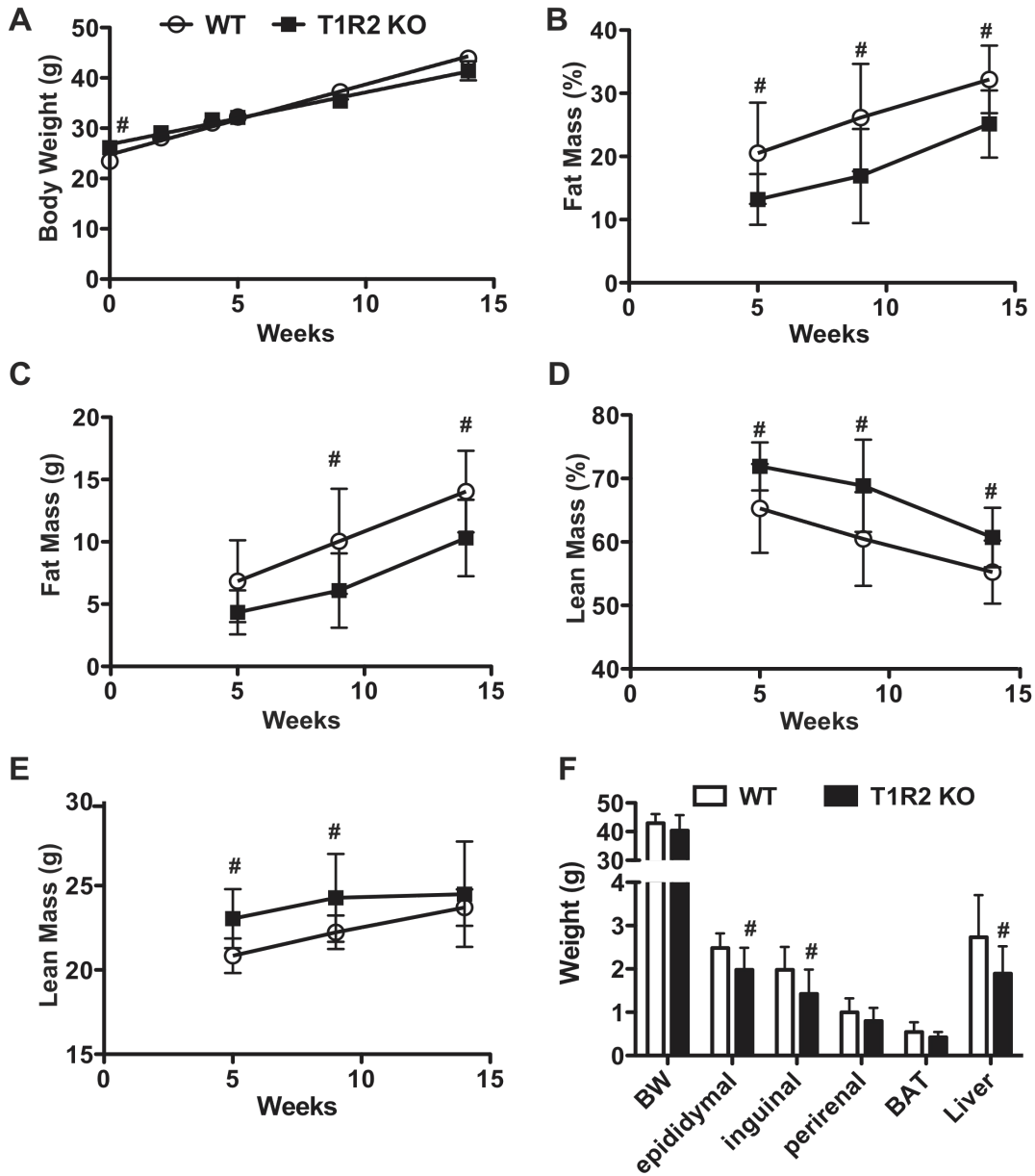


Figure 3.5 T1R2 KO mice have reduced adiposity on Western Diet

A) Body weight in WT(n=9) and T1R2 KO (n=9) mice on Western Diet for 14 weeks. B) Fat as percent of body weight or C) as mass in WT and T1R2 KO mice on Western diet for 14 weeks. D) Lean mass as percent of body weight or E) as mass in WT and T1R2 KO animals on Western diet for 14 weeks. F) Adipose depot and liver weights following Western diet feeding. Data are expressed as mean and S.D. Significance was determined using Student's t-test. *P*-values <0.05 are indicated with #.

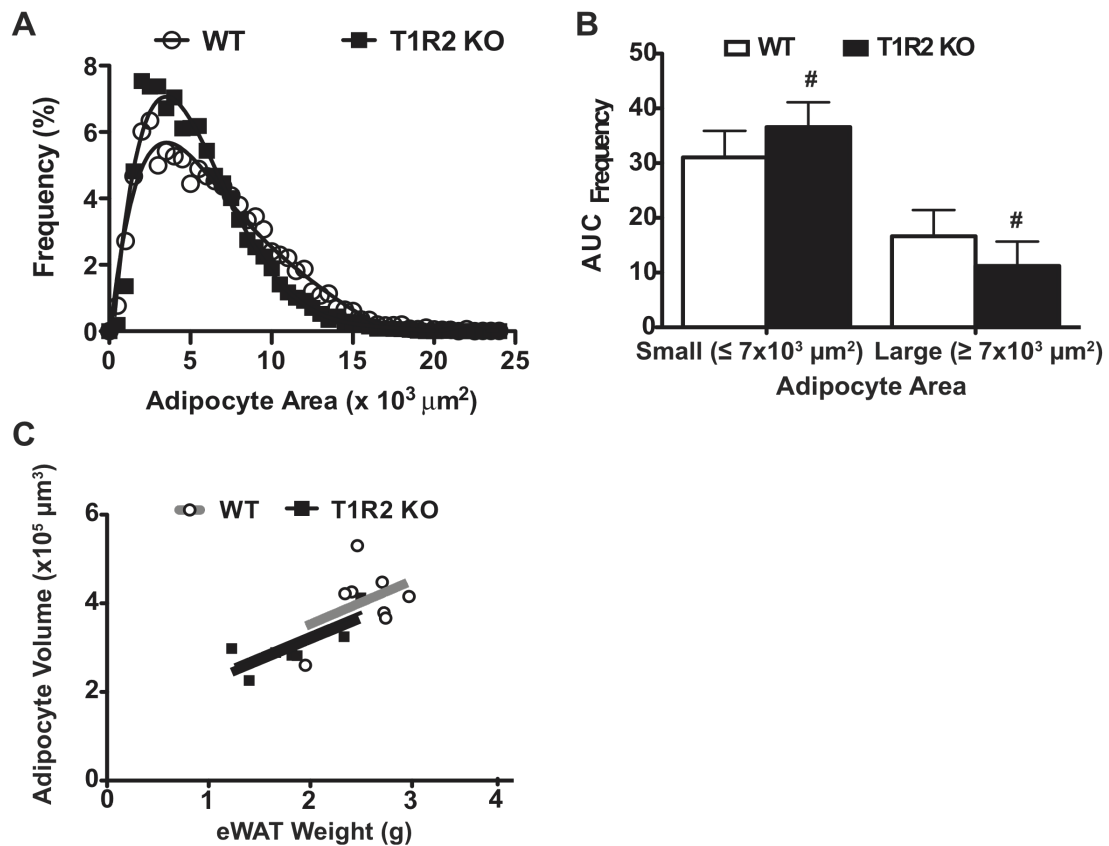


Figure 3.6 T1R2 KO mice have smaller adipocytes but equal adipocyte numbers.

A) Adipocyte size frequency distribution in WT and T1R2 KO mice on Western Diet shows a greater prevalence of smaller adipocytes in T1R2 KO animals. B) T1R2 KO animals show a decreased frequency of large adipocytes, defined as having a surface area greater than $7000 \mu\text{m}^2$, and in increased frequency of small adipocytes, defined as having a surface area smaller than $7000 \mu\text{m}^2$. Significance was determined using Student's t-test. *P*-values <0.05 are indicated with # in male mice. Data are expressed as mean plus S.D. C) Epididymal fat pad weight was correlated with average adipocyte volume of WT and T1R3 KO mice to estimate number of adipocytes per gram adipose tissue.

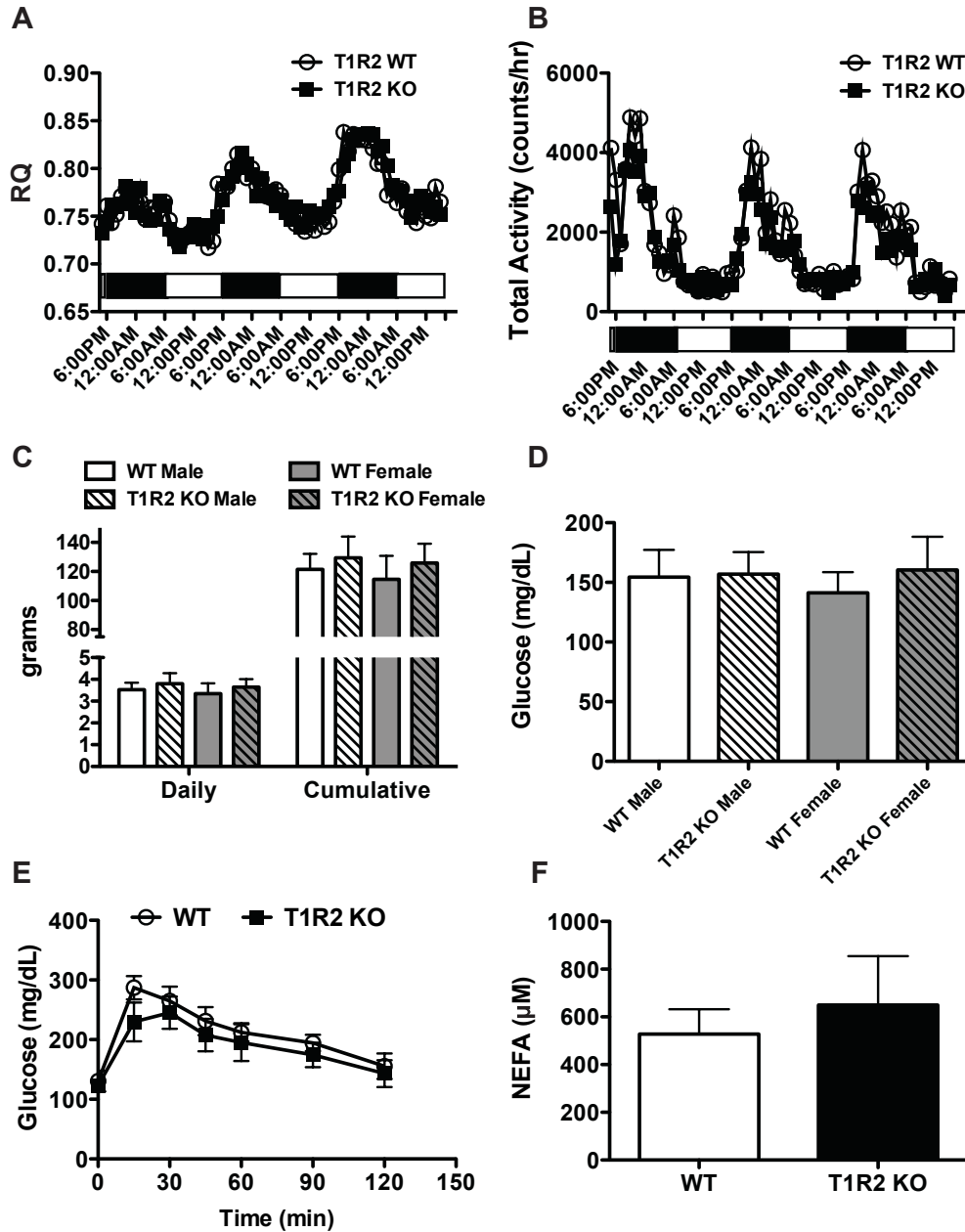


Figure 3.7. T1R2 KO mice have no changes in glucose sensitivity.

A) RQ and B) total activity were measured in WT (n=9) and T1R2 KO (n=9) male mice in Comprehensive Laboratory Animal Monitoring System (CLAMS) cages after 3 weeks on Western Diet. C) Food intake in T1R2 KO animals on Western Diet measured over 5 weeks. Data are expressed as mean plus S.D. D) Random fed glucose from WT and T1R2 KO animals following 3 weeks on Western Diet. Males n=11,9, females n=9,10. Data are expressed as mean plus S.D. E) Intraperitoneal glucose tolerance in WT (n=9) and T1R2 KO (n=9) male mice following 20 weeks on Western Diet. Data are expressed as mean plus S.D. Significance was determined using Student's t-test. F) Non-esterified fatty acids measured from serum of WT (n=9) and T1R2 KO (n=9) male mice following 18 weeks on Western Diet. Data are expressed as mean plus S.D.

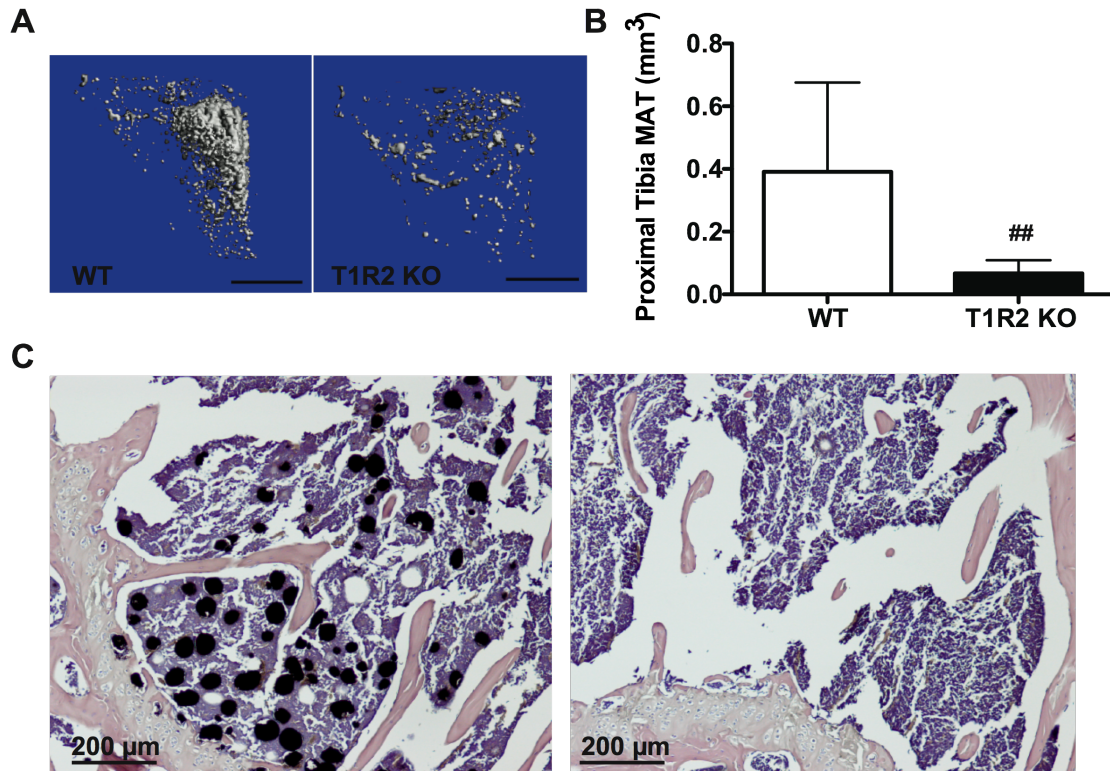


Figure 3.8. T1R2 KO mice have fewer bone marrow adipocytes.

A) Adult WT (left panel) and T1R2 KO (right panel) mice were placed on Western Diet for 14 wks, and bone marrow adipocytes were stained with osmium tetroxide before μ CT scanning. Representative μ CT shown, WT n=9, T1R2 KO n=9. B) Quantification of osmium tetroxide staining in tibia marrow adipose tissue from male WT and T1R2 KO mice on Western Diet for 14 weeks. Data are expressed as mean plus S.D. C)

Representative osmium tetroxide histology of bone marrow adipocytes in the proximal tibia. WT left panel, T1R2 KO right panel. Significance was determined using Student's t-test. *P*-values <0.05 are indicated with #, *P*-values <0.01 are indicated with ##.

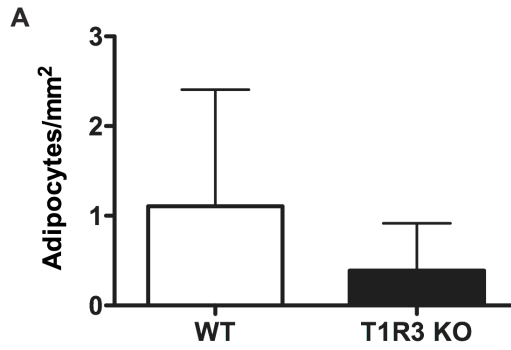


Figure 3.9. T1R3 KO animals trend towards fewer bone marrow adipocytes.

A) Bone marrow adipocytes from WT (n=7) and T1R3 KO (n=8) males on Western Diet for 24 weeks were quantified by manually counting adipocytes in stained femoral sections. Significance was determined using Student's t-test. Data are expressed as mean plus S.D.

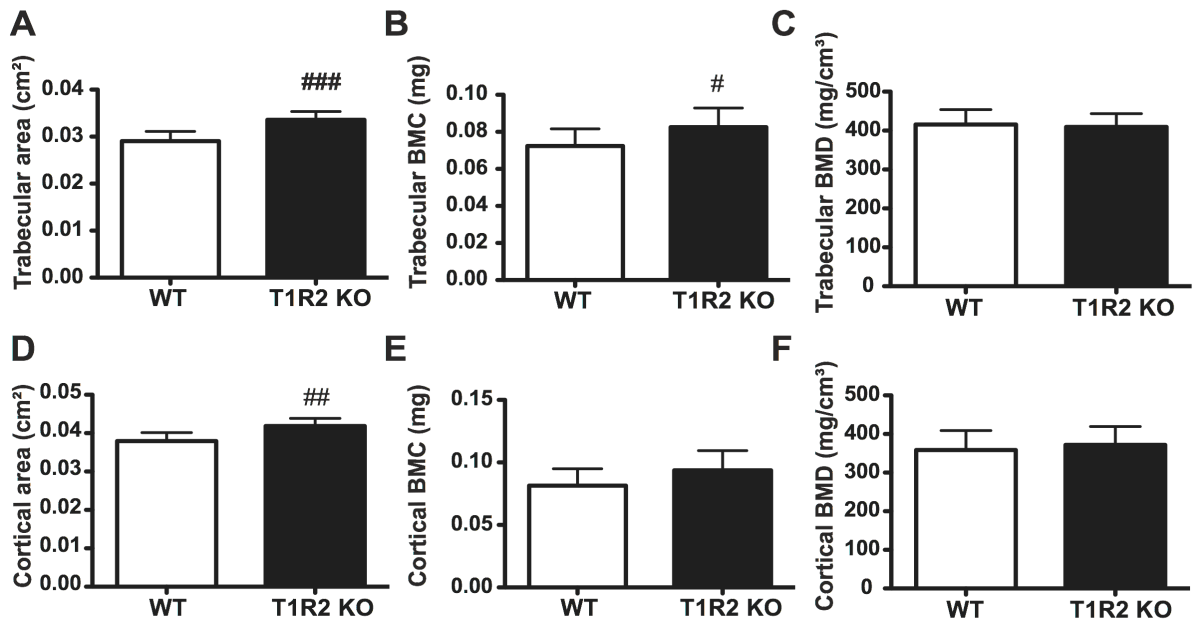


Figure 3.10. T1R2 KO animals have increased trabecular bone.

WT (n=9) and T1R2 KO (n=9) male mice were placed on Western Diet for 14 weeks, as in Fig 3.5. Cortical (A,B,C) and trabecular (D,E,F) parameters were evaluated by μ CT for the tibia. Significance was determined using Student's t-test. *P*-values <0.05 are indicated with #, *P*-values <0.01 are indicated with ##, and *P*-values <0.005 are indicated with ###. Data are expressed as mean plus S.D.

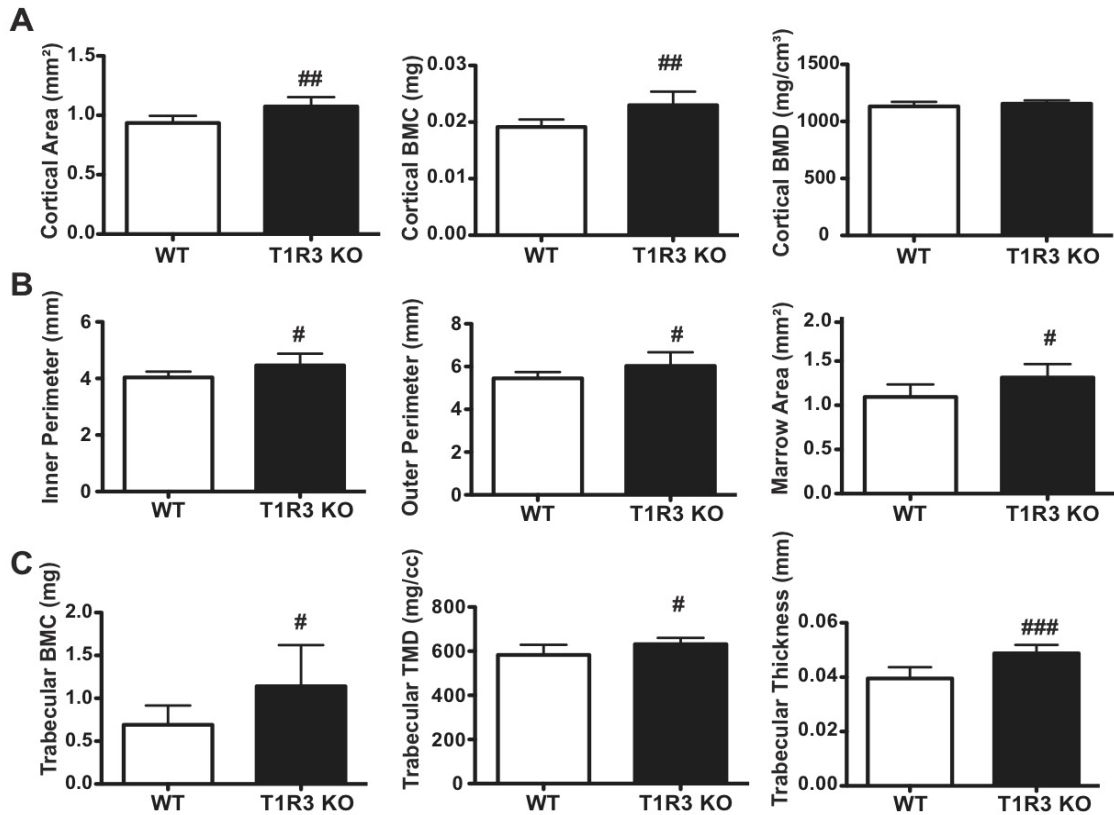


Figure 3.11. T1R3 KO animals have increased cortical and trabecular bone. WT (n=7) and T1R3 KO (n=8) mice were placed on Western Diet for 24 weeks, as in Fig 2. Cortical (A,B) and trabecular (C) parameters were evaluated in the femur by μ CT. Significance was determined using Student's t-test. *P*-values <0.05 are indicated with #, *P*-values <0.01 are indicated with ##, and *P*-values <0.005 are indicated with ###. Data are expressed as mean plus S.D.

References

- Akune, T., Ohba, S., Kamekura, S., Yamaguchi, M., Chung, U.I., Kubota, N., Terauchi, Y., Harada, Y., Azuma, Y., Nakamura, K., *et al.* (2004). PPARgamma insufficiency enhances osteogenesis through osteoblast formation from bone marrow progenitors. *J Clin Invest* *113*, 846-855.
- Davidson, T.L., Martin, A.A., Clark, K., and Swithers, S.E. Intake of high-intensity sweeteners alters the ability of sweet taste to signal caloric consequences: implications for the learned control of energy and body weight regulation. *Q J Exp Psychol (Hove)* *64*, 1430-1441.
- Elliott, R.A., Kapoor, S., and Tincello, D.G. Expression and distribution of the sweet taste receptor isoforms T1R2 and T1R3 in human and rat bladders. *J Urol* *186*, 2455-2462.
- Fretz, J.A., Nelson, T., Xi, Y., Adams, D.J., Rosen, C.J., and Horowitz, M.C. Altered metabolism and lipodystrophy in the early B-cell factor 1-deficient mouse. *Endocrinology* *151*, 1611-1621.
- Geraedts, M.C., Takahashi, T., Vignes, S., Markwardt, M.L., Nkobena, A., Cockerham, R.E., Hajnal, A., Dotson, C.D., Rizzo, M.A., and Munger, S.D. Transformation of postingestive glucose responses after deletion of sweet taste receptor subunits or gastric bypass surgery. *Am J Physiol Endocrinol Metab* *303*, E464-474.
- Glendinning, J.I., Gillman, J., Zamer, H., Margolskee, R.F., and Sclafani, A. The role of T1r3 and Trpm5 in carbohydrate-induced obesity in mice. *Physiol Behav* *107*, 50-58.
- Hirsch, J., and Batchelor, B. (1976). Adipose tissue cellularity in human obesity. *Clin Endocrinol Metab* *5*, 299-311.
- Jang, H.J., Kokrashvili, Z., Theodorakis, M.J., Carlson, O.D., Kim, B.J., Zhou, J., Kim, H.H., Xu, X., Chan, S.L., Juhaszova, M., *et al.* (2007). Gut-expressed gustducin and taste receptors regulate secretion of glucagon-like peptide-1. *Proc Natl Acad Sci U S A* *104*, 15069-15074.

Kawai, M., and Rosen, C.J. PPARgamma: a circadian transcription factor in adipogenesis and osteogenesis. *Nat Rev Endocrinol* 6, 629-636.

Kokrashvili, Z., Mosinger, B., and Margolskee, R.F. (2009). T1r3 and alpha-gustducin in gut regulate secretion of glucagon-like peptide-1. *Ann N Y Acad Sci* 1170, 91-94.

Kyriazis, G.A., Soundarapandian, M.M., and Tyrberg, B. Sweet taste receptor signaling in beta cells mediates fructose-induced potentiation of glucose-stimulated insulin secretion. *Proc Natl Acad Sci U S A* 109, E524-532.

Lecka-Czernik, B. Marrow fat metabolism is linked to the systemic energy metabolism. *Bone* 50, 534-539.

Mace, O.J., Affleck, J., Patel, N., and Kellett, G.L. (2007). Sweet taste receptors in rat small intestine stimulate glucose absorption through apical GLUT2. *J Physiol* 582, 379-392.

Margolskee, R.F., Dyer, J., Kokrashvili, Z., Salmon, K.S., Ilegems, E., Daly, K., Maillet, E.L., Ninomiya, Y., Mosinger, B., and Shirazi-Beechey, S.P. (2007). T1R3 and gustducin in gut sense sugars to regulate expression of Na⁺-glucose cotransporter 1. *Proc Natl Acad Sci U S A* 104, 15075-15080.

Masubuchi, Y., Nakagawa, Y., Ma, J., Sasaki, T., Kitamura, T., Yamamoto, Y., Kurose, H., Kojima, I., and Shibata, H. A novel regulatory function of sweet taste-sensing receptor in adipogenic differentiation of 3T3-L1 cells. *PLoS One* 8, e54500.

Merigo, F., Benati, D., Cristofolletti, M., Amaru, F., Osculati, F., and Sbarbati, A. Glucose transporter/T1R3-expressing cells in rat tracheal epithelium. *J Anat* 221, 138-150.

Nakagawa, Y., Nagasawa, M., Yamada, S., Hara, A., Mogami, H., Nikolaev, V.O., Lohse, M.J., Shigemura, N., Ninomiya, Y., and Kojima, I. (2009). Sweet taste receptor expressed in pancreatic beta-cells activates the calcium and cyclic AMP signaling systems and stimulates insulin secretion. *PLoS One* 4, e5106.

Nelson, G., Hoon, M.A., Chandrashekar, J., Zhang, Y., Ryba, N.J., and Zuker, C.S. (2001). Mammalian sweet taste receptors. *Cell* 106, 381-390.

Nestel, P.J., Austin, W., and Foxman, C. (1969). Lipoprotein lipase content and triglyceride fatty acid uptake in adipose tissue of rats of differing body weights. *J Lipid Res* 10, 383-387.

Nie, Y., Vignes, S., Hobbs, J.R., Conn, G.L., and Munger, S.D. (2005). Distinct contributions of T1R2 and T1R3 taste receptor subunits to the detection of sweet stimuli. *Curr Biol* 15, 1948-1952.

Pasarica, M., Xie, H., Hymel, D., Bray, G., Greenway, F., Ravussin, E., and Smith, S.R. (2009). Lower total adipocyte number but no evidence for small adipocyte depletion in patients with type 2 diabetes. *Diabetes Care* 32, 900-902.

Ren, X., Zhou, L., Terwilliger, R., Newton, S.S., and de Araujo, I.E. (2009). Sweet taste signaling functions as a hypothalamic glucose sensor. *Front Integr Neurosci* 3, 12.

Shockley, K.R., Lazarenko, O.P., Czernik, P.J., Rosen, C.J., Churchill, G.A., and Lecka-Czernik, B. (2009). PPARgamma2 nuclear receptor controls multiple regulatory pathways of osteoblast differentiation from marrow mesenchymal stem cells. *J Cell Biochem* 106, 232-246.

Swithers, S.E., and Davidson, T.L. (2008). A role for sweet taste: calorie predictive relations in energy regulation by rats. *Behav Neurosci* 122, 161-173.

Zhao, G.Q., Zhang, Y., Hoon, M.A., Chandrashekar, J., Erlenbach, I., Ryba, N.J., and Zuker, C.S. (2003). The receptors for mammalian sweet and umami taste. *Cell* 115, 255-266.

Chapter Four

Future Directions for Sweetener and Taste Receptor Biology

Summary

At the initiation of this thesis work, we hypothesized that sweet taste receptors functioned as nutrient sensors by sensing carbohydrate in adipose tissue. This receptor activation would serve as a positive nutrient signal to stimulate adipogenesis in preadipocytes and anabolic processes in adipocytes (Fig 1.4). This hypothesis was based on the known metabolic roles for sweet taste receptors in other non-gustatory tissues (Jang et al., 2007; Kyriazis et al., 2012) and microarray data indicating that chemosensory receptors were expressed in adipose tissue (Fig 2.1). We tested this hypothesis by treating adipocytes and adipocyte precursor cells with sweet taste receptor agonists to observe effects of receptor activation. Using this approach, we observed that saccharin or AceK treatment enhances adipogenesis in several model systems (Fig 2.3) and suppresses lipolysis in adipocytes (Fig 2.9). However, these effects were not dependent on expression of sweet taste receptors T1R2 or T1R3 (Fig 2.8 and 2.10). This observation suggests that sweeteners have metabolic input in the absence of a known receptor, and leaves the actual function of sweet taste receptors in adipose tissue an open question.

Concurrent with these *in vitro* studies, we also evaluated T1R2 and T1R3 KO mice for adipose tissue phenotypes, anticipating that KO animals would have failures in adipogenesis or anabolic processes that might result in metabolic dysfunction. We observed that both T1R2 and T1R3 KO mice have reduced adiposity (Fig 3.1 and 3.5) and smaller adipocytes (Fig 3.2 and 3.6) on a Western

diet, but have equal numbers of adipocytes and are metabolically normal by all tested parameters. These results suggest that while sweet taste receptor expression may play a role in regulating peripheral adipose expansion *in vivo*, this effect is not strong enough to robustly impact metabolic homeostasis. However, the loss of bone marrow adipocytes with T1R2 KO and increased bone mass in both T1R2 and T1R3 animals suggests that these receptors may play a more complex role in an adipogenesis-osteogenesis development axis.

While the above work represents the characterization of a novel role for sweet taste receptors and artificial sweeteners in adipose tissue and bone biology, it also engenders numerous questions for further study of chemosensory receptors in metabolic systems.

How are artificial sweetener effects mediated in the absence of taste receptors? Perhaps the most pressing question engendered by the present study is the mechanism by which saccharin and AceK mediate effects on adipogenesis and lipolysis in the absence of T1R2 or T1R3. In preadipocytes, saccharin treatment stimulates phosphorylation of Akt, which has never been reported in sweet taste receptor signal transduction. Sweetener treatment in this system also fails to generate calcium transients characteristic of sweet taste receptor signaling. These data, taken together with the observation that T1R2 and T1R3 expression are not necessary for any downstream effects of saccharin treatment, suggests that an independent receptor and signaling pathway are utilized for sweetener actions on adipocyte precursors.

Since the initiation of this study, Masubuchi *et al* have reported that T1R2 and T1R3 are expressed in 3T3-L1 cells (Masubuchi et al., 2013). This group shows constitutively low expression of T1R2 and a 90-fold increase in T1R3 expression throughout adipogenesis. In their model, saccharin and sucralose inhibit adipogenesis while stimulating cAMP accumulation, with no mention of calcium signaling. They show that while T1R3 expression is necessary in

HEK293 cells to drive sweetener-stimulated increases in cAMP concentrations, the addition of T1R2 blocks the T1R3 response. This would imply that T1R2 acts as an antagonist in this context, in contrast to numerous studies (Jiang et al., 2005; Nelson et al., 2001; Xu et al., 2004). They conclude that T1R3 acts as homodimer in 3T3-L1 cells because T1R2 expression is very low and T1R3 knockdown blocks saccharin-inhibited adipogenesis.

This study presents similarities and disparities with our own work that can hopefully be resolved with further experimentation. While we agree on a non-canonical model of taste perception, our results suggest that sweetener activity is independent of both T1R2 and T1R3, in contrast to their T1R3-dependent model. However, this group did not test for saccharin effects on adipogenesis in the absence of T1R2, which would add support to their T1R3 homodimer model. In addition, we show an enhancement of adipogenesis with saccharin treatment, while they report an inhibition. Although we have not identified any methodological differences that might cause such disparities, even after direct contact with the authors, repetition of these experiments in independent labs will hopefully clarify this issue. Though it seems most likely that divergent reagents and/or methods are the root cause of opposing phenotypes with sweetener treatment, the role of sweet taste receptors in adipogenesis is testable by independent means.

Homodimerization models suggest that both T1R2 and T1R3 are capable of independently binding ligand. Thus it is possible that saccharin might activate T1R2 in T1R3 KO cells and *vice versa*. Double T1R2;T1R3 KO cells would alleviate this confounding possibility. While our preliminary data indicates that saccharin robustly enhances adipogenesis in double KO eMSCs (data not shown), further experiments are necessary to better characterize this observation. A more direct assessment of saccharin binding in single and double KO eMSCs can also be performed by STD NMR, with quantification of receptor K_d values (Assadi-Porter et al., 2008). Using this technique to quantify saccharin

bound to membranes of eMSCs from a panel of genotypes, the capacity for homodimer binding can be directly measured. Additionally, NMR analysis of T1R2;T1R3 double KO eMSCs will quantitatively address whether any other receptors are present in these cells capable of binding saccharin.

What is the function of sweet taste receptors in adipose tissue *in vivo*? Is there an endogenous ligand for receptor activation?

In vitro, we have not observed any effects of sweetener treatment that were dependent on receptor expression. However, our *in vivo* results indicate that sweet taste receptor KO mice have reduced adiposity and adipocyte size. However, these receptors are also expressed in non-adipose tissues, and global receptor deletion in our mice makes a mechanistic interpretation of these observations more difficult. While we can hypothesize that the reduced adiposity and adipocyte size in KO animals supports a role for sweet taste receptors in regulating adipose tissue expansion or lipid utilization, a tissue-specific KO will be necessary to address these issues. A tissue-specific KO model may also uncover additional, specific roles for sweet taste receptors in adipose tissue *in vivo* that are obscured in a global KO model.

While T1R2 and T1R3 activity was stimulated *in vitro* with artificial sweeteners, these compounds are not predicted to circulate at high enough concentrations under normal dietary conditions to activate receptors *in vivo*; activation of sweet taste receptors on the tongue generally requires low millimolar concentrations of saccharin or ~100 mM of natural sugars, which are well above those generally circulating (Nelson et al., 2001; Piche et al., 2004; Sweatman et al., 1981). If sweet taste receptors are to be activated *in vivo*, this may necessitate the existence of additional, uncharacterized ligands present endogenously that can regulate their activity. Glucose has been shown to drive T1R2 and T1R3 activation *in vivo* in the gut, where local concentrations of sugars in the lumen can be much higher than those circulating (Ferraris et al., 1990; Olsen and Ingelfinger, 1968). In the pancreas, fructose has been shown to

stimulate insulin secretion at low millimolar concentrations in a T1R2-dependent manner, but only in the presence of adequate concentrations of glucose. This suggests a more complex synergy model for physiological ligand binding in this context (Kyriazis et al., 2012).

Candidate metabolites to activate adipose tissue sweet taste receptors *in vivo* also include glucose and fructose, though these sugars would presumably need to be circulating in higher concentrations or subject to ligand 'synergy' as seen in the pancreas. It is also possible that in adipose tissue, the presence of glycosylated surface proteins might provide a 'sticky' local environment that traps circulating sugars and raises local concentrations. Alternatively, some proteins have also been reported to activate sweet taste receptors (Assadi-Porter et al., 2005; Bohak and Li, 1976), and the amino acids glycine, alanine, and serine are mildly sweet (Schiffman et al., 1981). Whether dietary or synthesized and secreted, protein activation could also be the driving force for sweet taste receptor activation in adipose tissue.

Do sweet taste receptors play a role in bone biology?

We have reported that sweet taste receptor KO mice have increased bone mass. This result was unexpected, as we know of no reports of sweet taste receptor expression or activity in bone. This observation could be further explored by examination *in vitro*; osteogenesis can be compared between WT and taste receptor KO animals in bone marrow stromal cells, and in the presence or absence of artificial sweeteners. If the expected decreases in mineralization occur in response to sweetener treatment, these can then be evaluated for dependence on receptor expression using KO models. Observing repetition of KO effects in an *in vitro* system would add credence to the specificity of *in vivo* effects. A bone-specific KO of T1R2 and T1R3 would also further clarify whether increases in bone mass are secondary to increased lean mass or reflect endogenous sweet taste receptor activity in bone.

Are other chemosensory receptors functional in adipose tissue?

Our microarray results indicate that numerous chemosensory receptors, including olfactory, vomeronasal, and taste receptors, are expressed in adipose tissue. However, very few of these receptors have been investigated for physiological roles in adipose tissue. However, preliminary experiments suggest that some may be worth exploring.

T1R1

The umami taste receptor, a heterodimer of T1R1 and T1R3, is sensitive to L-amino acids and generates a 'savory' sensation from protein-rich food. Like sweet taste receptors, T1R1 is also expressed in non-gustatory systems (Daly et al.; Meyer et al.). The inherent amino acid-sensing capacity of T1R1 has led some groups to speculate that this receptor might also function as a nutrient sensor. Indeed, T1R1 was recently reported as a regulator of mTORC activity and autophagy in muscle (Wauson et al.). Interestingly, we have also observed that T1R1 is expressed in 3T3-L1 cells and eMSCs (Adam Bree, unpublished). Similar to sweet taste receptors, treatment of preadipocytes with amino acid stimulates Akt phosphorylation, but in a T1R3-dependent manner. This data supports a model for umami receptors acting as nutrient sensors in preadipocytes. Direct studies of umami receptor activity on adipogenesis are hampered by the relative dearth of non-metabolized receptor agonists; however, at least one such agonist has been synthesized (Zhang et al., 2008) that may allow investigation of effects of umami receptor activation on adipogenesis. Such a sensor could have role in autophagy as described in muscle, or in protein and hormone synthesis or secretion.

T2Rs

Bitter taste receptors were also detected in adipose tissue by our microarray, and have been shown to be active in the gut and trachea (Jeon et al., 2008; Shah et al., 2009). In these systems, bitter taste receptors are sensitive to potentially toxic compounds. However, bitter taste receptor polymorphisms have

also been associated with perturbed glucose and insulin homeostasis (Dotson et al., 2008). Additionally, treatment with the malarial drug and bitter tastant quinine causes hypoglycemia (Jones et al., 1986), though this side effect likely has complex causes (Gribble et al., 2000; Singh et al., 1998). Three bitter taste receptors were identified in adipose tissue by microarray (Fig 2.1), and all have been detected in 3T3-L1 cells by qPCR. While the pharmacology of these particular receptors is unknown, we have observed that treatment with the agonist quinine results in enhanced adipogenesis (data not shown). Further studies will be necessary to determine if this is a direct effect of taste receptor activity.

Olfactory receptors

Functional expression of olfactory receptors outside of the olfactory bulb has been a lofty but elusive goal of many sensory scientists. Most groups have described co-expression of known olfactory signaling components in the tissue of interest in lieu of demonstrated receptor activation (Itakura et al., 2006; Pluznick et al., 2009). However, the incredibly broad structural diversity of olfactory receptor ligands makes these receptors a perennial candidate for nutrient sensing studies. The majority of the chemosensory receptors detected in adipose tissue by microarray were olfactory receptors (Fig 2.1). We detected ~22 olfactory receptors in 3T3-L1 cells by qPCR, and have screened ~20 odorants for effects on adipogenesis; most compounds had no effect (data not shown). However, the complex pharmacology of olfactory receptors does not preclude the possibility that the correct agonist(s) for the receptors present were not used, or our *in vitro* conditions were not suited for detecting receptor activation. High-throughput screening may be a better method to address the question of olfactory receptor function in adipose tissue, perhaps combined with knockdown of canonical olfactory signaling components. While whether olfactory receptor function is involved in adipose biology is one of the most difficult questions presented here to definitely answer, but it could prove a fascinating and pharmacologically useful area of study.

References

- Assadi-Porter, F.M., Abildgaard, F., Blad, H., Cornilescu, C.C., and Markley, J.L. (2005). Brazzein, a small, sweet protein: effects of mutations on its structure, dynamics and functional properties. *Chem Senses* *30 Suppl 1*, i90-91.
- Assadi-Porter, F.M., Tonelli, M., Maillet, E., Hallenga, K., Benard, O., Max, M., and Markley, J.L. (2008). Direct NMR detection of the binding of functional ligands to the human sweet receptor, a heterodimeric family 3 GPCR. *J Am Chem Soc* *130*, 7212-7213.
- Bohak, Z., and Li, S.L. (1976). The structure of monellin and its relation to the sweetness of the protein. *Biochim Biophys Acta* *427*, 153-170.
- Daly, K., Al-Rammahi, M., Moran, A., Marcello, M., Ninomiya, Y., and Shirazi-Beechey, S.P. Sensing of amino acids by the gut-expressed taste receptor T1R1-T1R3 stimulates CCK secretion. *Am J Physiol Gastrointest Liver Physiol* *304*, G271-282.
- Dotson, C.D., Zhang, L., Xu, H., Shin, Y.K., Vignes, S., Ott, S.H., Elson, A.E., Choi, H.J., Shaw, H., Egan, J.M., *et al.* (2008). Bitter taste receptors influence glucose homeostasis. *PLoS One* *3*, e3974.
- Ferraris, R.P., Yasharpour, S., Lloyd, K.C., Mirzayan, R., and Diamond, J.M. (1990). Luminal glucose concentrations in the gut under normal conditions. *Am J Physiol* *259*, G822-837.
- Gribble, F.M., Davis, T.M., Higham, C.E., Clark, A., and Ashcroft, F.M. (2000). The antimalarial agent mefloquine inhibits ATP-sensitive K-channels. *Br J Pharmacol* *131*, 756-760.
- Itakura, S., Ohno, K., Ueki, T., Sato, K., and Kanayama, N. (2006). Expression of Golf in the rat placenta: Possible implication in olfactory receptor transduction. *Placenta* *27*, 103-108.
- Jang, H.J., Kokrashvili, Z., Theodorakis, M.J., Carlson, O.D., Kim, B.J., Zhou, J., Kim, H.H., Xu, X., Chan, S.L., Juhaszova, M., *et al.* (2007). Gut-expressed gustducin and taste receptors regulate secretion of glucagon-like peptide-1. *Proc Natl Acad Sci U S A* *104*, 15069-15074.

Jeon, T.I., Zhu, B., Larson, J.L., and Osborne, T.F. (2008). SREBP-2 regulates gut peptide secretion through intestinal bitter taste receptor signaling in mice. *J Clin Invest* 118, 3693-3700.

Jiang, P., Cui, M., Zhao, B., Liu, Z., Snyder, L.A., Benard, L.M., Osman, R., Margolskee, R.F., and Max, M. (2005). Lactisole interacts with the transmembrane domains of human T1R3 to inhibit sweet taste. *J Biol Chem* 280, 15238-15246.

Jones, R.G., Sue-Ling, H.M., Kear, C., Wiles, P.G., and Quirke, P. (1986). Severe symptomatic hypoglycaemia due to quinine therapy. *J R Soc Med* 79, 426-428.

Kyriazis, G.A., Soundarapandian, M.M., and Tyrberg, B. Sweet taste receptor signaling in beta cells mediates fructose-induced potentiation of glucose-stimulated insulin secretion. *Proc Natl Acad Sci U S A* 109, E524-532.

Masubuchi, Y., Nakagawa, Y., Ma, J., Sasaki, T., Kitamura, T., Yamamoto, Y., Kurose, H., Kojima, I., and Shibata, H. A novel regulatory function of sweet taste-sensing receptor in adipogenic differentiation of 3T3-L1 cells. *PLoS One* 8, e54500.

Meyer, D., Voigt, A., Widmayer, P., Borth, H., Huebner, S., Breit, A., Marschall, S., de Angelis, M.H., Boehm, U., Meyerhof, W., *et al.* Expression of Tas1 taste receptors in mammalian spermatozoa: functional role of Tas1r1 in regulating basal Ca(2)(+) and cAMP concentrations in spermatozoa. *PLoS One* 7, e32354.

Nelson, G., Hoon, M.A., Chandrashekar, J., Zhang, Y., Ryba, N.J., and Zuker, C.S. (2001). Mammalian sweet taste receptors. *Cell* 106, 381-390.

Olsen, W.A., and Ingelfinger, F.J. (1968). The role of sodium in intestinal glucose absorption in man. *J Clin Invest* 47, 1133-1142.

Piche, M.E., Arcand-Bosse, J.F., Despres, J.P., Perusse, L., Lemieux, S., and Weisnagel, S.J. (2004). What is a normal glucose value? Differences in indexes of plasma glucose homeostasis in subjects with normal fasting glucose. *Diabetes Care* 27, 2470-2477.

Pluznick, J.L., Zou, D.J., Zhang, X., Yan, Q., Rodriguez-Gil, D.J., Eisner, C., Wells, E., Greer, C.A., Wang, T., Firestein, S., *et al.* (2009). Functional

expression of the olfactory signaling system in the kidney. *Proc Natl Acad Sci U S A* 106, 2059-2064.

Schiffman, S.S., Sennewald, K., and Gagnon, J. (1981). Comparison of taste qualities and thresholds of D- and L-amino acids. *Physiol Behav* 27, 51-59.

Shah, A.S., Ben-Shahar, Y., Moninger, T.O., Kline, J.N., and Welsh, M.J. (2009). Motile cilia of human airway epithelia are chemosensory. *Science* 325, 1131-1134.

Singh, B., Choo, K.E., Ibrahim, J., Johnston, W., and Davis, T.M. (1998). Non-radioisotopic glucose turnover in children with falciparum malaria and enteric fever. *Trans R Soc Trop Med Hyg* 92, 532-537.

Sweatman, T.W., Renwick, A.G., and Burgess, C.D. (1981). The pharmacokinetics of saccharin in man. *Xenobiotica* 11, 531-540.

Wauson, E.M., Zaganjor, E., Lee, A.Y., Guerra, M.L., Ghosh, A.B., Bookout, A.L., Chambers, C.P., Jivan, A., McGlynn, K., Hutchison, M.R., *et al.* The G protein-coupled taste receptor T1R1/T1R3 regulates mTORC1 and autophagy. *Mol Cell* 47, 851-862.

Xu, H., Staszewski, L., Tang, H., Adler, E., Zoller, M., and Li, X. (2004). Different functional roles of T1R subunits in the heteromeric taste receptors. *Proc Natl Acad Sci U S A* 101, 14258-14263.

Zhang, F., Klebansky, B., Fine, R.M., Xu, H., Pronin, A., Liu, H., Tachdjian, C., and Li, X. (2008). Molecular mechanism for the umami taste synergism. *Proc Natl Acad Sci U S A* 105, 20930-20934.